VECTOR DESIGN FOR MONOCLONAL ANTIBODY PRODUCTION USING CHINESE HAMSTER OVARY CELLS

HO CHENG LEONG STEVEN

B.ENG (HONS), NTU

A THESIS SUBMITTED

FOR THE DEGREE OF

DOCTOR OF PHILOSOPHY

DEPARTMENT OF BIOENGINEERING

NATIONAL UNIVERSITY OF SINGAPORE

2014

Declaration

I hereby declare that this thesis is my original work and it has been written by me in its entirety. I have duly acknowledged all the sources of information which have been used in the thesis.

This thesis has also not been submitted for any degree in any university previously.

HO CHENG LEONG STEVEN

4th August 2014

Acknowledgements

My PhD journey has been an extremely enriching and fulfilling process. I would like extend my sincerest thanks to my supervisors, Dr Yang Yuansheng and Prof Tong Yen Wah, for their supervision and guidance. I am eternally grateful for their patience and all the pearls of wisdom they have generously shared with me.

Special thanks to Prof Miranda Yap and Prof Lam Kong Peng for their support of my scholarship. My sincerest wishes that Prof Yap's condition improves. The financial support from Bioprocessing Technology Institute (BTI), A*STAR is gratefully acknowledged. I would also like to thank all members of my qualifying exam and thesis committee for their advice and guidance.

The work done in this thesis would not have been possible without the sincere and professional assistance from my colleagues in BTI with special thanks to members of my group, Animal Cell Technology. I am grateful to the support from Dr Muriel Bardor, Dr Miranda van Beers and Dr Wang Tianhua and their analytics group, Dr Bi Xuezhi and his proteomics group and especially Dr Song Zhiwei.

Everything I have achieved in life is all only possible thanks to the care and love from my family. Thanks to my dad for his advice on work and life, my mom for her awesome meals and my siblings for their support. Not forgetting my partner-in-crime, my travel buddy, my late-night overtime workmate, my playmate—my girlfriend. Thanks to my loved ones for putting up with my grumpiness when an experiment fails or a deadline approaches.

From the bottom of my heart, thank you everyone.

Contents

Summary

Monoclonal antibodies (mAb) for treating various cancers and autoimmune diseases are the top-selling class of biologics. A plasmid vector was designed to express the light chain (LC), heavy chain (HC) and selection marker genes required for generating stable mAb producing Chinese hamster ovary (CHO) cells together on a single transcript by linking the genes using internal ribosome entry site (IRES) elements. Compared to traditional co-transfection and multi-promoter single vector systems, the IRES tricistronic vector generated fewer non-expressing cells and gave higher mAb productivity (chapter 3). We observed that only clones from the IRES tricistronic system exhibited similar LC:HC ratios. The strict control of LC and HC relative amounts by linking the genes on one transcript was important as LC:HC ratio has been shown to be important to mAb expression in transient, clonal and in-silico modelling experiments.

Another DNA element which is able to link multiple genes is the 2A peptide coupled to a furin cleavage site (F2A). F2A was expected to give balanced ratios of the two linked genes while when using IRES, the gene upstream of IRES would always be in excess compared to the downstream gene. F2A could possibly be used to express LC and HC peptides in equal amounts to study LC:HC ratio in stable cell lines. We compared a series of vectors generated using IRES and F2A for expressing mAb (chapter 4). F2A was not appropriate for expressing mAb as there was presence of fusion proteins, eg. LC-F2A-HC or HC-F2A-LC, that arose due to failure of the 2A peptide processing or furin cleavage. Extra 2A peptide amino acid residues

also possibly affected signal peptide cleavage. Use of F2A to control LC:HC ratio for further studies would require further optimization of the system.

We next proceeded with studying the effect of LC:HC ratio on stable mAb expression using variations of the IRES tricistronic vector described in chapter 3 to generate CHO cell lines with LC:HC ratios of 3.4, 1.2, 1.1 and 0.3 (chapter 5). The LC:HC ratio of 3.4 was the best for both mAb expression level and quality. At the ratio of 0.3, mAb expression level was low, aggregated easily, had undesired highly matured glycans and was less stable. In chapter 6, we observed that the aggregates could be dissociated in reducing and denaturing conditions, revealing possible disulfide and hydrophobic bonding between the molecules. Cell engineering by over-expressing BiP chaperone could reduce the amount of unwanted products. Re-transfection of the cells having excess HC with more LC greatly improved mAb products secreted and the cells started to only produce IgG monomers.

The IRES tricistronic vector presented in this thesis presents an attractive and flexible alternative to existing vector systems. The vector and its variants were also used for the first report of controlled LC:HC in stably transfected mAb expressing CHO cells to study its effects on mAb expression and quality. Possible solutions to remedy cells expressing mAb with high aggregation due to poor control of LC:HC ratio giving excess HC were also presented.

List of tables

List of figures

List of symbols and abbreviations

ADCC	Antibody dependent cell-mediated cytotoxicity
BiP	Binding immunoglobulin protein
CHO	Chinese hamster ovary
CMV	Human cytomegalovirus immediate early gene promoter
CPP	Critical process parameters
CRISPR	Clustered regularly interspaced short palindromic repeats
CQA	Critical quality attributes
DHFR	Dihydrofolate reductase
DSB	Double strand breaks
ELISA	Enzyme linked immunosorbent assay
EMCV	Encephalomyocarditis virus
ER	Endoplasmic reticulum
F2A	Furin-2A peptide
FBS	Fetal bovine serum
FMDV	Food-and-mouth disease virus
GFP	Green fluorescence protein
HC	mAb heavy chain
IgG	Immunoglobulin G
IRES	Internal ribosome entry site
IRESatt	Attenuated internal ribosome entry site
IVCD	Integrated viable cell density
LC	mAb light chain

mAb	Monoclonal antibody
MTX	Methotrexate
NHEJ	Non-homologous end joining
NPT	Neomycin phosphotransferase
ORF	Open reading frame
PAT	Process analytical tools
pcd	pg $cell^{-1}$ day^{-1}
PCR	Polymerase chain reaction
PI3K	Phosphatidylinositol-3 kinase
QbD	Quality by design
qRT-PCR	Quantitative real-time PCR
qmAb	Specific cell antibody productivity (pg $cell^{-1}$ day^{-1})
RVD	Repeat variable diresidue
SEC	Size exclusion chromatography
SpA	Simian virus 40 early polyadenylation signal
SV40	Simian virus 40 promoter
TALEN	Transcription activator like effector nuclease
TNF	Tissue necrosis factor
UPR	Unfolded protein response
VEGF	Vascular endothelial growth factor
ZFN	Zinc finger nuclease

Chapter 1: Introduction

This chapter introduces the motivation, hypotheses and objectives of the thesis.

1.1 Motivation

Monoclonal antibodies (mAb) are the top selling class of biologics with an annually growing market demand. The highly specific mAbs are used to treat various cancers, battle transplant rejections and fight autoimmune diseases by recognition of cell surface antigens or secreted activating factors. In contrast to small molecule drugs like paracetamol which are produced by chemical synthesis, mAbs are complex protein molecules requiring the use of live cellular machinery in a recombinant protein production process. Recombinant protein production involves transferring foreign genes encoding proteins not normally produced by the target cell into the cell to allow its expression by the cell. Mammalian cells like the Chinese hamster ovary (CHO) cells are commonly used for their ability to perform the required protein modifications for product safety and efficacy. DNA plasmid vectors are used to transfer the required genes into the cell and its design is critical to ensuring good mAb production. It is required that the cells are producing mAbs at a high level for maximal production efficiency and the product having the required critical product quality attributes, like molecular weight, aggregation level, glycosylation, stability, charge and antigen binding, for safety and efficacy. It is not uncommon to screen thousands of clones before the final candidate clone is selected. The process is labor intensive and time consuming if expensive automated systems are not available. One reason for the need to screen clones is due to problems associated with the commonly used vector systems.

The most commonly produced mAbs are multimeric immunoglobulin G (IgG) molecules assembled from two heavy chain (HC) peptides and two

light chain (LC) peptides and is the product of interest in this report. Three exogenous genes, HC, LC and a selection marker, are expressed when producing mAb using CHO cells. Gene expression requires a basic expression cassette consisting of a promoter, the gene of interest and a polyadenylation signal and each of the three genes are in separate expression cassettes on most plasmid vectors (further discussed in section 2.5). Issues like vector fragmentation causing false positives (Ng et al. 2010), transcriptional interference due to multiple promoters in close proximity (Eszterhas et al. 2002) and poor control of LC:HC ratios (Chusainow et al. 2009; Lee et al. 2009) can plague mAb cell line generation processes using these vectors. As LC and HC peptides are translated separately before assembly, their relative amounts could potentially affect mAb titer and quality attributes. As such there are conflicting reports which either encourage the expression of more HC as it is the rate-limiting reagent (Dorai et al. 2006) or discourage excess HC as it slows down assembly (Gonzalez et al. 2002). There is still no consensus LC:HC ratio which is best for both mAb expression level and quality. To date, there has been no studies where LC:HC ratio is effectively controlled in all cells of a stably transfected CHO cell lines. In this thesis, a novel vector for generating mAb producing CHO cells would be designed to address the issues faced when using the existing vectors.

It is possible to link all the three genes (LC, HC and selection marker) together using internal ribosome entry site (IRES) element from the encephalomyocarditis virus (EMCV) or 2A peptide from the food-and-mouth-disease virus (FMDV) to express the multiple required genes using a single promoter in one mRNA transcript. Using such vectors should minimize the

occurrence of non-expressing clones due to vector fragmentation and provide better control of LC:HC ratio. An IRES-based vector system which can achieve high mAb product titers in CHO cells is currently not available. In the only available report of an IRES vector for mAb expression, the expression levels obtained was more than two magnitudes below the desired levels and the experiments were also not performed in CHO cells (Mielke et al. 2000). While 2A peptides shown to generate mAb expression similar to that of co-transfection, 2A's have been reported to have cleavage errors and proper evaluation is still required for our application.

1.2 Hypothesis

It is hypothesized that a vector with the LC, HC and selection marker genes linked on a single transcript using IRES can be designed to generate stable CHO cell lines producing high levels of mAb product.

1.3 Aim and Objectives

The main aim of this thesis was to design a novel vector to improve the process of generating mAb producing CHO cell lines. The designed vector should be able to generate CHO cell lines capable of producing high amounts of mAb product (above 20 pcd) with low levels of aggregates and consistent glycosylation profiles. The vector should be able to help control LC:HC ratio at a similar level in all transfected cells to assist in achieving the targets. The following objectives were designed to explore and evaluate the above hypothesis.

Objective 1: Evaluate a vector design which expresses LC, HC and selection marker genes on a single transcript using IRES elements for controlling LC:HC ratio. Optimize the selection marker to obtain high mAb producing CHO cell lines.

Objective 2: Compare the use of 2A peptide with IRES for expressing mAb in CHO cells.

Objective 3: Investigate the effect of different LC:HC ratios on stable mAb production in CHO cells to ensure optimized gene arrangement on the vector for high mAb titer and good product quality.

Chapter 2: Literature review

This chapter describes the uses and market for monoclonal antibodies (mAb). It also reviews the recent developments made towards generating mAb producing mammalian cell lines.

*Parts of the following were first published in "**Ho, S. C. L.**, Tong, Y. W. and Yang, Y. (2013). "Generation of monoclonal antibody-producing mammalian cell lines." Pharmaceutical Bioprocessing **1**(1): 71-87".*

2.1 Monoclonal antibodies for therapy

Immunoglobulins (Ig) are produced by B cells as cell-surface receptors for disease and foreign antigens. Upon antigen stimulation, the B cells differentiate to plasma cells, which now secrete soluble effector molecules known as antibodies (Baumal and Scharff 1973). Each antibody is made up of light chain (LC) and heavy chain (HC) peptides which can both be separated into variable and constant regions. There are five main antibody isotypes, IgA, IgD, IgE, IgG and IgM that differ in the heavy chain constant regions. IgG is the simplest form, composed of two identical LC peptides and two identical HC peptides linked by disulfide bonds to form a "Y" shaped structure (Fig. 2.1). The paratope at the tip of the variable region on Fab fragment is responsible for the highly specific antigen recognition and binding and the Fc fragment commonly elicits the effector functions.

Recombinant therapeutic antibodies are copies of the antibody generated by a single, selected B cell candidate and are referred to as monoclonal antibodies (mAb). IgG is the dominant form of marketed therapeutic mAbs (Reichert 2012). Early attempts at mAb therapy were foiled by low protein amounts and highly immunogenic rodent sera cocktails (Gura 2002). These issues were addressed later by the development of hybridoma technology to generate larger amounts of product (Kohler and Milstein 1975) and antibody humanization to reduce the immunogenic segments (Jones et al. 1986) . Fully human mAbs can now be generated with the recent inventions of phage display (Winter et al. 1994) and transgenic mice (Lonberg et al. 1994; Wagner et al. 1994; Fishwild et al. 1996). The improvement in efficacy and

safety brought about by the aforementioned technologies has seen mAbs develop into the best-selling class of biologics.

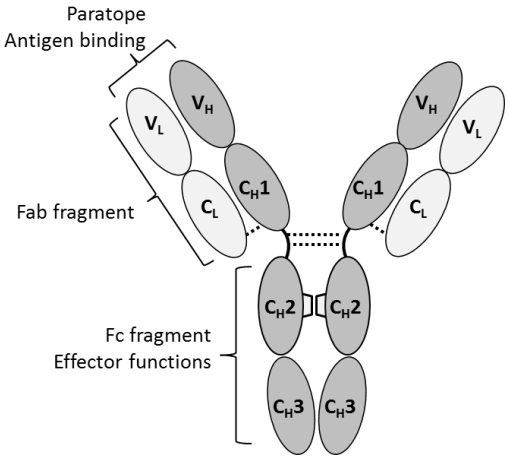

Figure 2.1 Structure of an IgG antibody molecule. Each IgG is a multimeric protein molecule composed of two identical light chains with MW ~25 kDa (white ovals) and two identical heavy chains with MW ~50 kDa (grey ovals). Each peptide chain has variable (V) and constant (C) regions. The paratope end is responsible for antigen binding while the Fc fragment composed of C_H2 and C_H3 domains are required for effector functions. The solid black line between C_H1 and C_H2 domains is the hinge region. Dotted lines represent disulfide bonds and the white squares on the C_H2 domain represent the N-glycosylation oligosaccharide residues.

Therapeutic mAbs function by binding to cell surface receptors or cytokines to either disrupt signal pathways or elicit immunogenic reactions like antibody dependent cell-mediated cytotoxicity (ADCC) and complement dependent cytotoxicity (CDC). Bevacizumab (Trade name: Avastin®) approved for the treatment of various tumors including metastatic colorectal cancer, an example of a cytokine binder, is an anti-vascular endothelial growth factor (VEGF) antibody. VEGF is an angiogenic factor which is promotes formation of vessels in tumors (Ferrara 2004). Bevacizumab binds to the VEGF released by the tumor cells to render the factors inactive to the VEGF receptors and aid in inhibiting tumor growth (Ferrara et al. 2004). Tumor

necrosis factor (TNF) is up-regulated in autoimmune diseases, including rheumatoid arthritis, psoriasis and Crohn's disease, resulting in uncontrolled inflammation and tissue destruction due to formation of osteoclasts (Brennan et al. 1989; Pfeilschifter et al. 1989; Tracey et al. 2008). Adalimumab (Humira®) is an antagonist which binds to TNF when administered to prevent activation of the TNF receptor and alleviate the symptoms (Chan and Carter 2010). Some mAbs can function through multiple mechanisms of action. Trastuzumab (Herceptin®) recognizes the human epidermal growth factor receptor 2 (HER2), a tyrosine kinase receptor, is most commonly used for treating HER2 positive metastatic breast cancer patients. HER2 receptor binding inhibits downstream phosphatidylinositol-3 kinase (PI3K) and Akt signaling leading to cell cyle arrest of the tumor cells (Yakes et al. 2002). The Fc fragment on the constant region also activates ADCC by engaging the Fcγ receptors on effector immune cells like natural killer cells (Barok et al. 2007).

2.2 MAb market and production

The market for mAbs saw 8.3% growth and $18.5 billion in sales for 2010, followed by similarly robust 10.1% growth and $20.3 billion of sales in 2011 in the US (Aggarwal 2011; Aggarwal 2012). The highly specific targeting capability of mAbs is now used to treat various cancers, battle transplant rejections and fight autoimmune diseases. 28 mAb products are approved for the market and over 350 are at various stages of clinical testing (Reichert 2012). Five full IgG mAb products that are currently listed as blockbusters (with over $1 billion in annual sales each): Remicade®, Avastin®, Rituxan®, Humira® and Herceptin®. As the market continues to mature, two

new trends are also forming. Biotech companies are starting to target the smaller markets of orphan diseases as seen by the record number of biopharmaceuticals approved for such indications (Kling 2012). Biosimilars of existing blockbuster products are also being developed and gaining approval outside of the US (Kling 2012; Reichert 2012). The increasing demand for existing mAbs and rapid innovation in mAb therapeutics has stimulated a parallel improvement in mammalian cell culture technologies used to produce a majority of the products. Faster and more efficient cell line development technologies for mAb production are now of utmost importance.

MAb production in mammalian cells can be performed either in transient or stable transfections. Transient transfections allow quick generation of small amounts of product for use during early stages of drug discovery (Pham et al. 2006). There are several review articles available for information on large-scale transient transfections of mammalian cells (Pham et al. 2006; Geisse 2009; Geisse and Voedisch 2012). Stably transfected cell lines are more widely used in large scale industrial production. Cell lines used for manufacturing are from a single cell clone in order to get high amounts of consistent product. The cell line development process (Fig. 2.2) starts from transfection of a mammalian cell line with plasmid vectors carrying the light chain (LC) gene, heavy chain (HC) gene, and a selection marker gene (Birch and Racher 2006). The plasmid vector comes in various designs, optimized for mAb production. Several cell types can be used but mammalian cells are the main workhorse for producing the safest and most effective mAb products. Plasmid delivery can be performed using calcium-phosphate precipitation, electroporation, lipofection and polymer-mediated techniques (Norton and

Pachuk 2003). After transfection, positive transfectants are selected by their drug resistance or growth advantage. If an amplifiable selection marker is used, gene amplification can be carried out to increase gene copies, leading to increase in product expression. Single clones are then chosen for scale up and characterization of product quality and long-term expression. The following sections will look at existing and upcoming materials and methods for generating stably transfected mammalian cell lines.

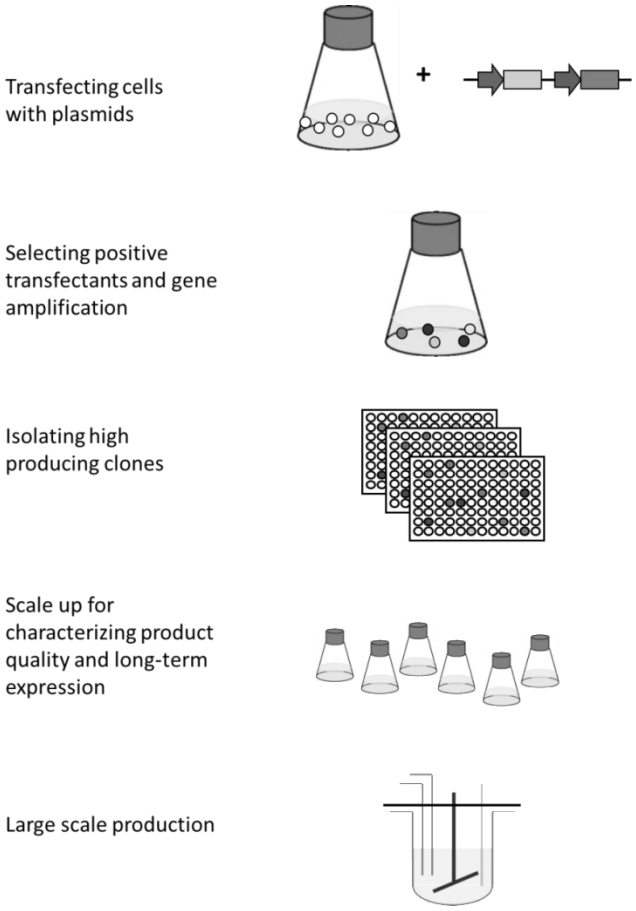

Figure 2.2 Generating a monoclonal antibody producing cell line. Mammalian cells are first transfected with plasmids carrying the light chain, heavy chain and selection marker genes. Drug selection is then carried out to select for positive transfectants. An initial round of screening is carried out to identify high producers. Selected clones are scaled up to collect sufficient mAb for characterization of product quality before production cell lines are selected for large scale production.

2.3 Mammalian cells for producing mAb

A survey of the mAbs currently approved by US or EU for the market shows a heavy reliance on mammalian cells for production. Of the 28 products, 12 are produced in Chinese hamster ovary (CHO) cells, 12 are produced in murine lymphoid cell lines NS0 or Sp2/0 and two are from hybridomas (Reichert 2012). *E. coli* microbial systems are only used for producing two antigen binding fragments products. Mammalian cell types have become dominant for manufacturing due to their abilities to produce high amounts of mAb with consistent quality and to adapt well to culturing in large scale suspension bioreactors (Butler 2005; Birch and Racher 2006; Costa et al. 2010). Another reason for the dominance is the capabilities to perform the required protein folding, assembly and post-translational modifications such as glycosylation (Walsh and Jefferis 2006; Jenkins 2007; Hossler et al. 2009). The mAb produced would be biochemically similar to human forms for increased product efficacy and safety (Matasci et al. 2009).

2.3.1 Chinese hamster ovary cells

Chinese hamster ovary (CHO) cells were first isolated in 1958 and they quickly gained recognition for ease of culture and fast generation times (Tjio and Puck 1958). Pathogenic human virus like HIV, influenza and polio do not replicate in CHO cells, greatly increasing safety of the mAb produced and simplifying the downstream purification process (Jayapal et al. 2007). The ease of genetic modification is another advantage of using CHO cells for mAb production (Jayapal et al. 2007). CHO cells have proven track record of producing safe, biocompatible and bioactive mAbs, enabling products from these cells to gain regulatory approval more easily (Butler and Meneses-

Acosta 2012; Kim et al. 2012). They will remain as the most widely used mammalian cells for therapeutic protein production in the near future as evidenced by the continued usage of the cells for producing new mAb therapeutics (Bronson et al. 2012; Reichert 2012). The recently assembled genomic sequence of the ancestral CHO-K1 cell line will increase understanding of these cells and their popularity (Xu et al. 2011).

2.3.2 Murine lymphoid cells

Murine lymphoid cells (NS0 and SP2/0) originate from differentiated B cells, which have the innate ability to produce large amounts of immunoglobulin, making them good candidates for manufacturing mAbs. Although there are currently a similar number of approved products from CHO cells and murine lymphoid cells, CHO derived cells are becoming the preferred hosts. Four of the six products approved before the year 2000 were from NS0 or Sp2/0 cells while two were from CHO. This changed in favor of CHO cells for products approved since 2010 where four were from CHO and only one from NS0. One reason for moving away from these cells is that glycoproteins from NS0 and Sp2/0 can have residues which are immunogenic and have reduced in-vivo half-life (Baker et al. 2001; Brooks 2004; Durocher and Butler 2009).

2.3.3 Human cells

To ensure mAbs produced do not carry any antigenic carbohydrate groups, cells from a human source can be used for production (Butler 2005). Possible candidates include the human embryonic kidney derived HEK293 cell line, immortalized human amnioctyes from CEVEC and human embryonic retinoblast derived Per.C6 cell line from Crucell (Swiech et al.

2012). HEK293 and amniocytes are reported to be better suited for transient protein production (Pham et al. 2006; Fischer et al. 2012). Per.C6 is currently the most promising candidate. This cell line can reach cell densities ten folds higher than CHO cells and been reported to produce up to 8 g L^{-1} of protein in fed-batch reactors (Kuczewski et al. 2011; Swiech et al. 2012). Several Per.C6 based products are currently undergoing clinical trials. Regulatory concerns exist regarding use of human based cell lines for production due to their lack of resistance against adventitious agents (Swiech et al. 2012).

2.4 Host cell engineering

Mammalian cell culture performance can be improved by genetic engineering of either enzymatic or regulatory activities. Modifications to the cell phenotype can be achieved through traditional recombinant DNA techniques to over-express target genes or to knockdown/knockout target genes by using more recent cell engineering techniques like RNA interference (RNAi) and zinc-finger nucleases (Wu 2009; Krämer et al. 2010; Lim et al. 2010; Liu et al. 2010; Dietmair et al. 2011).

2.4.1 Apoptosis

Apoptosis is a form of programmed cell death which occurs during high stress conditions in dense and productive mAb producing mammalian cell cultures (Singh et al. 1994). Delaying the onset of apoptosis would benefit culture health and lifespan, making genes involved in the pathway interesting cell engineering targets (Arden and Betenbaugh 2006; Wong et al. 2006). One approach is to over-express anti-apoptotic genes, like those in the Bcl-2

family, which had been shown to improve cell viability and increase mAb production (Tey et al. 2000; Chiang and Sisk 2005; Majors et al. 2009; Carlage et al. 2012). Another approach involves down-regulating pro-apoptosis genes like Bax and Bak by RNAi (Lim et al. 2006) or deleting the genes using zinc-finger nucleases (ZFN) (Cost et al. 2010). Deleting the genes inhibited activation of downstream caspases in the presence of apoptotic stimuli, improving cell viability and increased mAb expression by up to five folds (Cost et al. 2010).

2.4.2 mAb folding and secretion

mAb folding is a intricate process which is mediated by a series of chaperones and foldases (Feige et al. 2010; Braakman and Bulleid 2011) and is a possible bottleneck for mammalian cells producing high levels of the recombinant mAb (Dinnis and James 2005). Over-expression of protein disulfide isomerase (PDI), a foldase which catalyzes formation of disulfide bond, only saw moderate increases in mAb expression of CHO cells (Borth et al. 2005; Mohan et al. 2007) or no effect (Hayes et al. 2010). BiP, a protein in the folding pathway which helps retain incompletely folded proteins by binding to exposed hydrophobic regions, caused a drop in mAb expression when over-expressed either alone or in tandem with PDI (Borth et al. 2005). The unfolded protein response (UPR) is a cellular reaction to increased demand of the cells folding capacity by regulating the expression of a number of chaperones and foldases (Schröder and Kaufman 2005). XBP-1 plays a major role in the UPR but its over-expression generated no effects on mAb expressing CHO cells (Ku et al. 2008). The limited success of these attempts shows that engineering of the mAb folding pathway alone is likely not the

ideal approach to improve mAb expression level. Cell engineering studies of chaperones have mainly focused on the expression level and it is still unclear how it could affect product qualities like aggregation.

2.4.3 Glycosylation

mAb glycosylation is important for the product's pharmacokinetics, pharmacodistribution, stability, receptor binding and effector functions (Werner et al. 2007). Despite its importance, there is no consensus for the "correct" mAb glycosylation due to inherent heterogeneity of the process and differences in activity (Higgins 2010). It is still of great interest to both research and industry to generate mAbs with specific glycoforms to improve efficacy and safety. Although mAb glycosylation can vary through control of culture conditions (Wong et al. 2005; Butler 2006), genetic approaches can be more efficient (Omasa et al. 2010). Many mAbs function through eliciting antibody dependent cell cytotoxicity (ADCC) and significant improvements were seen in ADCC activity for fucose deficient IgG1 mAbs (Shields et al. 2002). Knockout of the α-1,6 fucosyltransferase (FUT8) gene has been achieved by homologous recombination (Yamane-Ohnuki et al. 2004) and ZFN deletion (Malphettes et al. 2010). Afucosylated Rituxan® exhibited 100-fold improvements in ADCC activity (Yamane-Ohnuki et al. 2004). It has also been demonstrated that normal mAb producing cells can generate afucosylated product through siRNA knockdown of FUT8 and GDP mannose 4,6-dehydratase (GMD) (Imai-Nishiya et al. 2007). Fucose modification is currently the most successful method to improve mAb efficacy and the first glyco-modified afucosylated mAb produced from engineered CHO cells was recently approved in Japan in March 2012 (Beck and Reichert 2012). This

approval will pave the way for more glycosylation optimized biobetters produced from modified CHO cells.

2.4.4 MicroRNA

Engineering of singular targets in complex mammalian pathways have yielded limited or mixed results (Dietmair et al. 2011). MicroRNAs (miRNA) are non-coding double-stranded RNA molecules able to globally modify gene expression levels to affect entire pathways (Müller et al. 2008). Use of miRNA in CHO cells is a recent cell engineering technique first reported in 2007 (Gammell et al. 2007). The number of identified CHO miRNAs has increased exponentially since that report (Hackl et al. 2011; Johnson et al. 2011; Hammond et al. 2012). Although more studies still need to be done using mAb producing cell lines to verify the usefulness of miRNAs, existing reports are promising. Over-expression of cgr-miR-7 produced effects similar to temperature-shifting with arrested growth and increased specific productivity (Barron et al. 2011) and miRNAs in the cgr-miR-17-92 cluster was beneficial to cell growth (Jadhav et al. 2012).

Despite all the promise of cell engineering, none of the cell lines reported with improved growth or productivity have been used in industrial mAb production. Approval of glyco-modified mAb from an engineered CHO cell line and with over 10 others under testing, we would likely see an increase in such products in future (Beck and Reichert 2012). Increased knowledge of CHO genome (Omasa et al. 2009; Hammond et al. 2011; Xu et al. 2011), transcriptome (Becker et al. 2011; Hackl et al. 2011) and proteome (Baycin-Hizal et al. 2012) would allow better understanding of the complex interactions taking place for better cell engineering approaches. Construction

of dynamic computational models have worked well in production microbial cells and this extra information would eventually allow similar implementations in mammalian cells (Dietmair et al. 2011; Dietmair et al. 2012; Nolan and Lee 2012).

2.4.5 Targeted gene modification using programmable nucleases

Targeted and controlled gene modification is desirable for both cell line generation and cell engineering of CHO cells. Transfected plasmids can be targeted into sites which are active and resistant to epigenetic silencing to obtain high and sustained mAb expression (Zhou et al. 2010). Specific gene knockouts can also be carried out at higher efficiency compared to traditional homologous recombination techniques to generate novel CHO cell variants (Yamane-Ohnuki et al. 2004; Fan et al. 2012).

Programmable nucleases can be used to cleave the target cell's chromosome at pre-determined, specific sites to engage the endogenous DNA repair system for modification. Available programmable nucleases include zinc-finger nucleases (ZFNs), transcription activator-like effector nucleases (TALENs) and the recently reported RNA-guided engineered nucleases based on the clustered regularly interspaced short palindromic repeat (CRISPR)-CRISPR associated (Cas) bacterial adaptive immune system (Kim and Kim 2014). The nucleases produce double-strand breaks (DSB) which can enhance homologous recombination efficiency for gene insertion from an exogenous template by more than two orders of magnitude (Rouet et al. 1994). DSBs can also activate a non-homologous end joining (NHEJ) repair mechanism which often produces small insertions or deletions (indel) to alter the original genetic sequence.

Zinc finger proteins are eukaryotic DNA binding proteins of ~30 amino acids with conserved Cys_2-His_2 residues coordinating a zinc atom and each finger is able to recognize and bind three specific base pairs. Activity of the fingers are modular and can be linked together to recognize specific sequences. At least three fingers are needed for sufficient binding specificity and affinity (Fig. 2.7A) (Gersbach et al. 2014). A *FokI* cleavage domain is fused to the zinc finger chain to generate the sequence specific ZFN to generate DSBs (Bibikova et al. 2002). TALE proteins are 33-35 amino acid domains originating from the plant-pathogenic bacteria *Xanthomonas* which recognize singular DNA base pairs. Binding specificity is determined by repeat-variable-diresidues (RVD) at the 12^{th} and 13^{th} position. Similar to zinc finger proteins, TALE proteins are highly modular and can linked together to recognize specific DNA sequences in the chromosome. Fusing of a FokI domain similar produces TALENs for targeted DSBs (Fig. 2.7B). TALENs generally exhibit higher specificity compared to ZFNs due to their one domain-one base pair system. Greater optimization and engineering is required to reduce off-targets for ZFNs. One advantage ZFN has is the smaller size of the coding sequence required, ~1 kbp less than that required for TALEN.

CRISPR-Cas RNA guided systems are the adaptive immune system of bacteria to provide protection from foreign DNA and the newest tools for targeted modification. The system requires two main components, the Cas9 enzyme and a guide RNA (gRNA) (Fig. 2.7C). Major advantages of the CRISPR-Cas system compared to ZFN and TALEN include: the Cas9 nuclease is the same regardless of target and no protein engineering is

required; ease of designing and producing the gRNAs; possible to have multiple targets by simply using a mixture of gRNAs (Carroll 2014).

To date, there are only reports of ZFN being used to generate novel CHO cell hosts. The first report involved use of ZFN to knockout the FUT8 gene to generate novel CHO lines which produce defucosylated antibodies as mentioned in section 2.4.3 (Malphettes et al. 2010). Another group generated GS knock-out CHO cell lines for better selection efficiency (Fan et al. 2012). The CRISPR-Cas system development for CHO cell biotechnology is currently being carried out by Sigma-Aldrich as they hold the propriety rights to use of the system for CHO (personal communication). Issues with intellectual property for the more recent TALEN and CRISPR-Cas system could explain why their use is still not widespread in the industry.

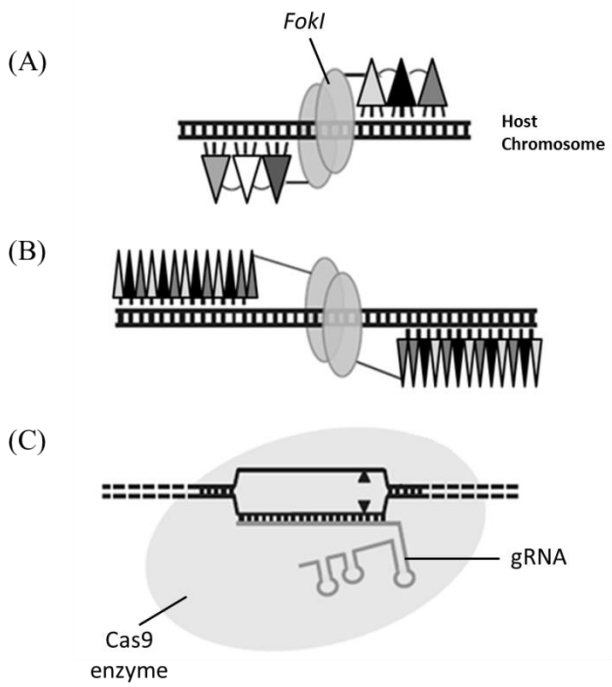

Figure 2.3 Programmable nucleases for targeted genome editing. (A) Zinc-finger nuclease, (B) transcription activator-like effector nucleases. The triangles in (A) and (B) represent the binding domains of ZFN and TALEN. Each different shading indicates different specificity.

2.5 Vector design

2.5.1 Co-expression of LC and HC genes

Complex interactions occur between LC and HC during folding and assembly of an IgG mAb. The LC: HC peptide ratio plays an important role in the kinetics of mAb formation (Gonzalez et al. 2002). Excess LC has been suggested to be beneficial for higher mAb expression levels (Gonzalez et al. 2002; Schlatter et al. 2005; Yang et al. 2009). There was also a study which correlated mAb expression to the amount of available HC, suggesting that HC is the limiting reagent and higher HC expression is beneficial (Dorai et al. 2006; Jiang et al. 2006; Fallot et al. 2009). It is also still unclear if equimolar amounts of LC and HC is optimal (Jostock et al. 2010). There is a report that at LC:HC mRNA ratios above 1.5 results in minimal product aggregation levels (Lee et al. 2009). As LC: HC ratio could affect mAb assembly, it has been suggested that mAb glycosylation could vary with ratio as well (Schlatter et al. 2005). It is of interest to express these mAb subunits at optimal stoichiometric ratios for better mAb production. LC and HC genes are traditionally introduced by co-transfecting on two separate vectors (Kim et al. 2001; Chusainow et al. 2009) or transfecting a single larger vector carrying all the required genes (Bebbington et al. 1992; Jun et al. 2005). LC and HC peptide ratios can be varied under transient conditions when co-transfecting the genes on separate vectors by changing the relative amounts of each plasmid (Fig. 2.3A) (Lee et al. 1999; Schlatter et al. 2005). Controlling ratio by this method in stable transfections is inefficient as in the random integration process, gene copies and the site of integrated cannot be controlled (Trill et al. 1995; Fussenegger et al. 1999; Mielke et al. 2000). Single vectors

should provide better control of the ratio as all genes are integrated in the same site (Fig. 2.3B). One possible issue that could arise with having multiple promoters in close proximity is the resulting transcriptional interference (Eszterhas et al. 2002). This interference suppresses gene expression to different degrees depending on the site of integration. Suppression of a downstream gene in a tandem pair of expression cassettes was suspected to be due to obstruction of the downstream promoter region by the polymerase II complex coming from the upstream gene. Formation of the promoter complex on the first promoter might also inhibit formation of a second promoter complex in close proximity.

(A)

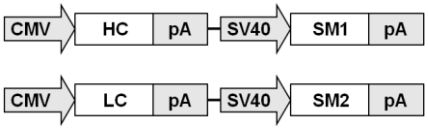

(B)

(C)

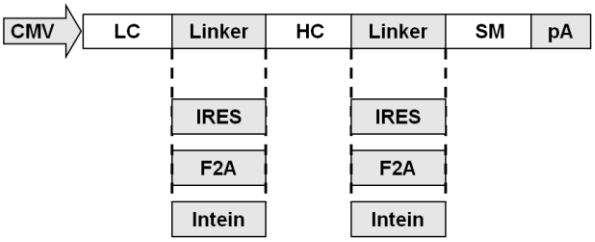

Figure 2.4 Different vector designs for expression of light chain (LC) and heavy chain (HC) for mAb production. (A) Co-transfection on two separate vectors. (B) Single vector with separate expression cassettes for each gene. (C) Single vector, single promoter vector with genes linked together on one expression unit. The linker element used can be an internal ribosome entry site (IRES)element, a furin-2A peptide (F2A) sequence or intein sequences. CMV: human cytomegalovirus immediate-early gene promoter, SV40: simian virus

40 promoter, LC: Light chain gene, HC: Heavy chain gene, SM: Selection marker, pA: Polyadenylation signal.

Single promoter, single vector systems for expressing LC and HC have the stricter control on LC: HC ratio (Fig. 2.3C). Typical eukaryotic mRNA translation is dependent upon 5'-cap mediated ribosome binding, following by scanning to identify the AUG start codon for initiation (Kozak 1989). An internal ribosome entry site (IRES) element when placed between two genes mediates cap-independent translation initiation of the second gene (Pelletier and Sonenberg 1988). IRES elements from the Encephalomyocarditis (EMCV) virus are known to be strong initiators and among the most commonly used (Borman et al. 1997). IRESes form complex secondary structures for the recruitment of eukaryotic initiation factors (eIF). Binding of the eIF4G protein helps recruit other initiation factors for interaction with the ribosome (Martinez-Salas 1999). The cap-independent translation of the second gene is less efficient than a typical cap-dependent translation, resulting in peptide levels ranging from 3- to 100-fold lower for the second gene (Hennecke et al. 2001) (Fig. 2.5). The difference varied based on the IRES, genes expressed and cells used. It is possible to use IRES elements to express LC, HC and selection marker genes on one transcript (Mielke et al. 2000). There only report available for mAb expression using IRES was using a mAb fusion protein and the final titers obtained was not clearly stated. CHO cells were also not used in the study (Mielke et al. 2000). No comparison with the co-transfection and single vector multi-promoter system was done to verify the benefits of using IRES.

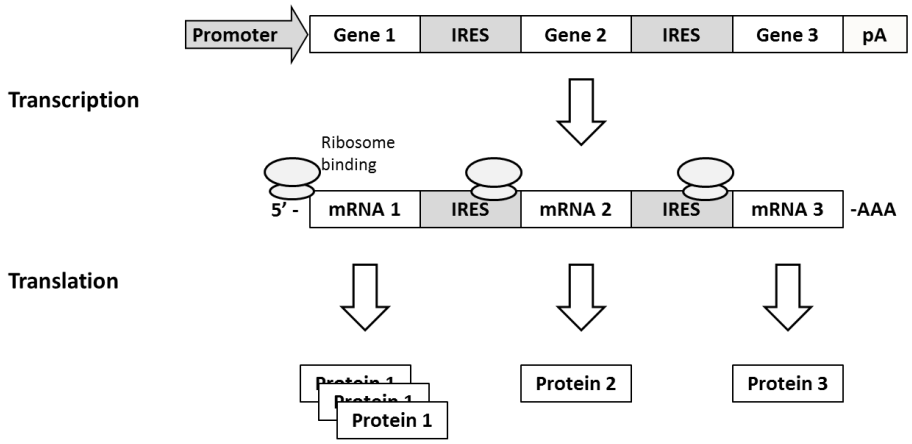

Figure 2.5 Internal ribosome binding on IRES for gene translation. Gene 1 is downstream of a promoter while genes 2 and 3 downstream of IRES elements. The three genes are transcribed together into a single long strand of mRNA with 5' cap protein and a polyA tail. mRNA1 is translated in a normal cap-dependent manner while mRNA2 and 3 are translated by ribosomes binding to the middle of the transcript on IRES. As IRES driven translation is less efficient, mRNA2 and 3 are translated into lower amounts of proteins 2 and 3 relative to protein 1.

The multiple genes required can be expressed at equal amounts in a single open reading frame by using either the foot and mouth virus derived 2A self-processing sequence combined with a furin cleavage site (F2A) (Fang et al. 2007; Jostock et al. 2010) and inteins (Kunes et al. 2009). 2A elements are only about 60 to 80 base pairs long, making it easy to incorporate them into vector designs. The 2A linked genes are expressed in one open reading frame and self-processing occurs to generate the two separate peptides (Ryan and Drew 1994; Donnelly et al. 2001; de Felipe et al. 2006; Jostock et al. 2010). Furin cleavage sequences are added to remove amino acids residue at the C-terminus of the protein upstream of 2A, while the terminal lysine is removed by carboxypeptidases (Fig. 2.5) (Fang et al. 2005; Jostock et al. 2010). Productivity of clones from a F2A based vector was comparable with clones generated using a reference vector using separate expression unit design

(Jostock et al. 2010). Interestingly, Davies et al. recently reported that LC was still detected in excess for higher producing clones generated using the F2A system due to increased HC degradation (Davies et al. 2011). One drawback of the F2A system is in the possible formation of unwanted residues or fusion proteins (De Felipe et al. 2010; Chan et al. 2011). Careful evaluation of each vector design is thus required before F2A can be used for production of mAb biologics.

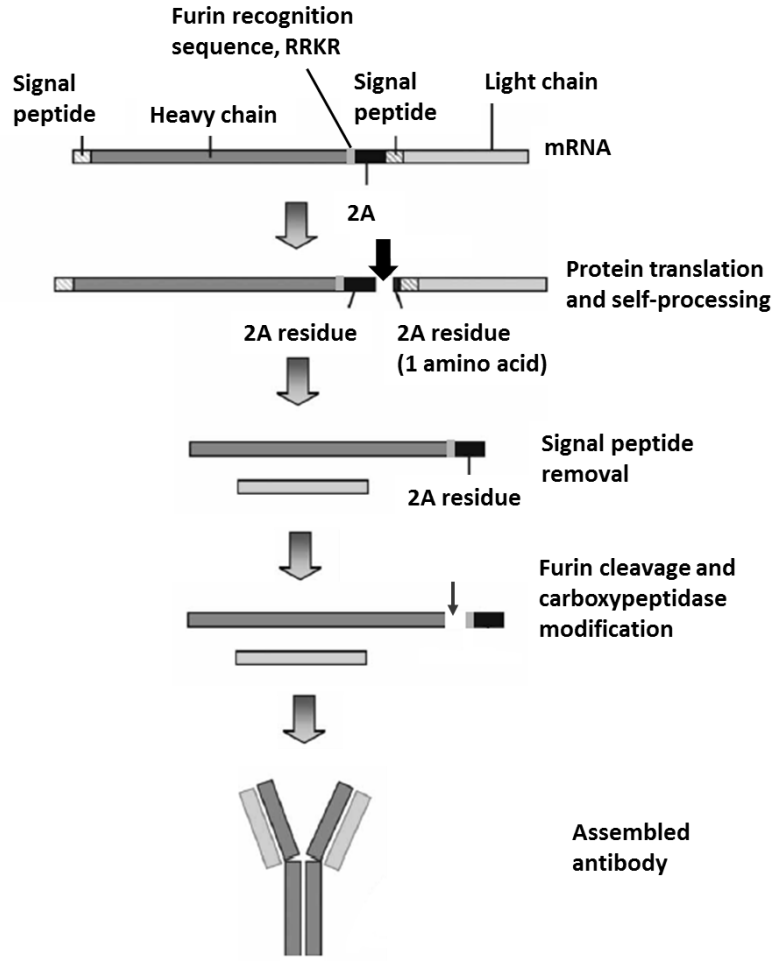

Figure 2.6 Using F2A for antibody expression. HC and LC are transcribed together onto one mRNA. During translation, a "ribosomal skip" occurs at the site indicated by the black arrow. 2A peptide residues are removed with the signal peptide or by furin endoprotease cleavage. HC and LC are then assembled into antibodies **(**Adapted from Fang et al., 2005).

2.5.2 Selection strategies

In order to efficiently select for stably transfected cells, selection marker genes which confer resistance to certain antibiotics or growth advantage in a nutrient deficient condition are used. Antibiotics commonly used for selection include geneticin (also known as G418), hygromycin and puromycin and can act by disrupting protein synthesis in the cell. The cells are transfected with neomycin phosphotransferase, hygromycin phosphotransferase or puromycin acetyltransferase genes to gain resistance to the respective antibiotics. Benefits of antibiotics selection include the ease of use and no requirements for modified cell lines. One major drawback is that gene amplification cannot be done to increase expression levels.

The dihydrofolate reductase (DHFR) is an amplifiable selection marker typically used together with the DHFR deficient DG44 or DXB11 CHO cells (Urlaub and Chasin 1980; Urlaub et al. 1983; Kaufman et al. 1985; Cacciatore et al. 2010). DHFR knockout CHO-K1 mutants have also been generated using ZFN to overcome deficiencies like poor growth and inefficient selection of current DG44 and DUXB11 cell lines (Sigma-Aldrich 2011). DHFR is involved in the reduction of dihydrofolate to tetrahydrofolate, which is in turn needed for nucleic acid metabolism. First selection is done in media devoid of hypoxanthine and thymidine. Amplification can be further carried out by adding a folic acid analog, methotrexate (MTX), which inhibits DHFR activity. In order to survive, cells will start to amplify the DHFR gene copy. The mAb genes located on the same transfected vector or in nearby sites are amplified as well, increasing the gene copies and thus expression levels after

several stepwise increases in MTX levels (Kim et al. 1998; Kim et al. 2001; Jun et al. 2005; Chusainow et al. 2009).

Glutamine synthetase (GS) selection marker catalyzes formation of glutamine from glutamate and ammonia (Bebbington et al. 1992; Brown et al. 1992). This allows successfully transfected cells to survive in media lacking in glutamine. The GS selection system works well in NS0 cells which do not express their own GS. Using this system with mammalian cells with endogenous levels of GS requires using methionine sulphoximine (MSX), a GS inhibitor (Brown et al. 1992). Similar to using MTX with DHFR, using MSX with GS forces cells to co-amplify the GS gene and the product gene (Cockett et al. 1990). One advantage of using the GS system is typically only one round of amplification to obtain high expression levels (Bebbington et al. 1992; Brown et al. 1992). There are concerns of instability when using the GS/MSX amplification in CHO K1 cell lines (Jun et al. 2006). Effectiveness of the GS system in CHO cells was greatly improved when using the GS-knockout CHO cell lines. Usage of this mutant new cell line helped improve clone selection efficiency by six folds as compared to using regular CHO cell lines (Fan et al. 2012).

Two novel selection methods have been reported recently that could be useful with more optimization. An amplifiable selection marker based on hypoxanthine phosphoribosyltransferase (HPRT), which is required for purine synthesis, is currently under development (Costa et al. 2012). A toxin/anti-toxin method commonly used by bacterial cells to maintain plasmid stability has also been tested in mammalian cells (Nehlsen et al. 2010).

Vector integration is a random event with no control over whether integration is into an active or inactive site and incomplete vectors can get integrated resulting in non-expressing clones surviving selection. An active integration site leads to higher mAb expression levels. Enhancing selection stringency by reducing expression or activity of the selection marker can be used to identify integration into active sites. One way is using a weak promoter, such as one from SV40, to drive expression of the selection marker gene (Birch and Racher 2006). Various forms of selection marker sequence manipulation or mutations can be carried out in tandem to further improve stringency. Using a non-traditional AUG start codon results in inefficient translation initiation and can further reduce expression (van Blokland et al. 2007; Hoeksema et al. 2011). Deoptimizing codon usage of the wild-type (WT) DHFR sequence to reduce translation efficiency improved IgG expression level by three-fold (Westwood et al. 2010). Reducing enzymatic activity of a neomycin phosphotransferase (NPT) through amino acid mutations resulted in 15-fold improvement of expression level as compared to a WT-NPT (Yenofsky et al. 1990; Sautter and Enenkel 2005). Protein and mRNA destabilizing elements can be used reduce selection marker expression without modifying the sequence (Ng et al. 2007). This method could likely be applied with greater ease as no sequence modification is required.

When the selection marker gene is in an individual expression cassette, vector fragmentation can result in only the selection marker cassette being integrated intact (Barnes et al. 2007; Chusainow et al. 2009; Ng et al. 2010). Such clones would survive selection without expressing any mAb. Coupling of the selection marker to the product genes using IRES is a method to

minimize the number of these non-expressing clones (Gurtu et al. 1996; Rees et al. 1996; Hobbs et al. 1998). Fragmented IRES-based vectors would have incomplete expression units and no transcription occurs. The reduced translation efficiency of IRES compared to typical cap-dependent expression also helps improve stringency. Increased stringency can be achieved by modifying the principal translation start site on IRES and further attenuate the translation (Rees et al. 1996). Stringency of selection can be further improved by combining the two methods, such as using attenuated IRES with activity impaired NPT (Chen et al. 2004).

2.5.3 Signal peptide and codon optimization

Each IgG mAb molecule requires the expression two identical light chains (LC) and two identical heavy chains (HC) which are linked by disulfide bonds. Efficient expression of the genes requires an appropriate signal peptide for transport of the transcript to the endoplasmic reticulum (ER) for translation. Signal peptide derived from human albumin more than doubled the average specific productivity of a stable mAb producing CHO cell mini pools to almost 40 pg $cell^{-1}$ day^{-1} as compared to using a native IgG LC signal peptide (Kober et al. 2013). A signal peptide toolbox has also been generated to identify tailored signal peptides for each protein (Stern et al. 2011).

Codon optimization for gene expression is important due to differences in transfer RNA abundance in different cells and effects on the mRNA stability and secondary structures formed by the transcripts (Kim et al. 1997; Hung et al. 2010; Angov 2011). Early attempts at codon optimization for gene expression improved GFP expression in CHO cells by 42-fold using the empirical method of DNA shuffling (Crameri et al. 1996). More rational

approaches are now available with increased understanding of mammalian cells and a system known as codon adaptive indices (CAI) is used to score how optimized a gene is (Angov 2011). A comprehensive assessment of codon usage was performed in a recent proteomic analysis of CHO cells and preference for certain codons was observed to be especially prevalent for proline, threonine, aspartate and cysteine (Baycin-Hizal et al. 2012). Applying optimization based on codon usage in CHO and human cells have seen improvements in mAb expression by 1.5 to 4 folds (Kalwy et al. 2006; Hung et al. 2010). Combination of codon optimization and an optimized gene amplification protocol provides a way to get high yielding mAb producers with decreased efforts (Kotsopoulou et al. 2010). An interesting application of codon usage is to use it for generating mutant endogenous genes with "silent mutations" for use in RNAi rescue experiments (Fath et al. 2011). In another study which considered of both individual codon usage for each amino acid and additionally the surrounding codon context revealed that the commonly used design criteria of codon usage was less important than the codon context (Chung et al. 2013). Human interferon-gamma expression increased 13-fold with context optimization but only 10-fold with codon usage optimization. Another interesting observation made was that optimization based on the highly expressed genes was less effective for CHO as compared to microbial hosts.

2.5.4 Chromatin modifying DNA elements

Epigenetic status of the integration site can be altered by the DNA elements surrounding the site. Some of these elements have been isolated and

been tested in vector systems used for cell line generation and shown to improve expression level and stability.

The ubiquitous chromatin opening element (UCOE) is a un-methylated CpG fragment isolated from a region around house-keeping genes that keep the region in a transcriptionally active and open configuration (Benton et al. 2002; Nair et al. 2011). UCOE from both human and mouse sources have been identified. The element is placed upstream of the promoter on the vector. Using UCOE increase the number of clones with higher expression levels (Benton et al. 2002). Recombinant protein expression is also maintained for long periods as DNA silencing due to methylation is prevented (Nair et al. 2011). The element is promoter specific and some optimization of UCOE-promoter combinations is required (Nair et al. 2011).

Matrix attachment regions (MAR) create active chromatin loops within the chromosome and can regulate the epigenetic switching of the integration site to being transcriptionally active (Girod et al. 2005; Galbete et al. 2009; Harraghy et al. 2011). Transfecting it together with the plasmid vector helps maintain the integration site in an active configuration for a more homogeneous population with high and sustained product expression. Expression becomes gene copy number dependent instead of site dependent. mAb expression was most improved by either inserting one element upstream of the promoter and co-transfecting another MAR only plasmid or at both 5' and 3' ends of the expression cassette (Girod et al. 2005; Wang et al. 2010). MAR from chicken lysozyme, human genome and mouse genome have been identified and evaluated to have positive effects in CHO cells (Girod et al.

2005; Girod et al. 2007; Harraghy et al. 2011). Due to reported tissue specific effects, the MAR should be tested with the cell line to be used.

UCOE and MAR elements have been successfully used in gene expression platform technologies from Millipore and Selexis respectively. Other DNA elements which could also prove to be useful with more evaluation include the expression augmenting sequence elements (EASE) (Aldrich et al. 2003) and the stabilizing and anti-repressor (STAR) elements (Kwaks et al. 2003; Otte et al. 2007).

2.6 Clone selection

Random integration and amplification creates highly heterogeneous pools, making the selection of high mAb producing clones an extremely time-consuming and tedious process. Most estimates place the number of clones required to be picked to ensure sufficient high producers can be isolated to range between several hundred to up to thousands (Birch and Racher 2006; Pichler et al. 2010). Subsequent evaluation of long-term expression stability and product quality identify the few rare clones that satisfy requirements of production cell lines. Recent developments in methods for selecting high producing clones have also seen a heavier reliance on use of automation to save on labor and improve process consistency (Eisenstein 2006).

Flow cytometry applied to fluorescent activated cell sorting (FACS) is one method of high-throughput selecting for high mAb producers (Kumar and Borth 2012). Millions of cells can be screened rapidly and specific subpopulations isolated from the highly heterogeneous pools. FACS can be applied to sorting of surface labeled mAb producing cell lines. The level of

secreted proteins is proportional to the protein found on the cell surface. After three rounds of reiterative sorting, a 100-fold enrichment of a MTX amplified CHO cell line was observed with specific mAb productivity reaching 42 pcd (Brezinsky et al. 2003). The cells can be chilled to below room temperature to slow down the protein release from the membrane and endocytosis of the product-label complex to maximize the signal intensity (Pichler et al. 2009). Another way to use surface labeling for sorting is to co-express a surface protein not found in CHO cells, such as CD20 (DeMaria et al. 2007). This allows surface labeling for cell sorting without worry of signal loss. Surface labeling can also be done using a capture matrix composed of biotin, avidin and an antibody targeting the product. The matrix will cover the cell surface to trap the secreted mAb. The captured mAb can be detected using another biotinylated secondary antibody for FACS sorting (Böhm et al. 2004).

Linking the product gene to a fluorescent reporter by IRES is another way to allow use of FACS for sorting. Cells sorted for high fluorescent levels will be co-expressing high levels of the product gene (Freimark et al. 2010). High mAb producing cells can be sorted by dual fluorescent activated sorting where green fluorescent protein (GFP) and yellow fluorescent protein (YFP) are linked to HC and LC expression respectively (Sleiman et al. 2008). Another alternative is to use two GFP fragments which reassemble to allow FACS of high producers (Kim et al. 2012).

Automated colony pickers are becoming an indispensable part of many cell line generation platforms. Clonepix from Genetix (Serpieri et al. 2010; Dharshanan et al. 2011) and CellCelector from Aviso (Cairns et al. 2011) are two systems that have been used for selecting recombinant protein producing

colonies. Cells expressing mAb are plated in semi-solid media containing a fluorescent detection antibody against the mAb product. The viscous medium slows down dispersion of the secreted mAb, keeping it around the colony. This allows the detection antibody to label the product. Imaging software is used to identify colonies with high productivities that fluoresce with a bright halo and are sufficiently isolated from low-expressing or non-expressing cells for picking.

Production stability is a parameter as critical as productivity in mAb cell line development. Long-term stability required of a production clone was estimated to be around 60 generation to ensure sufficient time for expansion (Brown et al. 1992). Studies have shown that intraclonal expression can be stochastic in nature, giving rise to heterogeneous clonal populations (Pilbrough et al. 2009). Identification of homogeneous clonal populations would identify those with expression at a steady state and more likely to be stable (Pilbrough et al. 2009). Screening can be performed by using flow cytometry to check population distribution (DeMaria et al. 2007). Automated colony pickers can also be used by re-plating a clonally derived population back in the semi-solid media. Stable cell lines would have all subcolonies expressing mAb and the presence non-expressing colonies would hint of unstable production. Methylation status of the promoter and gene copy number can also be used as early markers to identify unstable cell lines (Osterlehner et al. 2011). Other studies have also shown unstable cell lines to be more prone to apoptosis and relevant apoptosis related markers like caspase 3, Annexin V (Dorai et al. 2012) and GADD153 (Bailey et al. 2012) could also be used for early stage screening.

Development of high throughput analytical methods and frameworks would help alleviate some existing bottlenecks in the characterization process (Konstantinidis et al. 2013). Early prediction of production level and product aggregation can be performed by screening LC:HC mRNA of clones and selecting those with ratios above 1.5 (Lee et al. 2009). ER stress related protein, GRP78, was recently shown to be an indicator of high producing cell lines and could be used as a marker to identify clones with high productivity (Kober et al. 2012) . Miniaturized bioreactor systems like ambr^{TM} are also being used to mimic bioreactor conditions for medium throughput characterization of clone performance under production conditions (Tap Biosystems 2014). By using a combination of novel automated systems and recently identified early predictors for desirable cell phenotypes, significant effort can be conserved during clone selection process. Widespread use of automation is still inhibitive for many smaller labs due to the high costs and large footprint of such machines. One way to alleviate the labor and cost incurred is to use better designed vectors to reduce non-expressing clones and improve the clonal consistency.

2.7 Product Quality

According to guidelines agreed upon by International Harmonization Conference (ICH), characterization of each biologics can include the physiochemical properties, biological activity, immunochemical properties and purity (ICH 1999). The product has to be sufficiently characterized to have established specifications during preclinical and clinical studies. These

specifications help ensure product consistency and safety. Some product parameters would be discussed in this section.

2.7.1 Aggregation

All proteins display the propensity to aggregate. Aggregates can be classified by covalent/non-covalent bonds, reversible/non-reversible, size and conformation (Mahler et al. 2009). The presence of aggregates in protein therapeutics can result in immunogenic reactions, complications during product administration and impair product quality and efficacy (Cromwell et al. 2006). Product aggregation can result during the various steps of the mAb manufacturing process, starting from the cell line generation to the scale up culture process followed by purification, formulation up to storage (Mahler et al. 2009; Joubert et al. 2011). The most commonly used protein-A affinity chromatography for mAb purification does not discriminate between monomers and aggregates as long as the Fc region is intact (Phillips et al. 2001). The presence of aggregates after filtration and centrifugation complicates the purification steps, requiring several other polishing steps like size exclusion chromatography (Phillips et al. 2001; Yoo and Ghosh 2012).

It is beneficial to minimize aggregation from the early steps of production during clone selection and culturing. In order to maximize yields, high amounts of recombinant mAb peptides are expressed. This could lead to intracellular aggregation due to the high amount of unfolded proteins or inefficiencies of the molecular chaperones at controlling proper protein folding (Zhang et al. 2004). This has been demonstrated in CHO cells where overexpression of a simple ATIII glycoprotein beyond a certain level triggered aggregation and lowered yield (Schröder et al. 2002). As mentioned in the

earlier section of co-expressing both LC and HC peptides, one study managed to successfully identify clones with high aggregation by screening for a threshold of LC:HC mRNA of 1.5 (Lee et al. 2009). Cell engineering of molecular chaperones have mostly been performed to improve cell productivity and reports of cell engineering to improve product aggregation are still lacking (Gomez et al. 2012).

2.7.2 Glycosylation

N-linked glycosylation takes place on the asparagine of an Asn-X-Thr/Ser consensus sequence where X can be any amino acid but proline. On a typical IgG, the oligosaccharides are attached to Asn297 on the C_H2 domain on the HC peptide (Fig. 2.1). Glycosylation is a multi-step process which begins with transfer of a high-mannose oligosaccharide (Glc3Man9GlcNac2) from a dolichol phosphate lipid carrier to the nascent HC peptide in the endoplasmic reticulum (ER). This is followed by further trimming and residue addition by a series of enzymes in the ER and golgi to form the final glycan complex (Werner et al. 2007). N-glycosylation takes place co-translationally with the peptide assembly (Sakaguchi 1997). The extent of glycan modification is influenced by the protein conformation and how various enzymes can access the glycan (Krambeck and Betenbaugh 2005; Butler 2006). Due to the complexity and number of steps involved, the secreted mAbs typically ends up with a heterogeneous population of glycan structures, such as absence of sialic acid, galactose or fucose residues (Werner et al. 2007). Structures of the main IgG glycans are shown in figure 2.8.

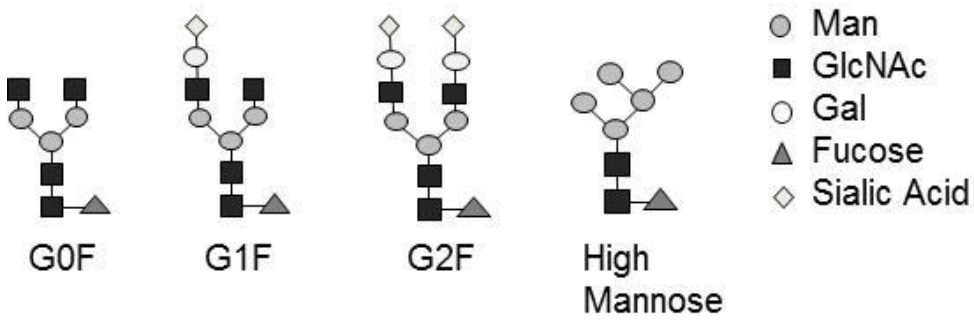

Figure 2.7 Major N-linked glycans found on human IgG produced in CHO cells. Note that the glycans can also exist as afucosylated and asialylated forms. G0F would be G0, G1F be G1 and G2F be G2.

N-linked glycosylation is linked to the therapeutic mAb efficacy and clearance. Fucosylation is a critical glycan modification for IgGs which function by ADCC. A Lec13 CHO mutant cell line with deficient fucose addition machinery produced afucosylated IgGs with up to 50-fold improved binding affinity to human FcγRIIIa receptor (Shields et al. 2002). This improved binding enhanced ADCC related action for Trastuzumab (Suzuki et al. 2007). C-type lectin mannose receptors expressed on the surface of macrophages and dentritic cells are able to recognize certain mannose and N-acetylglucosamine (GlcNac) residues (Walsh and Jefferis 2006). G0 and high mannose glycans would be more easily recognized by these receptors. The IgGs with these glycans would be cleared faster from the patient's system by macrophages after administration (Jefferis 2009; Goetze et al. 2011). There could also possibly be increased potentiation of immunogenicity due to greater recognition by dendritic cells (Jefferis 2009). Sialylated IgGs typically make up a small proportion of the mAb produced. Studies have shown that in a mouse model, IgGs bearing sialylated residues were shown to exhibit anti-inflammatory properties (Kaneko et al. 2006). Terminal galactosylation has

been reported to affect CDC related effector functions of antibodies by up to 2-fold (Raju and Jordan 2012). Studies which developed a cell line expressing GNTIII to increase the presence of a bisecting GlcNac, observed a 15-20 fold increase in ADCC activity (Jefferis 2009). As glycosylation plays such an important role in defining activity of the product, proper characterization of the glycol-profile and adherence to this profile is of the utmost importance.

2.7.3 Other product quality attributes

Other physiochemical properties of the product that are of concern include the mAb structure, the amino acid sequence and related modifications, free sulfhydryl groups and disulfide bridges (European Medicines Agency 2008). The structure and amino acid sequences would be determine the class of antibody and also be used to identify sequence variants that could arise during the culture or manufacturing process. Fragmentation of the product has the potential to cause loss of stability and efficacy and immunogenic responses due to the novel epitopes (Page et al. 1995; Eon-Duval et al. 2012). Modifications of the C-terminal due to lysine residues are unlikely to influence activity and potency of the mAb product (Khawli et al. 2010). Free sulfhydryl groups and unwanted disulfide bonding would affect protein folding and interactions, resulting in changes to the structure and its activity and immunogenic properties (Eon-Duval et al. 2012).

While general guidelines have been laid down for approval of mAb therapeutics, it is still mainly up to the manufacturers to validate that the specifications provided are sufficient to prove their product's safety and efficacy through toxicology and pharmacology tests. Biosimilars would be required to adhere to the specifications of the existing product in order to

obtain approval without extensive preclinical and clinical studies. Having a system and process which is able to generate product of consistent quality is thus of utmost importance.

2.8 Future perspectives

The expanding use of mAb therapeutics and development of the biosimilar market demands a parallel improvement of the production process. Initial issues of low production levels have been addressed with the past decade of research and development. Titers have increased from milligrams per liter to easily reach grams per liter in fed-batch cultures (Wurm 2004; Birch and Racher 2006). These improvements in cell line generation have been achieved through innovations in cell line engineering, vector design and optimization, high-throughput automated clone selection devices, media design and process development (Agrawal and Bal 2012). Instead of looking for ways to reduce cost of goods through increasing titers, there is now a shift towards shortening of development timelines, improving product quality and expression stability (Kelley 2009).

Technology advancement of the analytical tools like chromatography and mass spectrometry available has seen a greater emphasis being placed on implementation of process analytical tools (PAT) for analysis of products and control of processes. Critical process parameters (CPP) can be tracked to identify critical quality attributes (CQA) to enhance the consistency and safety of mAb products (Rathore and Winkle 2009). Recent innovations in areas of genomics, transcriptomics, proteomics and metabolomics enable the detailed study of cellular processes. With the added knowledge, cell line development

processes would move away from the empirical and towards more rational design, allowing quality by design (QbD) concepts to be applied with greater accuracy and effectiveness (Dietmair et al. 2012). Techniques like cell and vector engineering and high-throughput automation will also see further technological advancements.

Along with new mAb therapeutics, the rise of follow-ons for existing blockbusters with expiring patents will increase over the next few years (Nowicki 2007). The need to have robust platforms for biosimilar production is critical due to the number of competitors and importance of maintaining similar product quality as the original innovator drugs (Hou et al. 2011). Product characterization would need to be carried out with extra care as it is hard to compare quality and purity of biotherapeutics unlike chemical generics (Ahmed et al. 2012). Companies would rely more and more on smaller scale disposable bioreactors to allow them to adopt flexible production lines to a wider array of products (Kelley 2009). The approval of the first glyco-engineered mAb would also pave the way for biobetters of existing products and more novel products (Beck and Reichert 2012).

Chapter 3: Developing a IRES-mediated tricistronic vector for generating high mAb expressing CHO cell lines

In this chapter, we describe a vector utilizing internal ribosome entry site (IRES) elements to link the light chain (LC), heavy chain (HC) and an antibiotic selection marker on a single transcript. The vector is evaluated against commonly used vector designs to identify the benefits of using a single transcript for all genes and further optimized for high mAb titers.

*The following results were first published in "**Ho, S. C. L.**, Bardor, M., Feng, H., Mariati, Tong, Y. W., Song, Z., Yap, M. G. S. and Yang, Y. (2012). "IRES-mediated Tricistronic vectors for enhancing generation of high monoclonal antibody expressing CHO cell lines." Journal of Biotechnology **157**(1): 130-139".*

3.1 Abstract

A Tricistronic vector utilizing internal ribosome entry site (IRES) elements to express the light chain (LC), heavy chain (HC), and a neomycin phosphotransferase (NPT) selection marker from one transcript is designed for generation of mAb expressing CHO cell lines. As compared to commonly used vectors, benefits of this design include: (1) minimized non-expressing clones, (2) enhanced stable mAb productivity without gene amplification, (3) control of LC and HC expression at defined ratios, and (4) consistent product quality. After optimization of the LC and HC arrangement and increasing selection stringency by weakening the NPT selection marker, this Tricistronic vector is able to generate stably transfected pools with specific productivity (qmAb) greater than 5 pg $cell^{-1}$ day^{-1} (pcd) and titers over 150 mg L^{-1}. 5% of clones from these pools have qmAb greater than 20 pcd and titers ranging from 300 to more than 500 mg L^{-1} under non-optimized shake flask batch cultures using commercially available protein-free medium. The mAb produced by these clones have low aggregation and consistent glycosylation profiles. The entire process of transfection to high-expressing clones requires only 6 months. The IRES-mediated Tricistronic vector provides an attractive alternative to commonly used vectors for fast generation of mAb CHO cell lines with high productivity.

3.2 Introduction

Industrial production of monoclonal antibody (mAb) is carried out by transfecting mammalian cells like the Chinese hamster ovary (CHO) cells either with two vectors, referred to as Co-transfection (Fig. 3.1A) or with a Multi-promoter single vector (Fig. 3.1B) for expression of the light chain (LC), heavy chain (HC) and a selection marker. Each gene is driven by its own promoter and transcribed in separate units (Wurm 2004; Birch and Racher 2006; Costa et al. 2010). Upon entering the cell after transfection, the vector can be fragmented before integration or have parts of it removed from the genome after integration as a result of DNA rearrangement (Barnes et al. 2007; Chusainow et al. 2009; Ng et al. 2010). As each gene is independently expressed, if the expression units for the product genes are damaged while that of the selection marker remains intact, cells will only express the selection gene. These clones that are not expressing any mAb product will still survive the drug selection. For example, it has been reported that up to 50% of non-expressing clones generated using a Multi-promoter vector could escape drug selection (Barnes et al. 2007).

Another disadvantage of having individual expression units is the lack of control of the relative expression of LC over HC. It has been shown that when using Co-transfection, the relative amount of each vector integrated into chromosome varies from cell-to-cell (Fussenegger et al. 1999; Yahata et al. 2005; Underhill et al. 2007; Yang et al. 2009). Although using the Multi-promoter single vector system ensures introduction of LC and HC gene into each cell at equal amount, the expression ratio still varies between cells because the use of multiple promoters in close succession can result in

transcriptional interference. An active transcriptional unit can suppresses the expression of another unit and the degree to which gene expression is suppressed depends on the integration site in the genome (Eszterhas et al. 2002; Schlatter et al. 2005). Variations in LC:HC expression ratios have been observed in clones generated using both the Co-transfection and Multi-promoter vector systems (Chusainow et al. 2009; Lee et al. 2009). This change in the ratios of LC over HC expression can affect both mAb expression level and quality (Gonzalez et al. 2002; Schlatter et al. 2005; Jiang et al. 2006; Lee et al. 2009; Van Berkel et al. 2009).

Internal ribosome entry site (IRES) elements allow expression of multiple genes in one transcript (Mountford and Smith 1995; Fussenegger et al. 1998; Martinez-Salas 1999). IRES-based polycistronic vectors have been used in many studies where expression of multiple genes is desired (Gurtu et al. 1996; Fussenegger et al. 1998; Fussenegger et al. 1998; Greber and Fussenegger 2007). It has been demonstrated that IRES-based bicistronic vectors, which express the product gene and selection marker in one transcript, can eliminate non-expressing clones (Rees et al. 1996). However, there are currently few studies using IRES for mAb cell line generation probably because of its poor translation efficiency impeding generation of high producers. In designs which express the LC and HC under the control of one promoter *via* the use of an IRES element and the selection marker under the control of another promoter, the mAb expression is comparable with Co-transfection vector in transient and stable transfections (Jostock et al. 2004; Li et al. 2007). As the mAb genes and selection marker were expressed using different expression units, the advantage of IRES for alleviating problems

related to vector fragmentation is not realized and a large proportion of non-expressing clones may still exist. In another design which expressed the LC, HC, and puromycin selection marker in one transcript by using two IRES elements, the cell lines generated had low specific mAb productivity (qmAb) of a few pg $cell^{-1}$ day^{-1} (pcd) (Mielke et al. 2000). A head-to-head comparison with commonly used vectors and the mAb quality of the generated clones was not conducted in that particular study.

In this work, we designed an IRES-mediated Tricistronic vector, later referred to as Tricistronic vector (Fig. 3.1C) which expressed the LC, HC, and neomycin phosphotransferase (NPT) selection marker in one transcript and compared its performance with Co-transfection (Fig. 3.1A) and Multi-promoter (Fig. 3.1B) vectors for generation of mAb expressing CHO cell lines. We demonstrated that the Tricistronic vector could minimize non-expressing clones, enhance productivity and control LC over HC expression at defined ratios. High expressing clones were easily isolated through further improving the selection stringency and mAb produced by all the clones also had consistent N-glycosylation profiles and low product aggregation, simplifying the clone selection process.

(A)

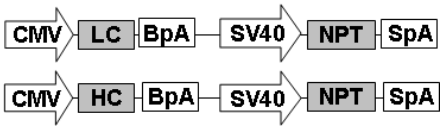

(B)

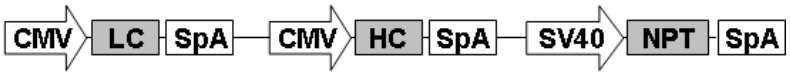

(C)

LC in first cistron

HC in first cistron


```
          10          11                12
IRESwt    ATGATAATATGGCCACAACCATG

          10                                                    NPT
IRESatt   ATGATAAGCTTGCCACAACCCCGGGAGATGAGGATCGTTTCGCATG
```

Figure 3.1 Schematic representation of vectors for expressing light chain (LC) and (HC) of recombinant monoclonal antibody (mAb) in CHO. (A) Co-transfection, expression of LC, HC and neomycin phosphotransferase (NPT) in two separate vectors. (B) Multi-promoter, expression of LC, HC and NPT in one vector using multiple promoters. (C) Tricistronic vectors, expression of LC, HC, and NPT in one vector using one promoter. Two different designs were tested, either LC or HC was placed as the first cistron. CMV, human cytomegalovirus IE gene promoter; SV40, simian virus 40 promoter; BpA, bovine growth hormone polyadenylation signal; SpA, simian virus 40 early polyadenylation signal; IRESwt, wild type encephalomyocarditis virus (EMCV) internal ribosomal entry site; IRESatt, mutated EMCV IRES with attenuated translation efficiency.

3.3 Materials and methods

3.3.1 Cell culture and media

Adherent CHO K1 cells (American Type Culture Collection, Manassas, VA) were grown in Dulbecco's modified Eagle's medium (DMEM) + GlutaMax^{TM} (Invitrogen, Carlsbad, CA) supplemented with 10% fetal bovine serum (FBS) (Sigma-Aldrich, St. Louis, MO), referred to as serum medium, in T-flasks. Suspension CHO K1 cells were obtained by in-house adaptation of the adherent cells into a protein-free medium, consisting of HyQ PF (HyClone, Logan, UT) and CD CHO (Invitrogen) at a 1:1 ratio and supplemented with 1 g L^{-1} sodium bicarbonate (Sigma-Aldrich), 6 mM glutamine (Sigma-Aldrich), and 0.05% Pluronic F-68 (Invitrogen) and grown in shake flasks. Routine subculture of both adherent and suspension cells was done every 3 to 4 days. Cell density and viability were measured using the trypan blue exclusion method on an automated Cedex counter (Innovatis, Bielefeld, Germany).

3.3.2 Vector construction

The Co-transfection vectors (Fig. 3.1A) were constructed by insertion of anti-HER2 LC and HC cDNA into the multiple cloning sites of pcDNA3.1(+) (Invitrogen). The Multi-promoter vector (Fig. 3.1B) was constructed by insertion of SV40-NPT-SpA cloned from pcDNA3.1(+) into a dual-CMV vector described previously (Yang et al. 2009). Construction of the Tricistronic vectors (Fig. 3.1C) were based on pcDNA3.1(+). The region between the bovine growth hormone polyadenylation signal (BpA) and SV40 promoter was replaced with an attenuated encephalomyocarditis virus (EMCV) IRES (IRESatt) designed based on literature, in which ATG-12 was

used as the start codon of NPT, ATG-11 was mutated and 23 extra bases were inserted upstream of ATG-12 (Rees et al. 1996). The anti-HER2 LC or HC cDNA was then inserted downstream of the human cytomegalovirus (CMV) promoter, followed by insertion of the wild type EMCV IRES (IRESwt)-HC or IRESwt-LC element. The IRESwt and HC or LC were linked by overlapping PCR. The EMCV IRESwt and IRESatt were cloned from pIRES-DsRed vector (ClonTech, Palo Alto, CA). The NPT mutants, M1 and M10, were generated using QuickChange site-directed mutagenesis kit (Stratagene, La Jolla, CA) , with amino acid E at 182 changed to D in M1, or D at 261 changed to G in M10 (Sautter and Enenkel 2005). All restriction enzymes used were from New England Biolabs (Ipswich, MA).

3.3.3 Transient transfections

Transient transfections were carried out in 6-well tissue culture plate using Fugene 6 (Roche, Indianapolis, IN). 2 mL of adherent CHO K1 cells at exponential phase were seeded at density of 3×10^5 cells mL^{-1} in 6-well plates 24 h prior to transfection. Duplicate transient transfections for each set of mAb vectors were performed using a Fugene 6 to plasmid ratio of 6 µL:2 µg. To normalize transfection efficiency, a third transfection was carried out in parallel for each vector with an added 0.2 µg of pMax-GFP (Amaxa, Gaithersburg, MD).

3.3.4 Generating stable cell lines

Comparison of stable cell lines generated by Co-transfection, Multi-promoter, and Tricistronic vectors (Fig. 3.1) was performed in adherent CHO K1 cells for easy isolation of clones. Transfections were carried out using Fugene 6 as described in transient transfection protocol. The plasmids were

linearized using a unique BglII site prior to transfection. Selection with G418 (Sigma-Aldrich) at 600 µg mL^{-1} in serum medium was started 48 h post-transfection. Non-transfected cells died after 7-10 days of selection and stably transfected pools were obtained after 2 weeks. Clones were isolated by limiting dilution in 96-well tissue culture plates.

Evaluation of stable cell lines from the Tricistronic vector containing the NPT mutants was performed using suspension CHO K1 cells because of their higher cell densities compared to adherent cultures. Another reason for using suspension cells was that we observed easier adaptation of suspension cells back into suspension cultures after selection in the more robust adherent conditions. In each transfection, 5×10^6 cells were transfected with 5 µg of plasmids linearized at BglII site using Nucleofector (Amaxa). The transfected cells were then resuspended with 2 mL of protein-free medium into 6-well suspension culture plates. At 24 h post-transfection, cells were centrifuged at ~100 x g rpm for 5 minutes, resuspended into 6-well tissue culture plates using 2 mL of serum medium with 600 µg mL^{-1} of G418. Changing from protein-free to serum medium allowed the suspension cells to become adherent. Selection with G418 followed by a recovery period took up to a total of 5 weeks before clone isolation was carried out using limiting dilution method. The stable pool and high expressing clones, based on specific productivity (qmAb), were adapted back into suspension in protein-free medium with G418 at 600 µg mL^{-1} by stepwise decrease of FBS from 10% to 1%, 0.5%, and 0%.

3.3.5 Determining cell productivity by ELISA and nephelometry

Productivities of stable pools and clones under adherent condition were determined in 6-well tissue culture plates by seeding 2 mL of culture in each well at a cell density of 2×10^5 cells mL^{-1}. After 72 h, cells were detached for cell density analysis using Cedex (Innovatis) and supernatant was collected for analysis of mAb concentration using enzyme-linked immunosorbent assay (ELISA). Each well of a 96 well plate was first coated with 50 µL of goat anti-human IgA+IgG+IgM (H+L) (KPL, Gaithersburg, MD) in PBS at 37°C for 60 min. The plate was washed three times with a wash buffer of PBS + 0.1% Tween 20 (Promega, Madison, WI). 300 µL of blocking buffer, 3% bovine serum albumin (BSA) (Sigma), was added to each well and incubated again for 60 min at 37°C. Plate was washed again as before. 50 µL of diluted samples were added in duplicates together with purified myeloma IgG1 standard (Sigma) and incubated again at 37°C for 60min. After another round of washes, 50 µL of detection antibody of goat anti-human IgG (Fc-specific) conjugated to alkaline phosphatase (Sigma-Aldrich) was added, followed by another 60 min of incubation. A final round of washing was performed and 50 µL of p-nitrophenyl phosphate substrate (Sigma) added. The reaction was stopped after 30 min incubation at room temperature with 1 M sodium hydroxide (Sigma). Absorbance was read at 405 nm with 630 nm reference using microplate reader from Bio-Tek (Winooski, VT).

Productivities of suspension adapted stable pools and clones were determined in 250 mL shake flasks. Cells were seeded in 50 mL of medium at a cell density of 2×10^5 cells mL^{-1}. Growth and mAb concentration in the supernatant were monitored every other day until viability dropped below

50%. mAb concentrations were measured using a nephelometric method on an IMMAGE 800 immunochemistry system (Beckman Coulter, Buckinghamshire, England). The qmAb in both adherent and suspension cultures was calculated as the mAb concentration measured at the end of culture divided by the integrated viable cell density (Balcarcel and Stephanopoulos 2001).

qmAb was measured in units of pg cell^{-1} day^{-1} (pcd) and calculated using the formula below:

$$\boldsymbol{qmAb = \frac{[mAb]}{IVCD}}$$

where [mAb] is the mAb concentration in the culture supernatant. IVCD is the integrated viable cell density calculated by the following equation:

$$\boldsymbol{IVCD = \frac{(N - N_0) \times t}{\ln \frac{N}{N_0}}}$$

where N and N_0 are the initial and final viable cell densities and t is the length of culture.

3.3.6 Determining intracellular polypeptides of LC:HC ratios

2×10^6 cells collected from 6-well plate cultures were washed with 1X PBS (Sigma-Aldrich) and lysed in RIPA buffer (Thermo Scientific, Waltham, MA). The cell lysates were centrifuged at ~18,000 × g for 30 min at 4°C. The supernatants were quantified for concentrations of LC and HC polypeptides using ELISA. Steps were as described above in 3.3.5 except now detection antibodies used were goat anti-human IgG (Fc-specific) conjugated to alkaline phosphatase (Sigma-Aldrich) targeting HC and goat anti-human IgG (LC-

specific) conjugated to alkaline phosphatase (Sigma-Aldrich) targeting LC, respectively. The ratio of intracellular LC:HC polypeptides in each clone was calculated as the measured LC concentration divided by the HC concentration.

3.3.7 Western blotting analysis

The product pattern in different clones generated using Co-transfection, Multi-promoter, and Tricistronic vectors (Fig. 3.1) was determined using western blotting analysis. 12 µL of supernatant from 6-well plate cultures were mixed with 4 µL of loading buffer, boiled for 10 min at 70°C, separated on a E-PAGE^{TM} 48 protein Electrophoresis System, and transferred to PVDF membranes according to manufacturer's instructions (Invitrogen). Membranes were blocked in 5% blocking milk (Bio-Rad Laboratories) in TBS with 0.1% Tween-20 (Bio-Rad Laboratories) for 1 h at room temperature. AffiniPure mouse anti-human IgG (H + L) polyclonal primary antibody (Jackson ImmunoResearch, West Grove, PA) followed by horseradish peroxidase (HRP)-conjugated goat anti-mouse IgG secondary antibody (Jackson ImmunoResearch) were used. Proteins were detected using the ECL system (Amersham Biosciences). Membranes were exposed using Lumi-Film Chemiluminescent Detection Film (Roche).

3.3.8 Purifying mAb using protein A column

Culture supernatant containing mAb was loaded on a Tricorn 5/150 Protein A column packed with MabSelect SuRe (GE Healthcare, Uppsala, Sweden) using 1×PBS as a loading buffer and 0.1 M glycine buffer (Merck, Darmstadt, Germany) at pH 2.7 for elution. Samples were neutralized with 1M sodium bicarbonate at pH 8 (Merck). The purification was performed using a GE AKTA explorer 100 (GE Healthcare) and UV detection at 280 nm.

3.3.9 Glycosylation analysis of protein A purified mAb

The N-linked glycan distribution of mAb was analyzed using matrix-assisted laser desorption ionization-time of flight mass spectrometry (MALDI-TOF MS). Briefly, 200 μg of purified mAb was incubated with 8 μg of sequencing grade modified trypsin (Promega, Madison, WI) at 37°C in a 50 mM ammonium bicarbonate buffer (Merck) at pH 8.2. The digestion was stopped after 4 h by heating at 95°C for 15 minutes. The resulting mixture was deglycosylated overnight with 70 U of PNGase F (Prozyme, Hayward, CA) at 37°C. The released N-glycans were then purified using the Hypersep Hypercarb cartridges (Thermo Scientific). The N-glycan preparation was permethylated (Ciucanu and Kerek 1984; Dell et al. 1994) and cleaned-up using a Sep-Pack C18 cartridge (Waters Corporation, Milford, MA) (North et al. 2010).

The MALDI-TOF data was acquired on a 5800 MALDI-TOF/TOF mass spectrometer (AB Sciex, Foster City, CA) in positive reflectron mode. Permethylated samples were reconstituted in 30 μL of 80% (v/v) methanol in water and then spotted on a target plate on a ratio 1:1 with 2,5-dihydroxybenzoic acid matrix at 10 mg mL^{-1} (Water Corporation) dissolved in 80% (v/v) methanol in water. The 4700 calibration standard kit, calmix (AB Sciex) was used as an external calibrant for the MS mode. The laser intensity used to acquire the data was 50%. Relative quantification of the different N-glycan species was based on the MALDI-TOF MS data (Kang et al. 2007; Wada et al. 2007). Statistical significance at the 95% confidence level of the difference in glycan distribution between clones was compared using an ANOVA test.

3.3.10 Aggregation analysis of protein A purified mAb

The aggregation of protein A purified mAb was determined using size exclusion chromatography (SEC). The instrument setup consisted of a HPLC system (Shimadzu, Kyoto, Japan), with a binary pump, an auto injector, a thermostat column oven and a UV-visible detector. Dawn 8 (light scattering), Optilab (refractive index), and QELS (dynamic light scattering), were connected in series following the UV-visible detector. All the three detectors were purchased from Wyatt Technology Corporation (CA, USA) and operated using ASTRA software. The Chromatography columns used were TSK Guard column SWXL, 6×40 mm and TSK gel G3000 SWXL, 7.8×300 mm (Tosoh Corporation, Tokyo, Japan). Column Oven temperature was set at 25ºC and mobile phase included 0.2M sodium phosphate (Merck) and 0.1M potassium sulfate buffer at pH 6.0 (Merck). Flow rate was 0.5 mL min^{-1}.

3.4 Results

3.4.1 Design of Tricistronic vectors

IRES-mediated Tricistronic vectors were designed to express the LC, HC and NPT under the control of a CMV promoter (Fig. 3.1C). Arrangement of LC or HC as the first cistron allowed changing of the ratios of LC : HC expression. EMCV IRES was chosen to drive translation of the second mAb gene as it was reported to be less affected by the flanking coding sequences and mediates accurate translation (Borman et al. 1995; Borman et al. 1997; Hennecke et al. 2001). For higher translation efficiency, the sequence around ATG-10, ATG-11, and ATG-12 was maintained and ATG-12 was used as the start codon of mAb gene (Davies and Kaufman 1992; Kaminski et al. 1994;

Qiao et al. 2002; Bochkov and Palmenberg 2006; Martin et al. 2006). ATG-11 is known to be the dominant translation initiation site (Davies and Kaufman 1992) and the three extra amino acids added to the IRES-driven mAb gene would be cleaved together with the signal peptide (Li et al. 2007). In order to avoid gene amplification to reduce the time required for cell line generation, a NPT selection marker was chosen instead of amplifiable markers, such as DHFR. To enhance stringency of selection for high producer, a less effective IRESatt was applied on NPT to reduce its expression or using a combination of IRESatt and NPT mutants with reduced efficacy. The strategy is based on the principle that when the selection marker is weakened, only clones with greater transcriptional activity or more copies of the integrated vector can survive the selection process (Fussenegger et al. 1999; Ng et al. 2007).

3.4.2 Evaluation of Tricistronic vectors for transient mAb expression

Tricistronic vectors with either LC or HC as the first cistron were compared with the Co-transfection and Multi-promoter vectors in transient transfections in CHO K1 cells. The Co-transfection and Multi-promoter vectors exhibited similar mAb expression levels (Fig. 3.2). When compared to the Co-transfection system, expression was 33% lower for Tricistronic design with LC as the first cistron and 84% lower with HC as the first cistron. As cap-dependent translation of the gene in the first cistron is more efficient than IRES-driven translation, placement of LC downstream of CMV promoter would see LC expressed in excess of HC. HC would then be in excess when LC and HC positions were changed. Higher expression from the configuration that provided excess LC was consistent with the reports that excess LC was more favorable for mAb expression (Gonzalez et al. 2002; Schlatter et al.

2005). Having the LC as the first cistron was chosen as the optimal configuration for the Tricistronic vector design and used for subsequent experiments.

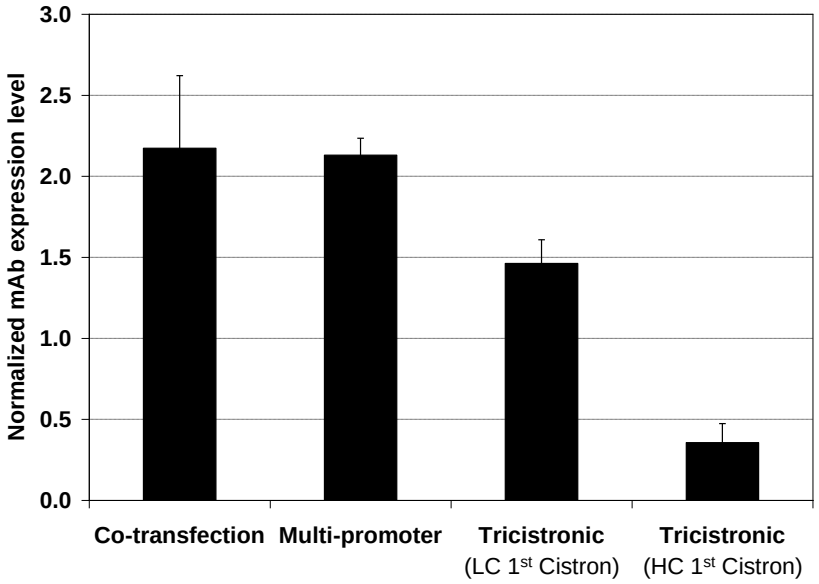

Figure 3.2 Comparison of different vectors for mAb expression levels in transient transfections. CHO K1 cells were transfected with different vector systems for expression of the anti-HER2 mAb. At 48-h post transfection, the mAb concentration in the culture supernatant was measured by ELISA. Results represent mAb concentration normalized to an internal control, GFP expression measured by FACS Calibur (Becton Dickinson, Bedford, MA). Each point represents the average and standard deviation of measurements of duplicates from two independent transfections.

3.4.3 Evaluation of Tricistronic vector for mAb expression in stable transfections

The Tricistronic vector with LC in the first cistron was then compared with the Co-transfection and Multi-promoter vectors in stable transfections. In stably transfected pools, the Co-transfection and Multi-promoter vectors gave similar qmAb of 0.02 and 0.03 pg cell^{-1} day^{-1} (pcd) respectively. In contrast to the lower expression in transient transfections, using the Tricistronic vector improved stable pool expression levels by 10-fold to 0.28 pcd (Fig. 3.3A).

Analysis of clonal productivities indicated that higher productivity in stable pools generated using the Tricistronic vector was a result of the enhanced proportion of positive clones and higher productivity of clones. Among 20 clones randomly picked from stable pools generated by each of the three vector systems, 40% of clones generated by Co-transfection system and 60% of clones generated by Multi-promoter system produced detectable levels of mAb using ELISA with Fc-specific antibody for detection, while 75% of the clones generated using the Tricistronic vector were positive (Fig. 3.3B). The average qmAb of 20 clones from the Tricistronic vector is 0.25 pcd and the highest expressing clone had qmAb of 1.16 pcd compared to average qmAb of 0.01 pcd and highest qmAb of 0.07 pcd for Co-transfection vectors, and average qmAb of 0.02 pcd and highest qmAb of 0.09 pcd for the Multi-promoter vector.

(A)

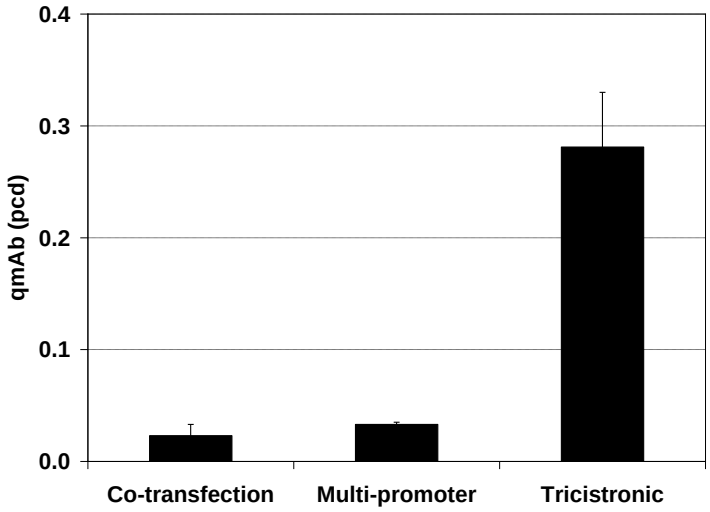

(B)

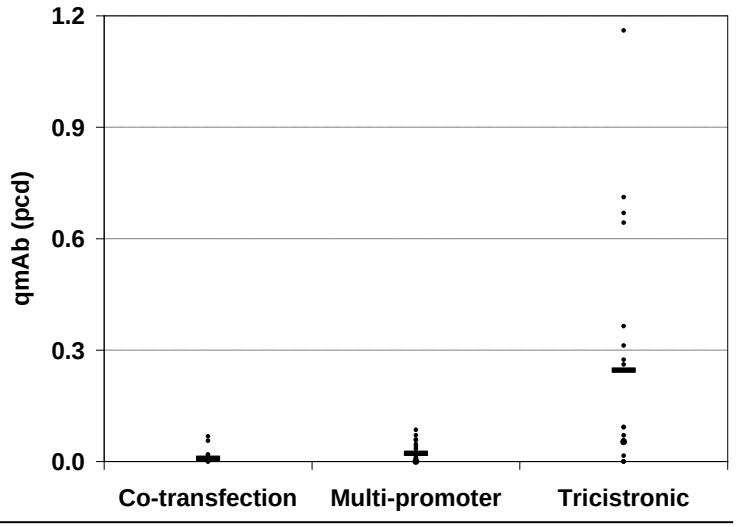

	Co-transfection	Multi-promoter	Tricistronic
Expressing clones%	40	60	75

Figure 3.3 Comparing mAb expression levels of different vectors in stable transfections. (A) Specific mAb productivity (qmAb) of stably transfected pools. Each point represents the average and standard deviation of three transfected pools. (B) qmAb and percentage of expressing clones out of 20 picked from each pool. Each point represents the mAb productivity of a single clone. mAb concentration was determined using ELISA and detection antibody targeting against the Fc region of mAb.

The clones were then sorted in ascending order based on their qmAb for further analysis using western blotting. Besides expressing complete antibody, HC_2LC_2, various combinations of antibody fragments including LC_2, LC monomer and HC_2 were observed in different clones. Among the clones examined, only two clones generated using Co-transfection vectors and four clones generated using Multi-promoter vector produced complete antibodies, the rest of the clones produced mainly fragments or no detectable antibody components (Fig. 3.4A and B). These results suggested that a portion of the positive clones detected using ELISA were in fact false positive clones expressing HC fragments. In contrast, the Tricistronic vector had 15 out of 20 clones expressing mainly complete mAb (Fig. 3.4C).

(A)

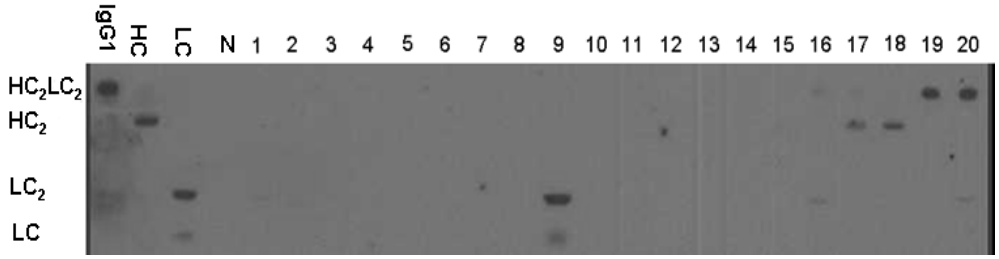

(B)

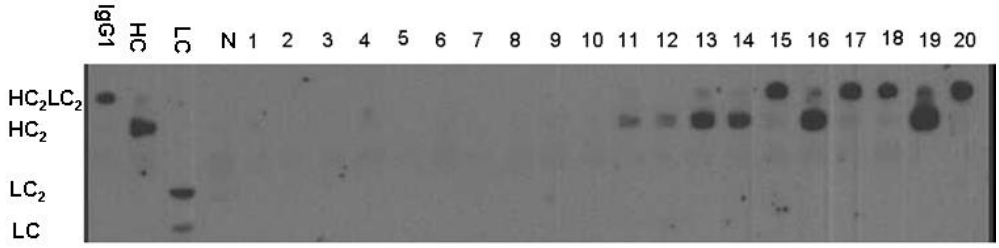

(C)

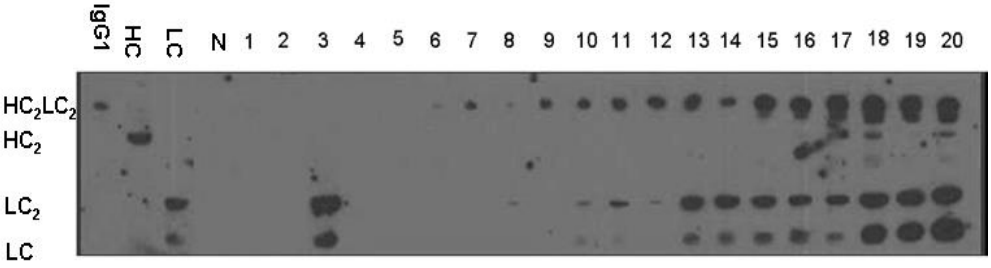

Figure 3.4 Western blot analysis of HC and LC polypeptides secreted from different clones generated using (A) Co-transfection, (B) Multi-promoter, and (C) Tricistronic vector. Non-reduced supernatant from different clones was loaded in each lane. A commercial human affinity purified myeloma IgG1 (Sigma-Aldrich) and supernatant from cells transfected with either a vector expressing only HC or a vector expressing only LC were loaded in separate lanes as controls. Supernatant from non-transfected cells (N) was loaded as negative control. Migration of the different secreted forms, HC_2LC_2, HC_2, LC_2, and LC, are indicated in the left side.

Further analysis of the ratios of intracellular abundance of LC over HC polypeptides provided insights to the different product patterns observed in clones generated using different vectors. Corresponding to the different product patterns in clones generated using the Co-transfection and Multi-

promoter vectors, the intracellular LC:HC polypeptides ratios varied from more than 7 to close to 0 (Fig. 3.5A and B). When the ratio was close to one like in Multi-promoter clones 15, 17, 18 and 20, the secreted product was mainly complete mAb. Unbalanced LC over HC expression could have resulted in secretion of mAb fragments, like Co-transfection clone 9 and Multi-promoter clone 11 to 14. The Tricistronic vector controlled the ratio of LC:HC polypeptides around 4:1 in all positive clones (Fig. 3.5C). This matched with the consistent product pattern of a mixture of HC_2LC_2, LC_2 and LC in all clones and could explain the secreted LC fragments.

(A)

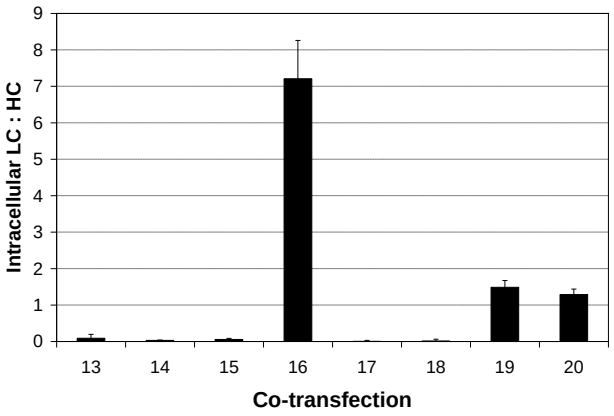

(B)

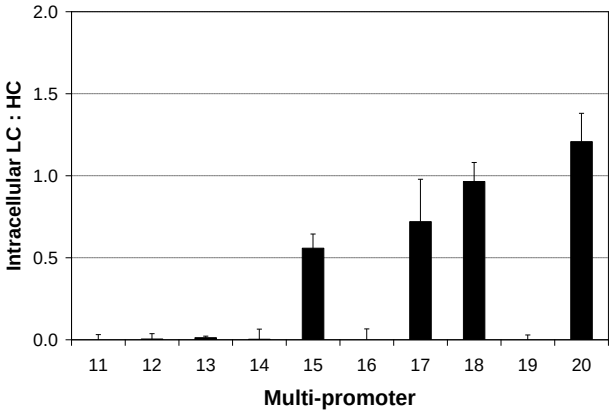

(C)

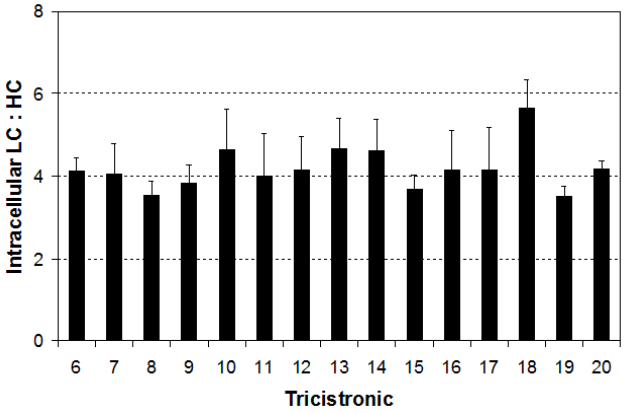

Figure 3.5 Ratios of intracellular abundance of LC over HC polypeptides in different clones generated using (A) Co-transfection, (B) Multi-promoter, and (C) Tricistronic vector. Clone numbers are represented on the horizontal axis. Equal numbers of cells from each clone with detectable levels of mAb production were lysed in RIPA buffer. The concentration of LC and HC polypeptides in the lysates was determined by using ELISA, with detection antibody targeting against LC and Fc region, respectively.

3.4.4 Weakening selection marker in Tricistronic vector for selection of high producers

To improve the stringency of selection for high producers, the NPT selection marker on the Tricistronic vector was further weakened through the use of NPT mutants, M1 and M10. M1 and M10 mutations reduced the enzymatic activity of NPT to 22% and 3% as compared to the wild-type NPT (Fig. 3.6) (Sautter and Enenkel 2005). In preliminary attempts, stable pools were successfully generated using Fugene 6 for the Tricistronic vectors containing wild type NPT and M1 mutant, but no clones could survive selection in cells transfected with the Tricistronic vector containing M10 mutant. This was likely a result of the high stringency of selection and low transfection efficiency. To address this issue, suspension cells were transfected using nucleofection to obtain more transfectants and selection was done under

adherent condition. This protocol allowed successful generation of stable pools for all three vectors. As compared to the Tricistronic vector containing the wild type NPT which generated pools with qmAb of 0.28 pcd, the improved one containing M1 mutant increased the qmAb of the stable pool by over 2-fold to 0.72 pcd and using the even weaker M10 pushed qmAb higher to 4.73 pcd (Fig. 3.6). A stable pool generated using M10-mutant Tricistronic vector was adapted to suspension in protein-free medium. Specific productivity remained around 5 pcd after adaptation. The culture reached a peak cell density of $5.7x10^6$ cells mL^{-1} and a titer of 168 mg L^{-1} in a 9 days batch shake flask culture.

A total of 111 clones were randomly picked from a stable pool generated using the M10 Tricistronic vector and screened for high expressing clones in 6-well plates. Based on the qmAb measured, the top 20 clones were adapted to suspension in protein-free medium and characterized in shake flasks for growth and productivity. The results of the 5 clones with highest qmAb, clone 50, 63, 87, 97, and 98, were listed in table 3.1. In non-optimized shake flask batch cultures using commercial protein-free medium, the 5 clones maintained viability above 50% for 7 to 9 days, with peak cell density ranging from 2.1×10^6 to 7.6×10^6 cells mL^{-1}. The qmAb, calculated based on the entire culture process, ranged from 20 to 33 pcd and the peak titer of the highest expressing clone, 87, reached 513 mg L^{-1}. Productivities of these clones are considered high as the culture conditions were under non-optimized shake flask batch cultures.

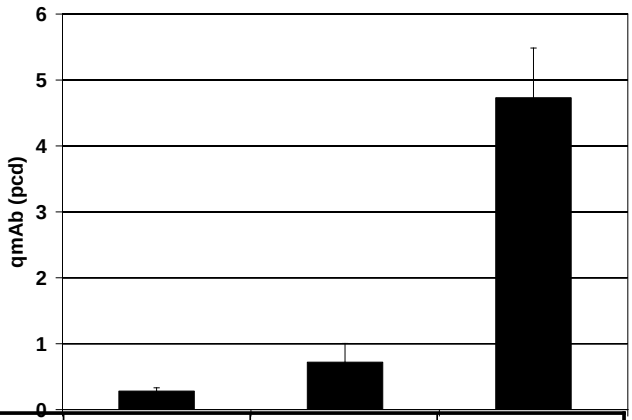

	WT	M1	M10
Amino acid substitution	None	E182D	D261G
Activity%	100	22	3

Figure 3.6 Specific productivity (qmAb) of stably transfected pools generated using Tricistronic vectors with the wild type NPT (WT), mutant M1, and mutant M10 as selection markers. The NPT mutants were generated based on literature (Sautter and Enenkel, 2005). The amino acid substitution and reported enzyme activity for each mutant were listed. Each point represents the average and standard deviation of measurements from three stable pools.

Table 3.1 Productivity of the 5 top mAb expressing clones in shake flask batch culture. VCD represents viable cell density.

Clone	Max. VCD ($X10^6$ cell mL^{-1})	Culture length (days)	Max. titer(mg L^{-1})	qmAb(pcd)
50	2.1	8	399	31
63	4.0	7	434	33
87	5.6	9	513	20
97	7.6	9	461	20
98	3.8	7	268	22

3.4.5 Product quality in clones generated using improved Tricistronic vector

Aside from high productivity, it is also desired that cell lines are able to produce mAb of good quality. Parameters to be considered include the glycosylation profile and protein aggregation, which can affect the mAb activity, immunogenicity and clearance (Rudd et al. 2001; Jefferis 2005; Cromwell et al. 2006). MALDI-TOF mass spectrometry was used to provide detailed identification and quantification of N-glycan on the mAb produced in the top 5 expressing clones (Fig. 3.7A and Table 3.2). 2% of the glycans were sialylated and around 80% fucosylated for all 5 clones (Fig. 3.7B). High-mannose type N-glycan composition ranged from 5% to 8%. Complex type G0, G1 and G2 glycan distribution ranged from 48% to 53%, 36% to 39% and 3.5% to 4.3% respectively for the 5 clones analyzed. The glycan distribution observed in these clones was similar to that reported by the manufacturer of anti-HER2 mAb (Fig 3.7C) (Junttila et al. 2010). Statistical analysis (ANOVA test) of all the observed glycoforms showed that there were no significant differences in glycan distribution between the clones.

(A)

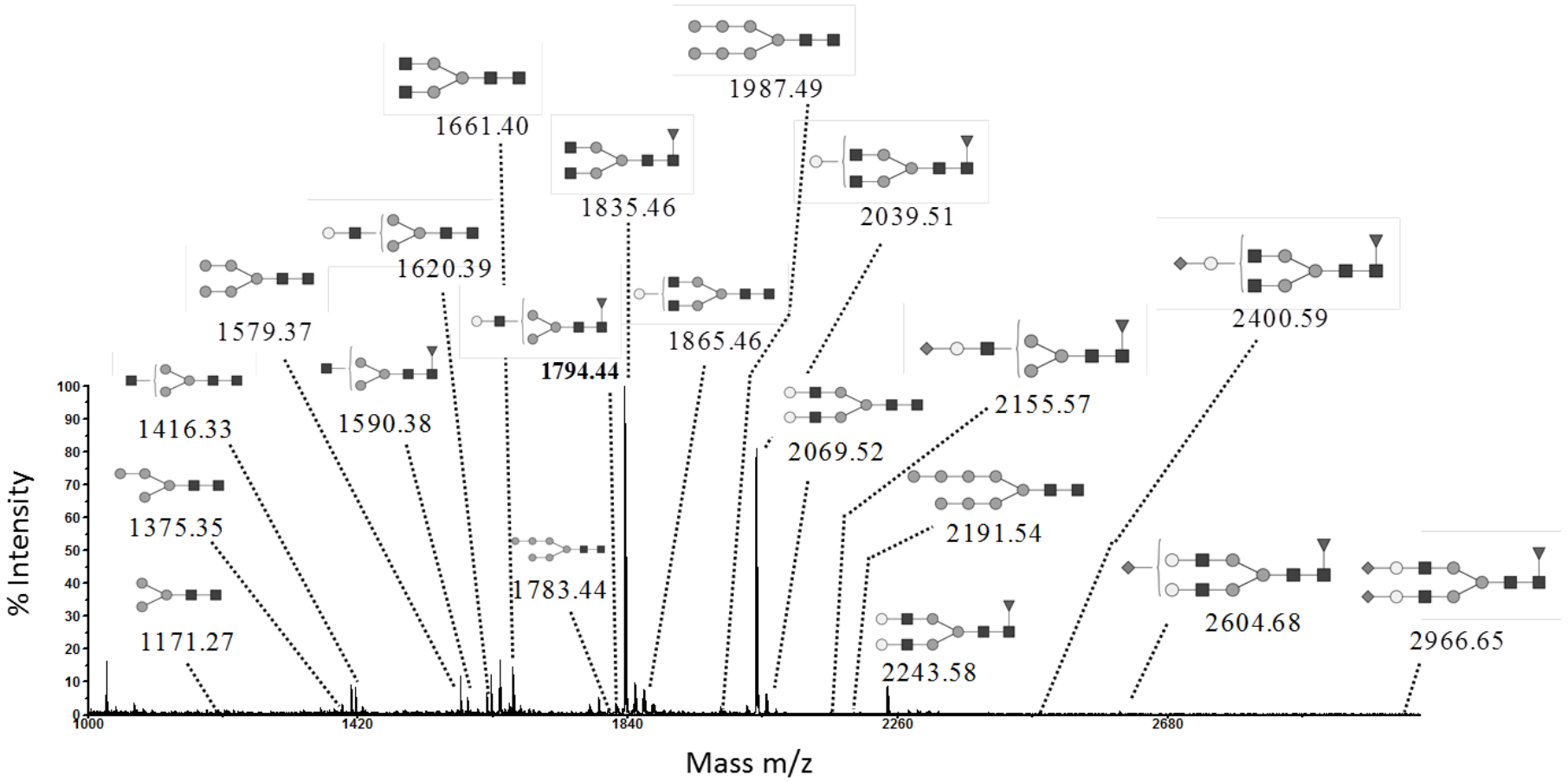
1661.40
1987.49
1835.46
2039.51
1620.39
1579.37
1865.46
2400.59
1794.44
1590.38
1416.33
2155.57
2069.52
1375.35
2191.54
1783.44
1171.27
2604.68
2966.65
2243.58
% Intensity
Mass m/z
100
90
80
70
60
50
40
30
20
10
0
1000
1420
1840
2260
2680

(B)

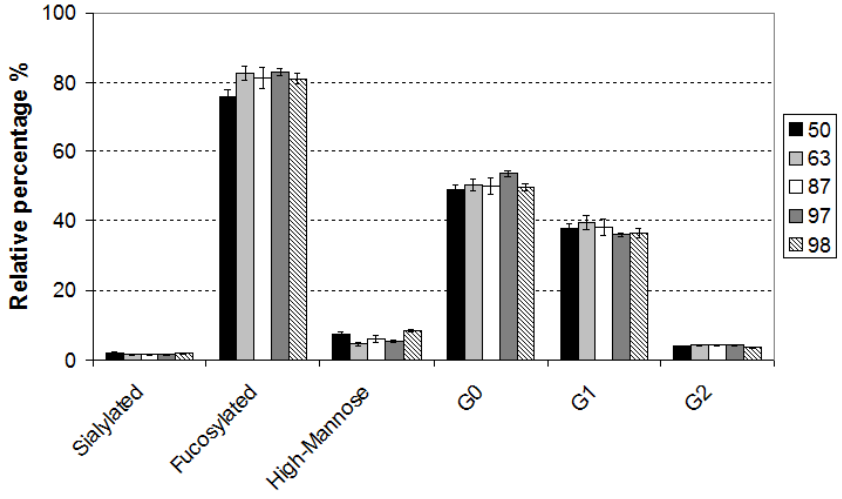

(C)

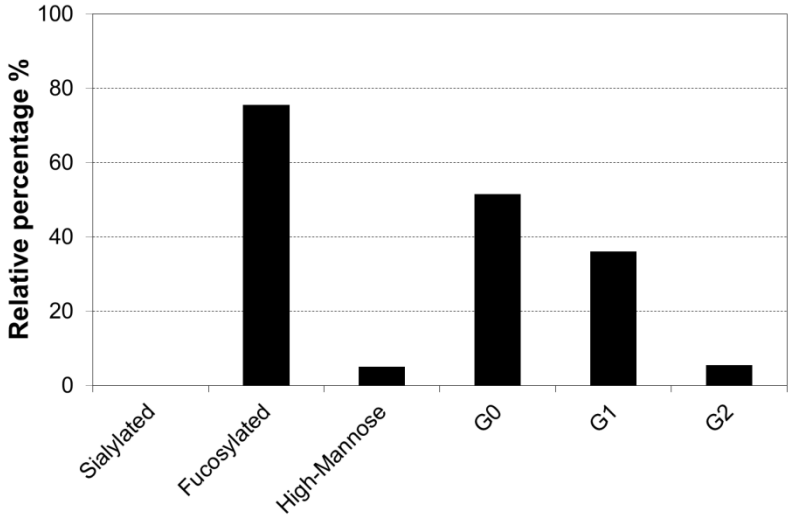

Figure 3.7 Glycan structures and distribution of recombinant mAb produced in the 5 top expressing clones. (A) MALDI-TOF analysis of the permethylated N-glycans released from the recombinant mAb produced in the clone 50 as an example. Solid square, N-acetylglucosamine; solid circle, mannose; open circle, galactose; solid triangle, fucose and solid diamond, sialic acid. (B) Glycan distribution on recombinant mAb produced in the 5 top expressing clones. N-glycans are categorized into sialylated which are substituted at least by one sialic acid residue in terminal position, fucosylated complex N-glycans, high mannose-type, G0 without bearing terminal galactose residue, G1 bearing one terminal galactose residue and G2 bearing two terminal galactose. The numbers presented here are the average and standard deviation of 3 independent N-glycan preparations. (C) Reported glycosylation profile for commercial anti-HER2 mAb (Juntilla T. 2010). Sialylated glycan values were not available.

Table 3.2 Microheterogeneity of N-glycan structures found on the purified mAb produced in the 5 top expressing clones.

Five categories of N-glycans have been distinguished: high mannose-type, complex-type G0 which are the ones bearing no terminal galactose residue, G1 which are having one terminal galactose, G2 which are the ones with two terminal galactose and then, sialylated which are the complex structures substituted by one or two sialic acids. The numbers reported here correspond to the percentage (%) of each N-glycan and are the mean of 3 independent analyses. Solid square, N-acetylglucosamine; solid circle, mannose; open circle, galactose; solid triangle, fucose; solid diamond, sialic acid.

Clones	50	63	87	97	98
Sialylated					
	0.63 +/- 0.12	0.59 +/- 0.16	0.48 +/- 0.10	0.48 +/- 0.10	0.79 +/- 0.17
	0.43 +/- 0.25	0.35 +/- 0.05	0.34 +/- 0.04	0.37 +/- 0.04	0.44 +/- 0.06
	0.47 +/- 0.23	0.39 +/- 0.07	0.45 +/- 0.06	0.45 +/- 0.03	0.37 +/- 0.07
	0.36 +/- 0.22	0.26 +/- 0.04	0.25 +/- 0.05	0.29 +/- 0.06	0.23 +/- 0.07
High-Mannose					
	0.72 +/- 0.25	0.54 +/- 0.04	0.53 +/- 0.05	0.49 +/- 0.03	0.77 +/- 0.09
	4.93 +/- 0.32	2.35 +/- 0.45	3.58 +/- 0.84	3.12 +/- 0.343	6.36 +/- 0.30
	0.74 +/- 0.22	0.70 +/- 0.16	0.8 +/- 0.04	0.66 +/- 0.07	0.60 +/- 0.06
	0.63 +/- 0.20	0.59 +/- 0.16	0.76 +/- 0.22	0.62 +/- 0.07	0.48 +/- 0.07
	0.52 +/- 0.23	0.38 +/- 0.05	0.36 +/- 0.03	0.37 +/- 0.05	0.32 +/- 0.07
G0					
	0.62 +/- 0.24	0.49 +/- 0.01	0.56 +/-0.05	0.43 +/- 0.03	0.59 +/- 0.09
	3.36 +/- 0.67	2.52 +/- 1.26	2.58 +/-1	3.44 +/- 0.13	3.01 +/- 0.74
	2.16 +/- 0.19	1.18 +/- 0.08	1.47 +/-0.3	1.16 +/- 0.10	2.98 +/- 0.11
	5.80+/- 0.25	4.57 +/- 0.84	4.68 +/- 0.77	3.20 +/- 0.26	2.65 +/- 0.15
	36.96+/- 1.17	41.43 +/- 0.90	40.62 +/- 1.79	45.3 +/- 0.74	40.33 +/- 0.70
G1					
	2.84 +/- 0.47	2.22 +/- 0.97	2.2 +/- 0.6	2.54 +/- 0.10	2.35 +/- 0.48
	2.30 +/- 0.09	1.34 +/- 0.13	1.31+/- 0.19	1.19 +/- 0.05	2.80 +/- 0.02
	3.04 +/- 0.15	2.32 +/- 0.19	2.16 +/- 0.24	1.60 +/- 0.09	1.36 +/- 0.09
	29.64 +/- 1.3	33.45 +/- 1.77	32.59 +/- 2.25	30.67 +/- 0.50	30.00 +/- 1.26
G2					
	0.77 +/- 0.27	0.58 +/- 0.07	0.48 +/- 0.07	0.50 +/- 0.06	0.41 +/- 0.10
	3.08 +/- 0.02	3.75 +/- 0.17	3.80 +/- 0.24	3.12 +/- 0.21	3.16 +/- 0.24

The aggregation of protein A purified mAb was determined by SEC followed by detection using dynamic light scattering and UV. Typical SEC chromatograms of the purified mAb are shown in Fig. 3.8. The peak P1 was identified as aggregates and the second peak P2 as IgG monomers, based on their average molecular weights of 2.87 x 10^5 g/mol and 1.45 x 10^5 g/mol respectively as determined by dynamic light scattering (Fig. 3.8A). The level of aggregation was then quantified using the peak areas detected by the UV detector (Fig. 3.8B). In all samples, the IgG monomer fractions had hydrodynamic radius (Rh) of 5.6 nm and represented more than 98 % of total protein composition and the level of aggregation was less than 2%.

(A)

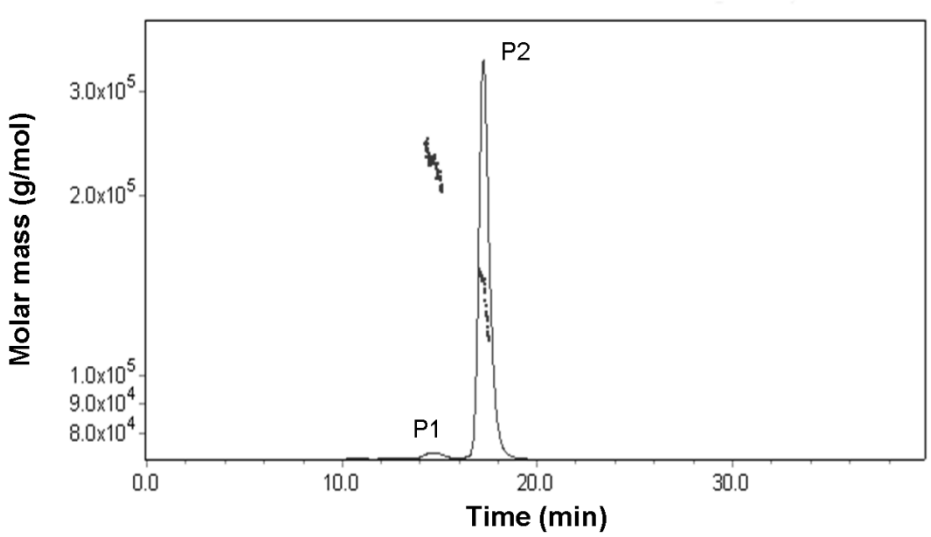

(B)

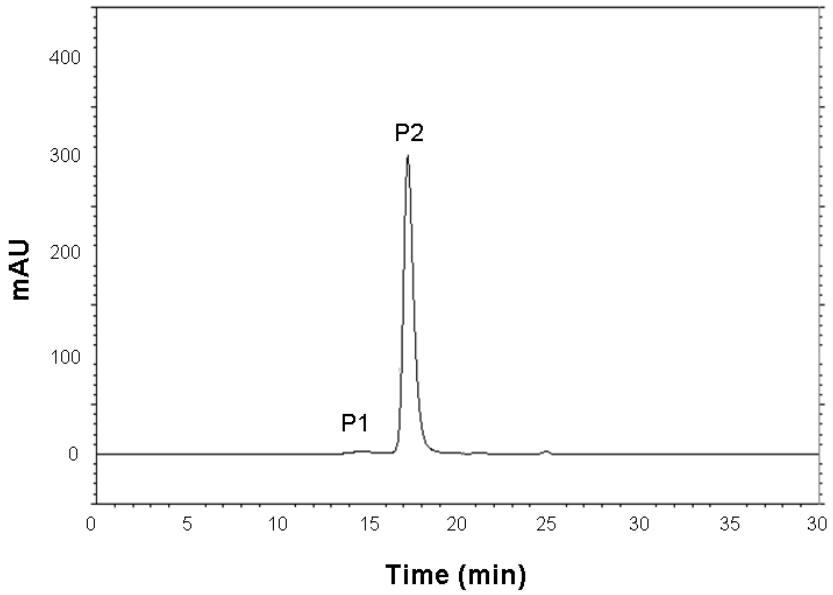

Figure 3.8 Typical chromatograms obtained for the top 5 expressing clones. (A) Species within protein A purified mAb from the top 5 expressing clones were separated by size exclusion chromatography followed by the identification of species based on molecular weight generated by light scattering detection. Peak P1 corresponds to aggregates and peak P2 corresponds to non-aggregated IgG monomers. (B) Chromatogram from UV detector showing similar peaks. Peak areas were used for the quantification of proteins detected as P1 and P2.

3.5 Discussion

As compared to Co-transfection and Multi-promoter vectors, using Tricistronic vectors minimized non-expressing clones, enhanced productivity, and controlled consistent product quality. These advantages obtained using the Tricistronic vector rely on three key designs: (1) expression of LC, HC, and selection marker in one transcript, (2) arrangement of LC as the first cistron, and (3) IRESatt driven translation of a weakened mutant NPT. The first observed benefit of using the Tricistronic vectors was the higher stable mAb expression although the transient expression levels were lower. This was likely due to the reduced non-expressing clones and better selection stringency using IRES compared to a weaker promoter. Tight coupling of the three genes

in one transcript minimized the non-expressing clones to 25%, as compared to 50 to 60% observed in those generated using Co-transfection and Multi-promoter vectors. It was expected that expression of the product and selection genes in one transcript would eliminate all non-expressing clones. The observation of non-expressing clones surviving drug selection is likely a result of insertion of an intact NPT gene from a fragmented Tricistronic vector downstream of an endogenous promoter. Expression of LC and HC in one transcript also enabled control of LC:HC at fixed ratios, giving consistent product patterns between clones which will simplify the clone selection process. Without a strict control of LC:HC expression in Co-transfection and Multi-promoter, clones generated could produce full mAb, HC fragments, LC fragments, or a mixture of them. While we observed no statistically significant differences in the mAb glycan distribution between our clones, variations of up to 18% and 14% for G0F and G1F respectively had been previously reported for mAb produced in clones generated using a Multi-promoter vector (Van Berkel et al. 2009). It was also suggested in the same study that N-glycosylation could be affected by the folding and assembly process, which in turn is affected by the LC:HC ratio. The fixed ratio of LC:HC expression of our clones generated using the Tricistronic vector could be the reason for the observed N-glycan distribution consistency.

Arrangement of LC as the first cistron in Tricistronic vectors expressed LC in excess, which had higher mAb expression than arrangement of HC as the first cistron. Extra expression of LC may be also beneficial for minimization of the mAb aggregation. In a study based on a Multi-promoter vector, it was observed that the level of mAb aggregation was reversely

correlated with the LC : HC mRNA levels (Lee et al. 2009). When the LC:HC ratio was greater than 3, most clones had aggregation less than 2% for the unspecified mAb. Another study has also shown that excess HC could be a reason explaining mAb aggregation (Vanhove et al. 2001). These results fit well with our observations that clones generated using the Tricistronic vector with a LC:HC ratio of 4 presented less than 2% of mAb aggregation.

Selection marker weakening is a common approach for enhancing selection of high producers. The Tricistronic design makes this strategy more effective by minimizing non-expressing clones. In theory, the weaker the selection marker is, the higher the threshold expression level is required for clones to survive selection. Application of IRESatt on the wild type NPT or mutant NPT M1 in the Tricistronic vector enhanced productivity but it was still less than 1.00 pcd in stable pools. High expression clones are expected to be still of a small proportion. Only further weakening selection marker, application of IRESatt on NPT mutant M10, enabled generation of clones with qmAb greater than 30 pcd by picking only a hundred clones. It is not clear whether further weakening NPT can further enhance productivity but we speculate that further reduction of NPT strength will result in failure of clone survival.

By avoiding gene amplification and enhancing stringency of selection, our optimized Tricistronic vector enabled generation of stably transfected pools with titers over 150 mg L^{-1} within two months and clones with specific productivities greater than 30 pcd within 6 months. The timeline could be further shortened by carrying out the drug selection and clone screening process under optimized suspension conditions. This shortened process is

beneficial to different stages of mAb development. High expressing pools can be quickly generated to provide mAb for preclinical studies, where smaller amounts of mAb are needed and timing is greater importance. In parallel, high expressing clones are picked for mAb production for late stage clinical trials and large scale manufacturing where high productivity is more critical. As compared to the use of transient transfection technology, use of stable pool for preclinical studies is preferred as product quality between stable pool and clones picked is more consistent.

Chapter 4: Comparing IRES and Furin-2A (F2A) for mAb expression in CHO cells

Using IRES to express LC and HC as in chapter 3 would result in higher expression of one of the genes due to the reduced translation efficiency of IRES. This might not be optimal for mAb production due to wastage of the excess peptides. It is still unclear if equimolar amounts of LC and HC would perform worse than having either one in excess in stable mAb producing cell lines. In this chapter we evaluated the use of F2A elements to link LC and HC genes for expression of biosimilar mAbs in CHO cells. Use of F2A should allow LC and HC to be expressed at equal amounts for subsequent studies on stable LC:HC ratio. This study would also allow us to compare the IRES vector design with a single transcript design which had been reported to generate high mAb titers.

*The following results were first published in "**Ho, S. C. L.**, Bardor, M., Li, B., Lee, J. J., Song, Z., Tong, Y. W., Goh, L.-T. and Yang, Y. (2013). "Comparison of Internal Ribosome Entry Site (IRES) and Furin-2A (F2A) for Monoclonal Antibody Expression Level and Quality in CHO Cells." PLoS One **8**(5): e63247".*

4.1 Abstract

Four versions of tricistronic vectors expressing IgG1 light chain (LC), IgG1 heavy chain (HC), and dihydrofolate reductase (DHFR) in one transcript were designed to compare internal ribosome entry site (IRES) and furin-2A (F2A) for their influence on monoclonal antibody (mAb) expression level and quality in CHO DG44 cells. LC and HC genes are arranged as either the first or the second cistron. When using mAb quantification methods based on the detection antibodies against HC Fc region, F2A-mediated tricistronic vectors appeared to express mAb at higher levels than the IRES-mediated tricistronic vectors in both transient and stable transfections. Further analysis revealed that more than 40% of products detected in stably transfected pools generated using the two F2A-mediated tricistronic vectors were aggregates. LC and HC from the F2A stably transfected pools were not properly processed, giving rise to LC+F2A+HC or HC+F2A+LC fusion proteins, LC and HC polypeptides with F2A remnants, and incorrectly cleaved signal peptides. Both IRES-mediated tricistronic vectors express mAb with correct sizes and signal peptide cleavage. Arrangement of LC as the first cistron in the IRES-mediated tricistronic vectors exhibits increased mAb expression level, better growth, and minimized product aggregation, while arrangement of HC as first cistron results in low expression, slower growth, and high aggregation. The results obtained will be beneficial for designing vectors that enhance mAb expression level and quality in mammalian cells.

4.2 Introduction

Monoclonal antibodies (mAbs) are currently the fastest growing class of biotherapeutic molecules (Aggarwal 2010; Nelson et al. 2010). Most mAbs in the market are immunoglobulin G (IgG) consisting of two identical heavy chain (HC) and two identical light chain (LC) polypeptides assembled via disulfide bridges. MAbs are commonly produced by stable transfection of Chinese hamster ovary (CHO) cells with the HC, LC and selection marker on either one or two separate vectors (Kim et al. 1998; Wurm 2004; Birch and Racher 2006; Costa et al. 2010). CHO DG44 cells are commonly used due to their compatibility with dihydrofolate reductase (DHFR), an amplifiable selection marker. Each gene is under the control of its own promoter and transcribed separately. One disadvantage of such designs is that vector fragmentation could result in non-expressing clones surviving drug selection (Barnes et al. 2007; Ng et al. 2010). The other disadvantage is the lack of control over the ratio of LC:HC expression. LC is required to facilitate the folding and release of HC from BiP to form a complete IgG monomer (Lee et al. 1999). While it has been demonstrated that expression of LC in excess was beneficial for mAb expression (Gonzalez et al. 2002; Schlatter et al. 2005; Jiang et al. 2006; Li et al. 2007; Chusainow et al. 2009; Ho et al. 2012). The ratio of LC:HC expression can also affect mAb qualities such as aggregation and glycosylation (Schlatter et al. 2005; Lee et al. 2009; Ho et al. 2012). Having HC in excess can cause ER stress (Lenny and Green 1991) and proteasome overloading (Fagioli et al. 2001), creating a burden to the cell machinery and can inhibit cell proliferation (Schlatter et al. 2005).

Tricistronic vectors that express LC, HC, and selection marker genes in one mRNA are able to alleviate the above problems of traditional vectors. When vectors get fragmented, the mRNA unit would be incomplete and no genes would be expressed. Internal ribosome entry site (IRES) elements, which have a length of several hundred base pairs, allow expression of multiple genes in one mRNA. When IRES elements are included between multiple open reading frames (ORFs), the first ORF is translated by the canonical cap-dependent mechanism while the rest are translated through a cap-independent mechanism (Mountford and Smith 1995; Hellen and Sarnow 2001). The IRES-driven cap-independent translation has lower efficiency than the cap-dependent translation, resulting in lower expression of IRES-driven genes (Kaufman et al. 1991; Houdebine and Attal 1999; Hennecke et al. 2001). A few studies have used IRES for expressing mAb in mammalian cells (Mielke et al. 2000; Jostock et al. 2004; Li et al. 2007; Li et al. 2007; Ho et al. 2012). It has been demonstrated that an IRES-mediated tricistronic vector expressing LC, HC and neomycin in one transcript reduced the occurrence of non-expressing clones and controlled the LC:HC ratios at similar levels for all clones (Ho et al. 2012). Clones generated using this vector expressed mAb at high levels with low aggregation and consistent glycosylation (Ho et al. 2012).

An alternative approach for co-expressing multiple genes in one mRNA is using 2A elements. 2A elements are much shorter than IRES, having only 60 to 80 base pairs. 2A linked genes are expressed in one single open reading frame and “self-cleavage” occurs co-translationally between the last two amino acids, GP, at the C-terminus of the 2A polypeptide, giving rise to equal amounts of co-expressed proteins (de Felipe et al. 2006; Doronina et al.

2008; Doronina et al. 2008). The exact mechanism involved is still unclear but it has been suggested to involve a "ribosomal skip" between the two codons with no peptide bond formation between G and P (Donnelly et al. 2001). Recent designs have added a furin cleavage sequence upstream of 2A to eliminate the additional amino acids which would otherwise remain attached to the upstream protein after cleavage (Fang et al. 2005; Fang et al. 2007). Furin-2A (F2A) elements have been used for mAb expression in mammalian cells (Fang et al. 2005; Fang et al. 2007; Jostock et al. 2010; Camper et al. 2011; Davies et al. 2011) and for *in vivo* gene therapy (Li et al. 2012). It has been demonstrated that the productivities of F2A-vector derived clones were comparable with those derived from an industry reference vector based on separate expression unit design (Jostock et al. 2010). The design of the F2A vector used in that particular study was not released.

In studies conducted using F2A for mAb expression, mAb quality has only been characterized by western blotting. Detailed quality characterization of mAb expressed using F2A has not been reported. Only one study has compared IRES and F2A for mAb expression in transient transfections in HEK293 cells (Fang et al. 2005) , in which the vector with a HC-F2A-LC arrangement gave higher mAb expression than the vector with a HC-IRES-LC arrangement. It is unclear which element is better when the positions of HC and LC are reversed. In this work, we sought to identify whether IRES or F2A works better for expression of humanized IgG1 in gene amplifiable CHO DG44 cells. We designed four tricistronic vectors expressing the LC, HC, and dihydrofolate reductase (DHFR) in one mRNA to compare transient and stable mAb expression in CHO DG44 cells. The quality of expressed mAb, including

LC and HC polypeptide size, signal peptide cleavage, and aggregation, was characterized by western blotting, LC-MS/MS, and size exclusion chromatography (SEC), respectively.

4.3 Materials and methods

4.3.1 Cell culture and media

Parental DHFR-deficient CHO DG44 cells (Life Technologies, Carlsbad, CA) were cultured in suspension using a protein-free medium consisting of HyQ PF (Hyclone, Logan, UT) and CD CHO (Life Technologies) at a 1:1 ratio and supplemented with 1 g L^{-1} sodium bicarbonate (Sigma-Aldrich, St. Louis, MO), 6 mM glutamine (Sigma-Aldrich), 0.1% Pluronic F-68 (Life Technologies), and 1% hypoxanthine and thymine (HT) (Life Technologies). Regular passaging was carried out every 3 to 4 days in 125 mL shake flasks (Corning, NY) by diluting cells to 2×10^5 cells mL^{-1} in 25 mL fresh medium. Cell density and viability were measured using the trypan blue exclusion method on an automated Cedex counter (Innovatis, Bielefeld, Germany).

4.3.2 Vector construction

Two tricistronic vectors, L-IRES-H and H-IRES-L (Fig. 4.1), were obtained by replacing neomycin with DHFR in the previously described IRES-mediated tricistronic vectors expressing a biosimilar IgG1 mAb, Herceptin (anti-HER2) in section 3.3.2. The IRES used to link the LC and HC genes is a wild-type encephalomyocarditis virus (EMCV) IRES (IRESwt). DHFR cDNA was cloned from the pSV2-DHFR vector (ATCC, Manassas, VA). Another

two tricistronic vectors, L-F2A-H and H-F2A-L, were constructed by replacing the region of LC-IRESwt-HC with either LC-F2A-HC or HC-F2A-LC (Fig. 4.1). F2A, the furin cleavage sequence linked to the foot-and-mouth disease virus (FMDV) 2A sequence, was designed based on the literature (Fang et al. 2007). The cDNA encoding F2A was synthesized by 1st BASE (Singapore). The LC cDNA, F2A, and HC cDNA were assembled by overlapping PCR. F2A vectors expressing biosimilar IgG1 Humira (anti-TNFα) and Avastin (anti-VEGF) were generated by changing the LC and HC variable regions of the anti-HER2 vectors. The anti-TNFα and anti-VEGF variable region DNA were synthesized by Genescript (Piscataway, NJ). All restriction enzymes used were from New England Biolabs (Ipswich, MA).

(A)

L-IRES-H

H-IRES-L

L-F2A-H

H-F2A-L

(B)

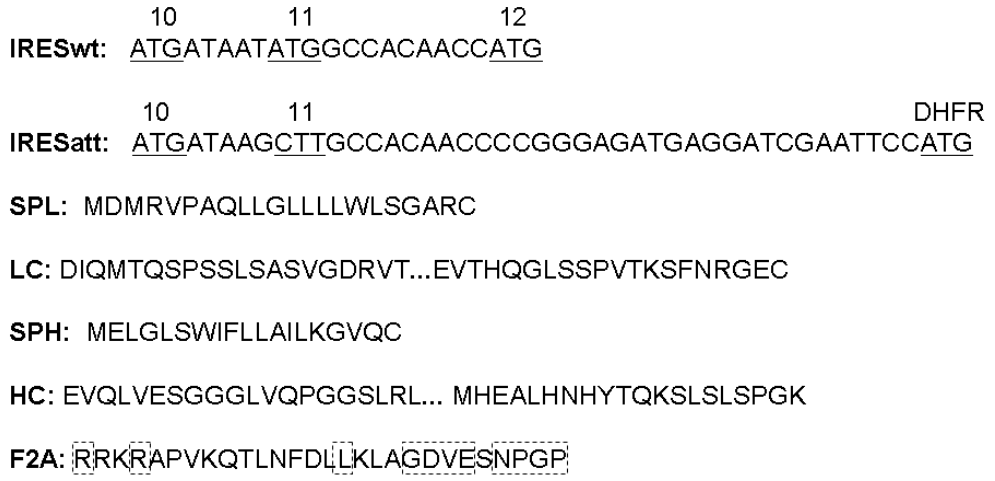

Figure 4.1Schematic representation of the four tricistronic vectors for mAb expression. (A) Structure of different vectors. (B) DNA sequences of the 3' end of IRESwt and IRESatt, amino acid sequences of signal peptide, F2A peptide, N- and C-termini of LC and HC are listed. The conserved regions of furin cleavage site and 2A peptide are highlighted in dotted boxes. CMV, human cytomegalovirus IE gene promoter; SpA, simian virus 40 early polyadenylation signal; IRESwt, wild type encephalomyocarditis virus (EMCV) internal ribosomal entry site; IRESatt, mutated EMCV IRES with attenuated translation efficiency; F2A, furin-2A peptide; LC, light chain cDNA; SP_L, LC signal peptide; HC, heavy chain cDNA; SP_H, HC signal peptide; DHFR, dihydrofolate reductase cDNA.

4.3.3 Transient transfections

Transient transfection of DG44 cells were carried out using Nucleofector kit V and program U-24 on a Nucleofector I system (Lonza, Cologne, Germany). In each transfection, 2×10^6 cells were co-transfected with 2 µg of the appropriate mAb encoding plasmid and 0.2 µg of a green fluorescence protein (GFP) encoding plasmid pMax-GFP (Lonza). The GFP plasmid acted as an internal control to account for variations in transfection efficiency. The transfected cells were then resuspended with 2 mL of HT-containing protein-free medium in 6-well suspension culture plates (Greiner Bio-One GmbH, Germany). Transfections were carried out in duplicates. At

48 h post-transfection, cells and supernatant were collected to measure GFP fluorescence intensity using a FACS Calibur (Becton Dickinson, MA) and to measure the mAb concentration using an enzyme-linked immunosorbent assay (ELISA) respectively. ELISA was performed as previously described in section 3.3.5 using capture antibody of affinity purified goat anti-human IgA+IgG+IgM (HC+LC) (KPL, Gaithersburg, MD) and detection antibody of goat anti-human IgG (Fc specific) conjugated to alkaline phosphatase (Sigma-Aldrich).

4.3.4 Stable transfections

Transfections to generate stably transfected pools were also performed using Nucleofector Kit V and program U-24 on a Nucleofector I system (Lonza). 1×10^7 CHO DG44 cells were transfected with 5 µg of BglII linearized mAb expressing plasmid. Transfection for each of the four vectors was carried out in duplicates. The transfected cells were each incubated in 2 mL HT-containing protein-free medium in a 6-well suspension culture plate for 24 h. Samples were next centrifuged at ~100×g for 5 min and cell pellets resuspended in 15 mL HT- and protein-free medium in 125 mL shake flasks to select for stable transfectants. Selection required around 2 to 3 weeks. When the stably transfected pools recovered with viability above 95%, gene amplification was induced by passaging in medium containing 50 nM methotrexate (MTX) (Sigma-Aldrich). The amplification process also required 2 to 3 weeks. Productivity of stable transfection pools at 50 nM of MTX was determined in 125 mL shake flask batch cultures. Cells were seeded in 25 mL of medium at a cell density of 2×10^5 cells mL^{-1}. Growth was monitored every day until the end of culture when viability measurements dropped below 50%.

Supernatant was collected at the end of culture and analyzed for mAb concentration using a nephelometric method on an IMMAGE 800 immunochemistry system (Beckman Coulter, Buckinghamshire, England). The IMMAGE 800 system utilized anti-human Fc region antibodies for IgG detection. The specific productivity (qmAb) was calculated as the mAb concentration divided by the integrated viable cell density (IVCD) which was determined based on the trapezoidal method (refer to section 3.3.5). Intracellular LC and HC amounts were performed as described in 3.3.6.

4.3.5 Western blotting analysis

Supernatants, which were collected from stably transfected pools at the end of culture, containing 10 ng of mAb as determined using the nephelometric method were mixed with NuPAGE sample loading buffer and reducing buffer (Life Technologies) and heated at 70°C for 2 min. Samples were loaded onto NuPAGE 4-12% Bis-Tris gel (Life Technologies) in MES buffer (Life Technologies). Precision plus protein dual color standards (Bio-Rad Laboratories, Hercules, CA) were used as molecular weight ladder and to check for transfer to the membrane. Proteins were transferred to polyvinylidene difluoride (PVDF) membranes (Life Technologies) using the iBlot system (Life Technologies). Membranes were blocked in 5% blocking milk (Bio-Rad Laboratories) in TBS with 0.1% Tween-20 (Bio-Rad Laboratories) for 1 h at room temperature and incubated overnight in HRP conjugated goat anti-human IgG Fc antibody (1:5000; Bethyl Laboratories, Montgomery, TX) and HRP conjugated goat anti-human IgG Kappa LC (1:20000; Bethyl Laboratories). Detection was done using ECL Prime (Amersham-GE Healthcare Life Sciences, Piscataway, NJ) and exposed on

Lumi-Film Chemiluminescent Detection Film (Roche Applied Science, Indianapolis, IN).

4.3.6 Purifying mAb using protein A column

mAb in the supernatant collected at the end of culture of stable transfection pools was purified by affinity chromatography using protein A column on a GE AKTA explorer 100 (GE Healthcare, Uppsala, Sweden) as previously described in section 3.3.8. This was carried out for duplicate transfected pools generated using each of the four tricistronic vectors.

4.3.7 SDS-PAGE separation of protein A purified sample

Protein A purified mAb in stable transfection pools generated using different tricistronic vectors were separated by SDS-PAGE. Prior to SDS-PAGE separation, 10 µg of each purified mAb sample was denatured by boiling in the presence of 2-mercaptoethanol (Sigma-Aldrich) at 95^{o}C for 5 min in the loading buffer containing 0.063 M Tris-HCl at pH of 6.8, 10.5% glycerol (BDH Chemicals, London, England), and 10% (w/v) SDS (Bio-Rad, Hercules, CA) and 0.1% bromophenol blue (GE Healthcare), and then ran at 15 mA for 90 min in a 10% T polyacrylamide gel (in-house created). Upon completion, the gel was immediately fixed and stained using 0.3% (w/v) Coomassie Brilliant Blue R-250 (Peirce, St. Louis, IL) in 45% methanol and 10% acetic acid, and washed with 10% methanol and 5% acetic acid to remove the background staining. The gel was scanned on Imagescanner III (GE Healthcare) and the relative intensities of the protein bands for each lane were quantified using the ImageQuant TL 7.0 software (GE Healthcare) based on the peak heights of each generated line graph.

4.3.8 LC-MS/MS analysis of protein A purified mAb

LC-MS/MS analysis was performed on each visible protein bands observed on the coomasie blue stained SDS-PAGE page gel. The bands on the gel were excised and washed in 150 µL of 50% acetonitrile (Fisher Scientific, Pittsburgh, PA) solution containing 25 mM ammonium bicarbonate. The washing solution was removed and the excised gels were dried using the Savant Speedvac (Savant Instruments, Holbrook, NY). Proteins within the excised gels were reduced by adding 25 µL of 20 mM DTT and incubated at 55°C for 60 min. Upon removal of the reducing agent, alkylation of the reduced proteins was facilitated by adding 25 µL of 55 mM iodoacetamide (Fluka, Steinheim, Germany) and incubated at room temperature in the dark for 45 min. The excised gels were then washed repeatedly in 100mM ammonium bicarbonate solution, followed by 100% acetonitrile. After drying the excised gels using the Savant Speedvac, 20 µL of trypsin (Promega, Madison, WI) at 0.04 µg μL^{-1} in 25 mM ammonium bicarbonate solution was added to each excised gel sample. The enzyme-sample mixtures were incubated with agitation at 37°C overnight. Each digested sample was extracted by adding 20 µL of acetonitrile with sonication. Each acetonitrile solution containing digested proteins was transferred to a new clean vial and dried using the Savant Speedvac. Prior to injecting the samples onto the LC-MS/MS system, each sample was reconstituted in 5 µL of aqueous buffer containing 0.1% formic acid (Sigma-Aldrich) and 1% methanol (Fisher Scientific).

LC-MS/MS analyses were performed on a Velos Orbitrap mass spectrometer (Thermo Fisher Scientific, San Jose, CA) coupled to a

nanoAcquity UPLC system (Waters, Milford, MA) fitted with a 180 µm x 20 mm Symmetry C18 peptide trap (Waters) and a 75 µm x 200 mm BEH130 C18 1.7-µm particle size analytical column (Waters). Depending on the peptide concentration of each sample, 1 to 2 µL of peptide digest was injected. Peptides were resolved by applying a linear binary gradient from 2 to 35% solvent B at 300 nL min^{-1} over 60 min at 35 °C, where solvent A and B were 0.1% (v/v) formic acid in Milli-Q water (Millipore, Billerica, MA) and 0.1% formic acid in acetonitrile, respectively. To minimize sample carryover, a dedicated column wash run (10 to 95% B in 30 min) followed by column re-equilibration (2% B for 30 min) was performed prior to the next sample injection. The nano-ESI source was fitted with a 30-µm stainless steel nano-bore emitter (Thermo Fisher Scientific) with 1.7 kV applied near the tip. The MS instrument method used was the data-dependent acquisition mode that specified each orbitrap survey scan (at resolution 60,000) to be linked to a maximum of 10 MS/MS events; each with maximum ion trap fill time of 25 ms and isolation window of 2 m/z. The threshold for triggering an MS/MS was set at 500 counts. The ion trap CID fragmentation employed an activation time of 10 ms, q value of 0.25 and normalized collision energy of 35%. Charge state screening was enabled, with unknown and singly charged states excluded. Dynamic exclusion was enabled with a list size of 500 and exclusion time of 60 s.

Acquired LC-MS/MS data were processed by the Proteome Discoverer 1.3 software (Thermo Fisher Scientific) using the Sequest search engine. The peptide and fragment ion mass tolerances used were ± 5 ppm and ± 0.5 Da, respectively. The specified search parameters were carbamidomethylation of

cysteine as fixed modification, oxidation of methionine as dynamic modification and tryptic digestion with 2 missed cleavages. Depending on the tricistronic vector configuration used (Fig. 4.1), each sample LC-MS/MS data was searched against the relevant full protein sequence to determine the actual expressed protein sequence for each excised gel band, with its corresponding sequence coverage calculated.

4.3.9 Aggregation analysis of protein A purified mAb

The aggregation of protein A purified mAb collected at the end of culture of stable transfection pools was determined using size exclusion chromatography (SEC) coupled to a UV-visible detector and a dynamic light scattering detector. Analysis was carried out for duplicate pools generated using each tricistronic vector. The instrument setup consisted of a HPLC system (Shimadzu, Kyoto, Japan) as previously described in section 3.3.10. The hydrodynamic radius measured by the light scattering detector was used to calculate the molecular weight of the different compounds present under each peak. The different fractions were assigned respectively to aggregates, monomer and fragments based on their measured molecular weights and elution time. The small rightmost peaks are a result of components in the buffer which the protein A purified samples are eluted in.

4.4 Results

4.4.1 Design of IRES- and F2A-mediated tricistronic vectors

An anti-HER2 IgG1 biosimilar was first used as a model mAb to compare IRES and F2A for mAb expression level and quality. Four

tricistronic vectors were designed to express the anti-HER2 LC, anti-HER2 HC, and DHFR under the control of one CMV promoter (Fig. 4.1). LC and HC were arranged in either the first or the second cistron. The two vectors in which LC and HC are linked by a wild type EMCV IRES (IRESwt) are designated as L-IRES-H and H-IRES-L, respectively. Vectors in which LC and HC are linked by F2A are designated as L-F2A-H and H-F2A-L, respectively. The DHFR selection marker downstream of an attenuated EMCV IRES (IRESatt) in the third cistron was used for all the vectors for fair comparison. Application of IRESatt on DHFR will reduce its expression and can enhance stringency of selection for high producers (Ng et al. 2007). Tight coupling of product gene and selection marker in one mRNA can reduce occurrence of non-expressing clones (Rees et al. 1996; Ng et al. 2007; Ho et al. 2012).

4.4.2 Comparing IRES and F2A for mAb expression

IRES and F2A were first compared for transient expression levels of anti-HER2 in 6-well plate cultures (Fig. 4.2A and B). As cap-dependent translation of the first cistron is more efficient than IRES-driven translation, the L-IRES-H vector will express LC in excess, and the H-IRES-L vector will express HC in excess. Consistent with previous reports that LC is more favorable for mAb expression (Gonzalez et al. 2002; Schlatter et al. 2005; Li et al. 2007; Ho et al. 2012), we observed that the mAb expression level from the L-IRES-H vector to be around double that from the H-IRES-L vector. A previous study had reported that mAb expression from a F2A vector similar to H-F2A-L was greater than that from a EMCV IRES vector similar to H-IRES-L in transient transfections performed using HEK293 cells (Fang et al. 2005).

We observed that both F2A-mediated tricistronic vectors, showed higher mAb expression levels than those from the IRES-mediated tricistronic vectors regardless of LC and HC positions. L-F2A-H had the highest expression with titers at around 500 ng mL^{-1}, three-fold higher than the titer of the best performing IRES vector, L-IRES-H.

Stable anti-HER2 expressions for the four vectors were next compared using shake flask batch cultures (Fig. 4.3A). Specific mAb productivity (qmAb) from the four vectors displayed a similar trend as that in transient transfections. The qmAb of the L-IRES-H stable pools was 3.9 pg $cell^{-1}$ day^{-1} (pcd). The H-IRES-L stably transfected pools had lower qmAb of 2.7 pcd, which was 70% of the L-IRES-H stable pools. Both F2A-mediated tricistronic vectors still exhibited higher qmAb than the IRES-mediated tricistronic vectors. Compared to L-IRES-H, L-F2A-H qmAb was 1.4-fold and H-F2A-L was 1.2-fold higher, reaching 5.4 pcd and 4.4 pcd, respectively.

Stably transfected pools generated using the four vectors also exhibited differences in growth (Fig. 4.3B). The L-IRES-H stable pools grew fastest, followed by pools generated using the L-F2A-H, H-F2A-L and H-IRES-L vectors. The viability of the former two pools dropped below 50% at day 10, one day earlier than the latter two pools. The L-IRES-H stable pools also had highest peak cell density and IVCD, followed by L-F2A-H, H-F2A-L, and H-IRES-L. Due to the lower qmAb and even lower IVCD as compared to L-IRES-H, the H-IRES-L stable pool had 50% lower titer (Fig. 4.3C). The lower IVCD of the F2A pools also resulted in titers of L-F2A-H dropping to 1.1-fold higher than L-IRES-H, and H-F2A-L dropping lower than L-IRES-H.

(A)

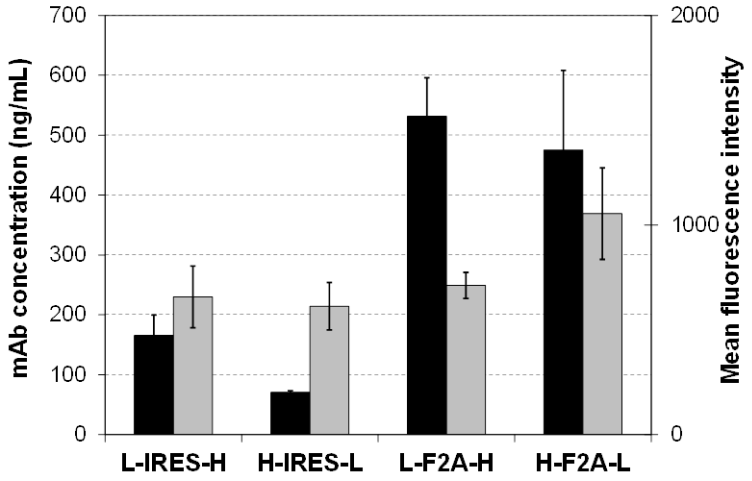

(B)

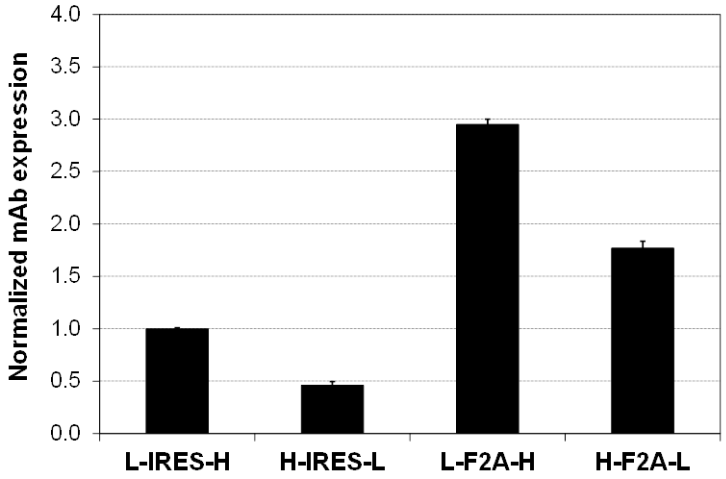

Figure 4.2 Comparison of the four tricistronic vectors for mAb expression in transient transfections. CHO DG44 cells were co-transfected with an appropriate mAb expressing vector containing IRES or F2A between the LC and HC gene and a GFP expressing vector. At 48 h post-transfection, supernatant and cells were collected for analysis of mAb concentration using ELISA and GFP expression using FACS, respectively. (A) Sample results of measured mAb concentration (black bars) and GFP mean fluorescence intensity (gray bars). Each value and standard deviation were obtained from a set of duplicate transfections. (B) Normalized mAb expression for each vector. Results represent mAb concentration measured in the culture supernatant normalized to firstly the internal control, GFP expression, to normalize the transfection efficiency and next mAb expression from the L-IRES-H vector. Each point represents the average and standard deviation of two measurements from two independent sets of duplicate transfections.

We next evaluated the stable intracellular LC:HC ratio for each vector using ELISA (Fig. 4.3D). The two IRES vectors L-IRES-H and H-IRES-L had ratios of around 4.5 and 0.5 respectively. This was expected as expression of the genes downstream of IRES was lower due to less efficient IRES translation. Surprisingly the F2A vectors L-F2A-H and H-F2A-L had ratios of 2.8 and 5.4 with significant variation. Based on the mechanism of F2A, ratios closer to one were expected. Follow-up western blotting of the products should help shed some light on these results.

(A)

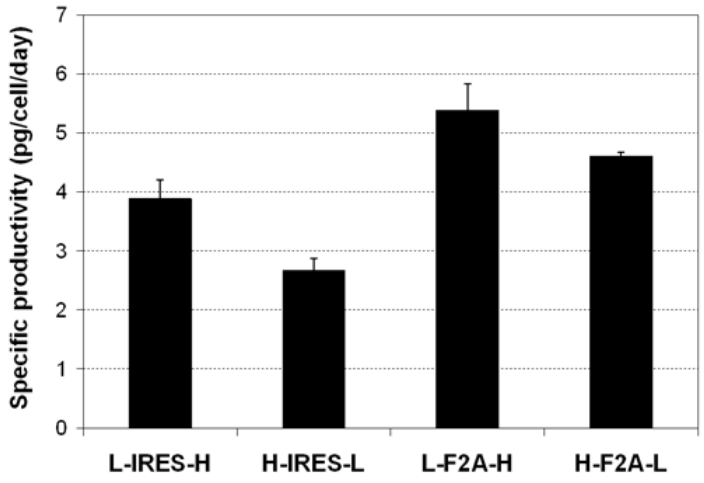

(B)

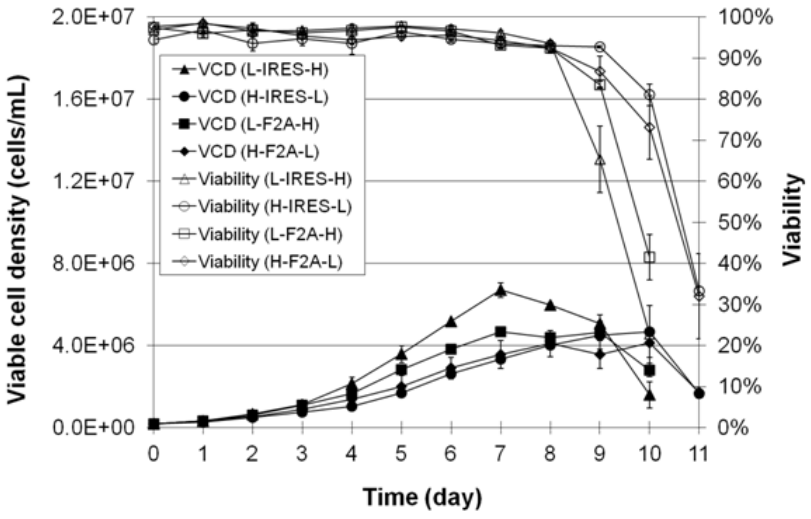

(C)

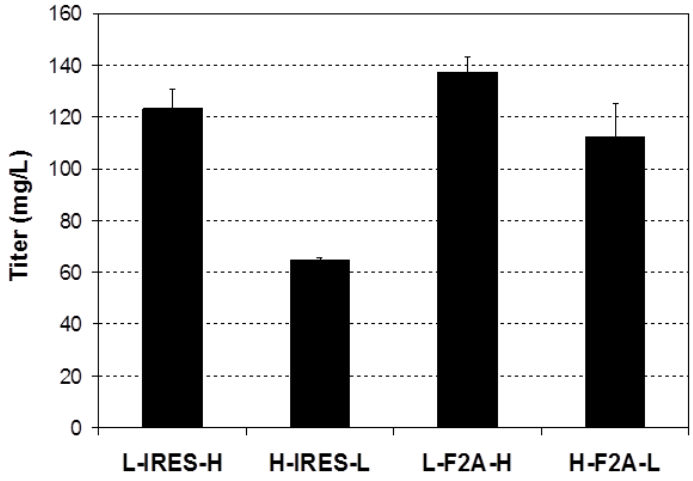

(D)

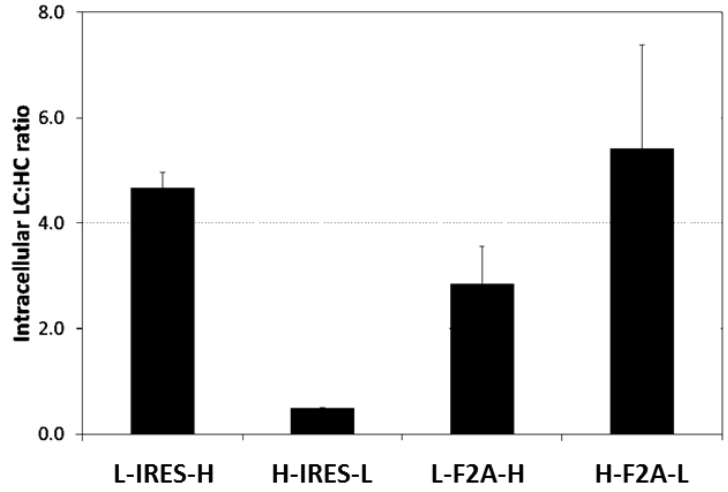

Figure 4.3 Comparison of the four tricistronic vectors for mAb expression in stable transfections. Stably transfected pools were generated by transfection of CHO DG44 cells with different tricistronic vectors containing either IRES or F2A between the LC and HC gene. Each pool was characterized for (A) specific mAb productivity (qmAb) measured in pg/cell/day (pcd), (B) growth data collected including viable cell density (VCD) and culture viability, (C) titer and (D) intracellular LC:HC ratio. Each point represents the average and standard deviation of two measurements of two stably transfected pools.

4.4.3 Western blotting analysis of mAb products expressed by IRES and F2A

Supernatant collected at the end of culture of CHO DG44 stably transfected pools generated using each of the tricistronic vectors were first analyzed under non-reducing conditions to characterize the products being secreted (Fig. 4.4A). Product from the L-IRES-H vector contained complete IgG1 monomers HC_2LC_2, LC_2 dimer, and LC monomer, a sign that the L-IRES-H vector expressed LC in excess. Product from the H-IRES-L vector consisted of HC_2LC_2 complete IgG1 and HC_2 dimers, providing evidence of expression of excess HC. Products from both F2A-mediated tricistronic vectors presented a smear with molecular weight greater than 100 kDa. The fractions above 150 kDa could correspond to mAb aggregates, and those around 150 kDa could be degraded IgG1 monomers, suggesting that mAb expressed from F2A was not stable. The two thin bands expressed from the L-F2A-H and H-F2A-L vectors with molecular weights of 100 kDa could be HC_2, and the one band from the L-F2A-H vector with a molecular weight of 80 kDa could be a fusion protein of LC+F2A+HC.

Western blotting analysis of reduced products in the supernatant was next performed to identify the different components in the IgG1 being produced using the various vectors (Fig. 4.4B). Two bands were detected within supernatants from the two IRES-mediated tricistronic vectors, L-IRES-H and H-IRES-L. Their molecular weights corresponded to the standard HC and LC, respectively. Comparing the relative intensities of these two bands indicated that the L-IRES-H vector expressed LC in excess and the H-IRES-L vector expressed HC in excess. Interestingly, three bands were detected in

reduced products from the L-F2A-H vector. The top band presents a molecular weight of approximately 80 kDa, which is equal to the sum of the molecular weights of LC, F2A, and HC suggesting that it is a fusion protein of LC+F2A+HC. The middle band exhibited similar size to the standard HC. The bottom band had slightly greater size than the standard LC, indicating a possible failed removal of 2A polypeptide residue by furin cleavage. Four bands were detected in products from the H-F2A-L vector. The top two bands could be the fusion proteins of HC+F2A+LC and HC+F2A based on their molecular weights. The other two bands had similar sizes to the standard HC and LC, respectively. Presence of these fusion proteins could also be affecting binding of the detection antibodies used for ELISA, causing the unexpected LC:HC ratios detected.

(A)

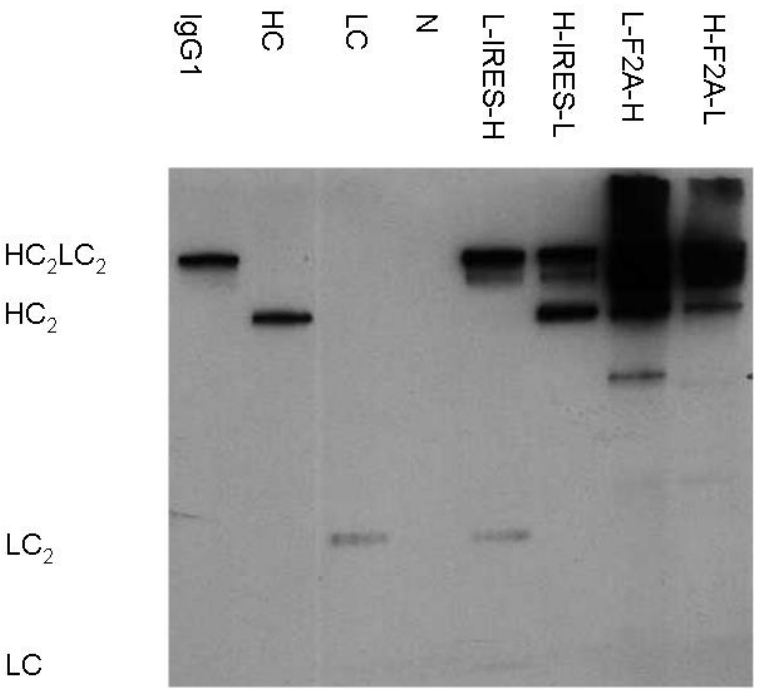

(B)

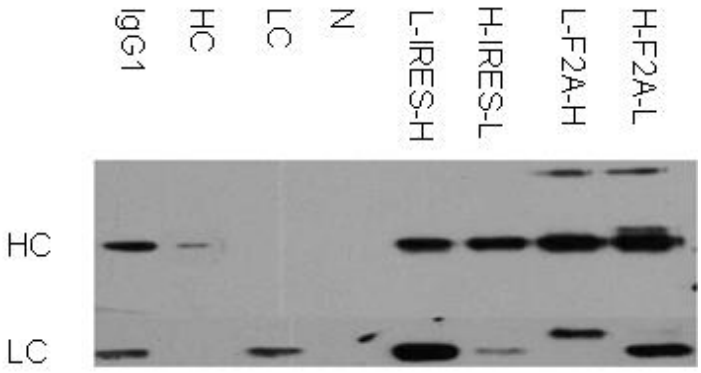

Figure 4.4 Western blot analysis of supernatant in stably transfected pools generated using the four tricistronic vectors. Each sample of crude supernatant was analyzed under both (A) non-reducing and (B) reducing conditions by western blot. A commercial human affinity purified myeloma Ig1 (Sigma-Aldrich) and supernatants from cells transfected with either a vector expressing only HC or a vector expressing only LC were used as positive control, and supernatant from non-transfected cells as negative control (N). All blots shown are only from the first replicates generated as duplicates were observed to exhibit the same product patterns.

IRESwt has three ATGs at the 3' end, which are designated as ATG-10, ATG-11, and ATG-12 as described previously (Kaminski et al. 1990). ATG-12 is used as the start codon of mAb gene for higher translation efficiency (Davies and Kaufman 1992; Kaminski et al. 1994; Qiao et al. 2002; Bochkov and Palmenberg 2006; Martin et al. 2006). Translation initiation of EMCV IRES-driven gene primarily occurs at ATG-11 and partially at ATG-12 (Davies and Kaufman 1992). Four extra amino acid residues, MATT, will be attached to the signal peptide of the IRES-driven LC or HC in those polypeptides which translation initiation occurs at ATG-11. "Self-cleavage" of 2A occurs between the last two amino acids, GP. Following self-cleavage, P will be attached to the signal peptide of LC or HC downstream of 2A and the rest of the 2A residues will attach to the C-terminus of the upstream gene.

Addition of a furin cleavage site upstream of 2A can eliminate the 23 amino acid residues which would otherwise be attached to the HC or LC (Fang et al. 2005). When HC is arranged upstream of F2A, design of a furin cleavage sequence with a second basic amino acid, such as RRKR, allowed carboxypeptidases to cleave both the RR residues left after furin cleavage together with the K on the C-terminus of HC (Fang et al. 2007).

To characterize the protein more accurately than just using western blotting, the reduced protein A purified mAb samples from duplicate pools of each vector were separated on SDS-PAGE (Fig. 4.5) and the bands were excised for LC-MS/MS analysis. The estimated molecular weight of each band, the polypeptide sequence as determined by peptide mapping and its associated sequence coverage, and the relative abundance of the expressed mAb chains are shown in Table 4.1.

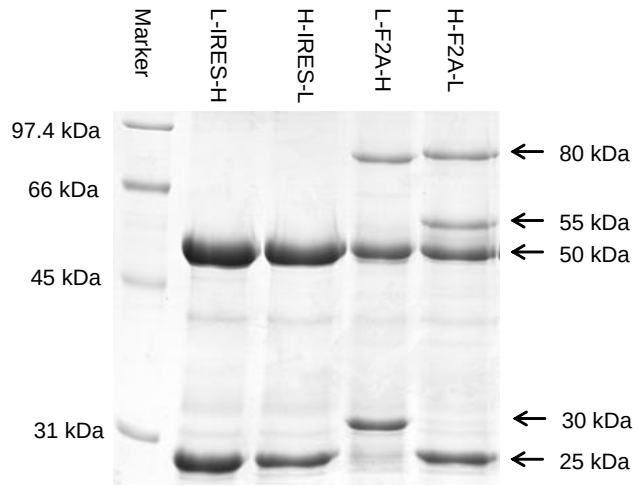

Figure 4.5 SDS-PAGE analysis of purified mAb in stably transfected pools generated using the four tricistronic vectors. Protein A purified supernatant was reduced and analyzed on a SDS-PAGE gel. Protein bands were visualized by coomasie blue staining. All gels shown are only from the first replicates generated as all duplicates were observed to exhibit the same product patterns.

Table 4.1 Relative abundance analysis of reduced antibody HC and LC variants by densitometry and sequence identity confirmation by peptide mapping.

Each point represents the average and standard deviation of two measurements from two stable transfection pools. "ND" means not detected.

Gel band (kDa)	Peptide mapping detected sequence (#Amino acids)	L-IRES-H		H-IRES-L		L-F2A-H		H-F2A-L	
		Sequence coverage (%)	Relative abundance (%)	Sequence coverage (%)	Relative abundance (%)	Sequence coverage (%)	Relative abundance (%)	Sequence coverage (%)	Relative abundance (%)
25	LC (214)	87.0 ± 1.4	47.5 ± 2.1	87.5 ± 6.4	44.0 ± 0.0	ND	ND	ND	ND
	SP_L+LC(236)	ND	ND	ND	ND	ND	ND	79.0 ± 1.4	39.0 ± 2.8
30	LC+F2A (242)	ND	ND	ND	ND	86.5 ± 12.0	37.0 ± 0.0	ND	ND
50	HC (450)	70.5 ± 0.7	52.5 ± 2.1	72.0 ± 0.0	56.0 ± 0.0	ND	ND	71.0 ± 1.4	32.0 ± 0.0
	SP_H+HC (469)	ND	ND	ND	ND	74.0 ± 0.0	42.0 ± 0.0	ND	ND
55	SP_H+HC+F2A (496)	ND	ND	ND	ND	ND	ND	45.5 ± 29.0	12.5 ± 0.7
80	LC+F2A+SP_H+HC (711)	ND	ND	ND	ND	67.0 ± 2.8	21.0 ± 0.0	ND	ND
	SP_H+HC+F2A+SP_L+LC (733)	ND	ND	ND	ND	ND	ND	62.5 ± 4.9	16.5 ± 2.1

The excised gel bands from the L-IRES-H or H-IRES-L vector at molecular weights of 25 and 50 kDa were confirmed by LC-MS/MS analyses as LC and HC polypeptides, respectively. The excised gel bands from the L-F2A-H vector corresponding to molecular weights of 30, 50, and 80 kDa were LC and F2A fusion proteins (LC+F2A), HC with incorrect or uncleaved signal peptide (SP_H+HC), and fusion proteins of LC+F2A+SP_H+HC, respectively. The four excised gel bands from the H-F2A-L vector with molecular weights of 25, 50, 55 and 80 kDa were LC with incorrectly cleaved signal peptide (SP_L+LC), HC, SP_H+HC+F2A, and SP_H+HC+F2A+SP_L+LC, respectively. No incorrect signal peptide cleavage was observed on LC and HC in the IRES generated pools. The four extra amino acids which might attach to the signal peptides during translation initiation at IRES ATG-11 did not seem to affect the signal peptide cleavage. In contrast, incorrectly cleaved signal peptides were detected in both LC and HC expressed downstream of F2A as indicated by the detection of SP_L+LC and SP_H+HC with signal peptide residues attached. This is possibly due to attachment of the extra P from F2A to the signal peptide.

Cleavage of F2A was less efficient in products expressed from the L-F2A-H vector than the H-F2A-L vector. Occurrence of LC+F2A+HC or HC+F2A+LC fusion proteins indicates cleavage failure at both furin and 2A recognition sites. Existence of LC+F2A or HC+F2A indicates successful cleavage at the 2A recognition site but cleavage failure at the furin recognition site. 21% of the LC and HC expressed from the L-F2A-H vector existed as a LC+F2A+SP_H+HC fusion protein. The rest were cleaved into similar abundances of LC+F2A (37%) and SP_H+HC (42%) as expected. 16.5% of

product expressed from the H-F2A-L vector was detected as SP_H+HC+F2A+SP_L+LC fusion proteins. The remaining was cleaved into products consisting of 32% HC, 12.5% SP_H+HC+F2A, and 39% SP_L+LC. The amount of SP_L+LC was similar to the sum of HC and SP_H+HC+F2A.

4.4.4 Aggregation analysis of mAb products expressed by IRES and F2A

Aggregation of protein A purified anti-HER2 IgG1 mAb produced in stable transfection pools was analyzed and quantified using SEC coupled to a UV and a dynamic light scattering detector. As replicate pools gave identical chromatograms, only one representative UV chromatogram is shown for each vector (Fig. 4.6A to D). Molecular weight of each peak was calculated based on their respective hydrodynamic radius. Peaks with average molecular weight greater than the complete IgG1 monomer were grouped as aggregates and those with lower molecular weight were grouped as fragments. Relative mass amounts of aggregates, monomers and fragments were determined using the respective peak area under the UV chromatograms. The IgG1 monomer, aggregate and fragment distributions for each vector design is shown in figure 4.6E. The level of aggregates was less than 1% in products from the L-IRES-H vector. In contrast, products from H-IRES-L vector had 28% of aggregates and 13% of mAb fragments. Products from both F2A-mediated vectors had approximately 45% of aggregates and less than 1% of mAb fragments. In contrast to multiple aggregate peaks observed in H-IRES-L (Fig. 4.6B), F2A-mediated vectors only had one aggregate peak (Fig. 4.6C and D), suggesting different aggregation mechanisms. Interestingly, aggregates in H-IRES-L did not show up on western blots performed using the unpurified supernatant while aggregates in the F2A vectors were visible (Fig. 4.4A). This is possibly

due to differences in the nature and components of the aggregates. The amount of fragments detected also appeared lower than the levels observed during western blotting in 4.4A. The fragments could possibly be composed mainly of incompletely processed peptides which do not bind as well to protein A and could be washed off during the wash step of protein purification. The fragments are thus not recovered during elution and do not show up in the chromatogram.

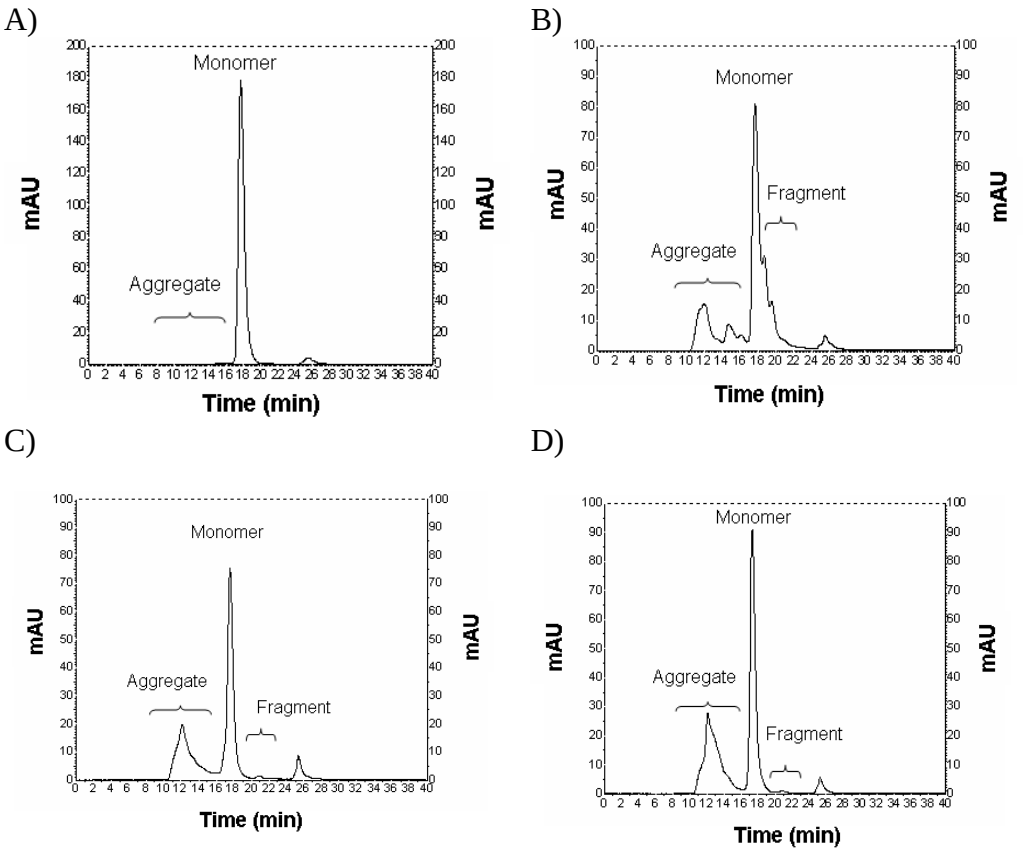

E)

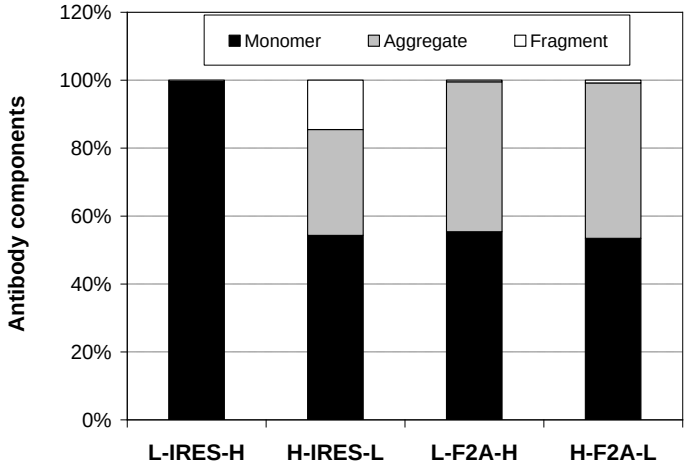

Figure 4.6 SEC analysis of protein A purified mAb in stably transfected pools generated using the four tricistronic vectors. Species within protein A purified mAb were separated by SEC followed by the identification and quantification of species by UV detection and light scattering, respectively. Analysis was done for duplicate stable transfection pools generated using each of the four tricistronic vectors. As results were consistent, only one typical chromatogram of the first pools analyzed from UV detector for vector (A) L-IRES-H, (B) H-IRES-L, (C) L-F2A-H, (D) H-F2A-L, are shown. (E) Quantitative comparison of aggregates, complete IgG1 monomers and incomplete IgG1 fragments of four vectors for different species. Each bar in figure E represents the average and standard deviation of four measurements from two stable transfection pools.

4.4.5 Cleavage efficiency of F2A for other IgG1 mAbs

Previous reports which utilized F2A for expressing mAb did not report any issues with 2A peptide cleavage under their tested conditions (Fang et al. 2005; Fang et al. 2007; Jostock et al. 2010; Davies et al. 2011) while we observed inefficient F2A cleavage for anti-HER2 IgG1 expression in CHO DG44 cells. To investigate whether cleavage efficiency is mAb product dependent, we expressed two more IgG1 mAbs, anti-TNFα and anti-VEGF, in transient transfections and checked for cleavage efficiency using western blotting under reducing conditions (Fig. 4.7). Bands corresponding to LC+F2A+HC fusion protein, HC and LC+F2A fusion protein was observed

for reduced anti-HER2 IgG1 expressed using the L-F2A-H vector and similar LC+F2A+HC, HC+F2A, HC and LC bands were observed for H-F2A-L. The products detected for anti-HER2 in the transient transfections are similar to that in products from stable transfections from both F2A vectors as shown earlier in figure 4.4B. Fusion proteins and uncleaved F2A residues were also observed for reduced samples of anti-TNFα and anti-VEGF. Reduced product bands similar to anti-HER2 were observed for the blots of both L-F2A-H and H-F2A-L except for an extra smaller band corresponding to LC for product from the L-F2A-H vectors in addition to the LC+F2A product band.

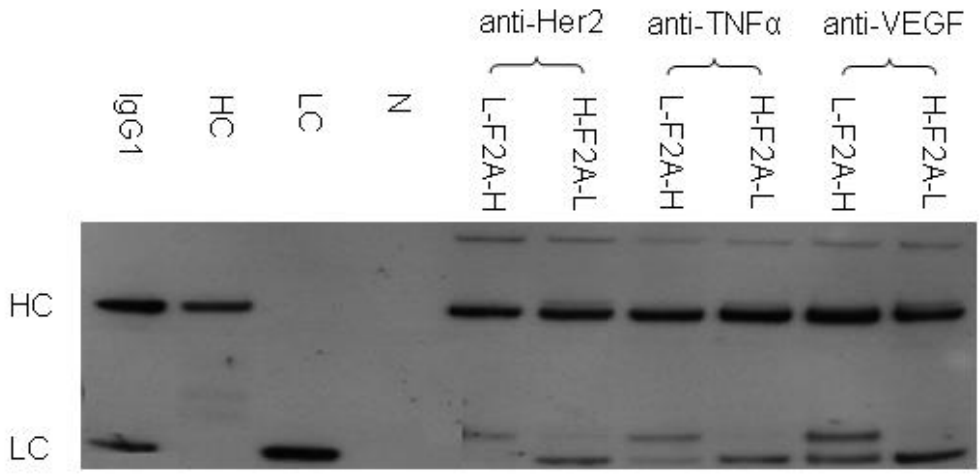

Figure 4.7 Western blot analysis of transiently expressed anti-HER2, anti-TNFα and anti-VEGF IgG1 mAbs. CHO DG44 cells were transfected with an appropriate mAb expressing tricistronic vector expressing anti-HER2, anti-TNFα, and anti-VEGF. At 48 h post-transfection, supernatant was collected for western blotting under reducing condition. The mAb loaded into each lane is identical as determined by ELISA. A commercial human affinity purified myeloma Ig1 (Sigma-Aldrich) and supernatants from cells transfected with either a vector expressing only HC or a vector expressing only LC were used as positive control, and supernatant from non-transfected cells as negative control (N). All blots shown are only from the first replicates generated as duplicates were observed to exhibit the same product patterns.

4.5 Discussion

We designed four tricistronic vectors to compare the use of EMCV IRES and F2A for IgG1 mAb expression level and quality in CHO DG44 cells. The mAb quantification methods that we used in this work, ELISA and nephelometric methods are based on detection antibodies against the Fc region of the product mAb. Besides the complete IgG monomer, these assays would detect any components containing HC, such as high molecular weight aggregate and HC_2 dimer, resulting in falsely high mAb titers. By measuring mAb in crude supernatant with these two assays, F2A vectors appeared to give higher mAb expression than IRES vectors in both transient and stable transfections. However, after considering the product distribution of complete IgG1 monomers, aggregates and fragments detected during SEC analysis (Fig. 4.6E), the amount of actual IgG1 monomer was significantly lower using H-IRES-L and the F2A constructs (Fig. 4.8). Actual titer in L-IRES-H stable transfection pools was unchanged and the highest at 123 mg L^{-1}, while titer of the H-IRES-L, L-F2A-H and H-F2A-L stable transfection pools dropped to 32 mg L^{-1}, 75 mg L^{-1} and 60 mg L^{-1} respectively.

Arrangement of LC as the first cistron gave higher mAb expression than arrangement of HC as the first cistron in both IRES- or F2A-mediated tricistronic vectors. This is understandable for the IRES-mediated tricistronic vectors as the L-IRES-H vector expressed LC in excess (Fig. 4.4) and extra LC is favorable for mAb expression (Gonzalez et al. 2002; Schlatter et al. 2005; Li et al. 2007; Ho et al. 2012). Both L-F2A-H and H-F2A-L vectors expressed LC and HC in similar amounts (Table 4.1). One possible explanation is LC+F2A from the L-F2A-H vector can still be processed and

does not create any burden to the cell's protein folding and assembly machinery while HC+F2A from the H-F2A-L vector has detrimental effects. Another possible explanation is that LC+F2A+HC and HC+F2A+LC mRNAs have different secondary structures, and the former one has higher translation efficiency and thus yielding higher mAb expression level.

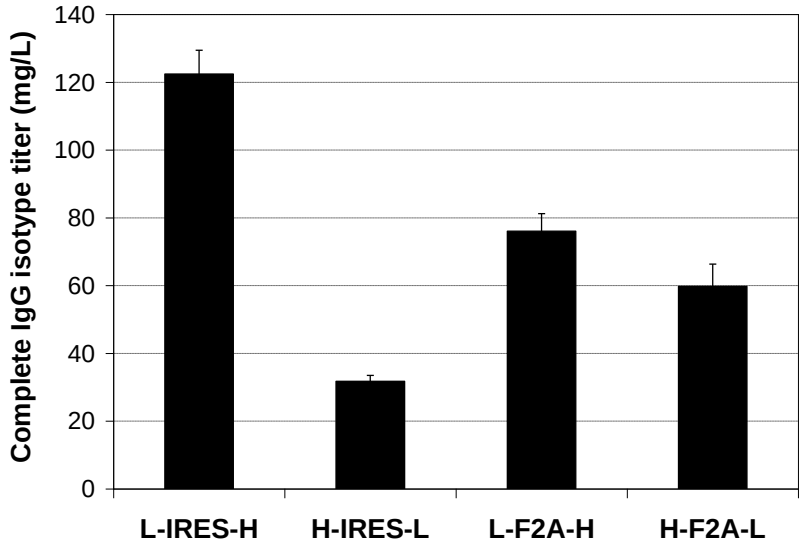

Figure 4.8 Estimation of the actual amount of complete IgG1 monomer produced in stably transfected pools generated using the four tricistronic vectors. The actual monomer amount was estimated based on the product titers measured by the nephelometer and the relative monomer peak area observed on SEC as shown in figure 4.6E. Each point represent the average and standard deviation of two measurements from two stably transfected pools.

Secretory proteins like the IgG1 LC and HC are bound by signal recognition particles (SRP) at their signal peptide sequence as they emerge from the ribosome within the cytosol and are targeted to SRP receptors of translocon complex on the ER membrane for translocation into the ER (Walter and Blobel 1983). Each signal peptide sequence is separated into three

regions: a hydrophilic and net-positively charged N-terminal region, a central hydrophobic region and a polar C-terminal region (von Heijne 1985). Studies have shown that an increase in the hydrophobicity of the N-terminal region can cause cleavage of the signal peptide to shift upstream (Nothwehr and Gordon 1990). In our vector designs, four additional amino acid residues, MATT, would be added to the IRES driven LC or HC peptides and one additional proline residue would be added for F2A driven peptides. Hydrophobicity index of the 19 amino acid HC signal peptide (SP_H), HC signal peptide with MATT residues (MATT+SP_H) and HC signal peptide with an additional P (P+SP_H) were analyzed using the Kyte and Doolittle hydrophobicity index (Fig. 4.9) (Kyte and Doolittle 1982). MATT residues would cause a lower net change in hydrophobicity of 0.533 as compared to addition of only one P residue causing a change of -1.067. This larger increased difference in hydrophobicity due to the P residue from F2A could be the reason causing incorrect cleavage of the signal peptide. Another reason for poor signal peptide cleavage could be due to the F2A reaction being inhibited by interactions between the nascent protein structure and the translocon complex (De Felipe et al. 2010). SRP binding to the signal peptide downstream of F2A does not occur and in turn proper signal peptide cleavage is inhibited. It is also interesting to note that signal peptide cleavage prediction using SignalP 4.1 (Petersen et al. 2011) did not indicate any changes to the cleavage site even with the additional residues.

Incomplete cleavage of F2A had been observed when used with various fluorescent reporter proteins (De Felipe et al. 2010; Chan et al. 2011). Previous reports of using F2A successfully for mAb expression had been in

CHOK1 (Fang et al. 2007; Jostock et al. 2010), CHOK1SV (Davies et al. 2011) and HEK 293 (Fang et al. 2005) cells and none of the reports stated that they were using humanized IgG1 as model mAb. This is the first report of using the F2A for humanized IgG1 expression in CHO DG44 cells and the possibility of cell and product specificity affecting cleavage should also not be discounted. All three humanized IgG1 products expressed using the F2A system in CHO DG44 cells exhibited the presence of incompletely processed LC and HC products showing that the processing issues was not specific to only the anti-HER2 mAb that was initially characterized. While the 2A peptide cleavage was an issue regardless of product or arrangement, we made some interesting observations regarding the furin cleavage. Firstly, the different cistron arrangements affected the furin cleavage efficiency. Arrangement of LC upstream of F2A inhibited cleavage efficiency more than arrangement of HC upstream of F2A. This can be seen from the greater abundance of uncleaved LC+F2A in the L-F2A-H pools as compared to HC+F2A in the H-F2A-L pools in the western blot (Fig. 4.4B). Secondly, furin cleavage appeared to be dependent on 2A processing as we did not observe fusion proteins with F2A attached to the N-terminal of the protein translated from the second cistron, e.g. F2A+HC or F2A+LC. Thirdly, the furin cleavage efficiency was higher for anti-TNFα and anti-VEGF as compared to anti-HER2 in the L-F2A-H vectors. It is unclear why this was observed as the C-terminal ends of the LC attached to the furin cleavage sequence were the same for all three IgG1 products. One reason could be due to differences in structure of the complete IgG1 monomers due to different variable regions. IgGs are typically fully assembled as HC_2LC_2 in the ER

(Feige et al. 2010) while furin endoproteases are mainly localized to the golgi (Nakayama 1997). The differences in structure of the three products within the golgi could affect furin cleavage efficiency. Less variation was observed for furin cleavage of the HC possibly due to the furin cleavage site being located further away from the differing Fab region.

The L-IRES-H was the best vector design for expressing IgG1 mAb in CHO DG44 cells among the four versions of tricistronic vectors. While the F2A system is a promising design, issues with 2A processing and furin cleavage affected product yield and quality. Further optimization of the type of 2A peptide to be used, addition of GSG linkers and the furin cleavage sequence need to be performed (Fang et al. 2007; Szymczak-Workman et al. 2012). It would be interesting for another comparison to be carried out after optimization.

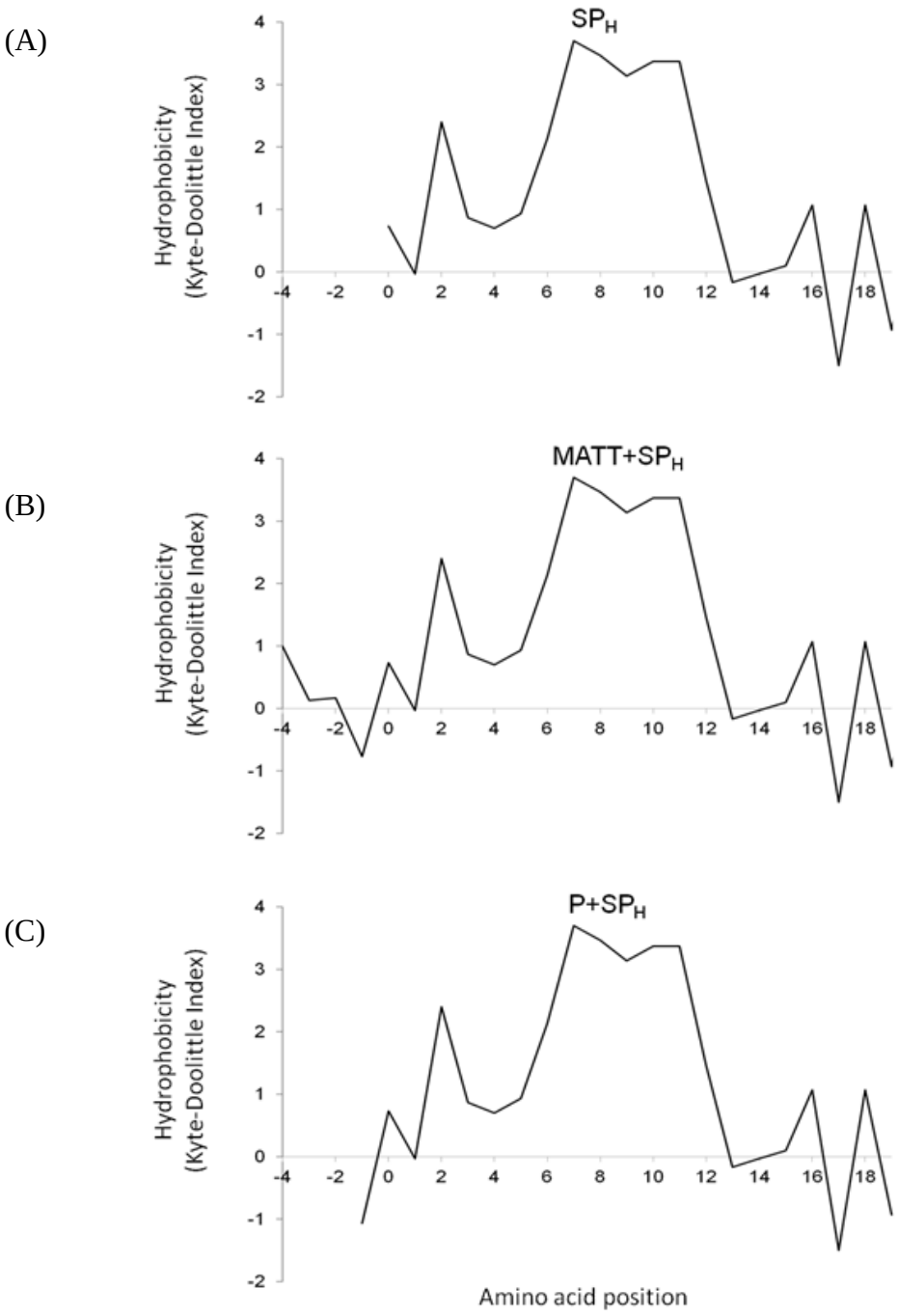

Figure 4.9 Hydrophobicity analysis of HC signal peptide attached with MATT and P amino acid residues at the N-terminal end. (A) Wild type HC signal peptide (SP_H). (B) SP_H with MATT amino acid residues attached to the N-terminal end ($MATT+SP_H$). (C) SP_H with amino acid P attached to the N-terminal end ($P+SP_H$). The 19 amino acids of the HC signal peptide are shown as amino acids 0 to 19. Additional residues at the N-termini due to IRES and F2A processing are numbered starting from -1. Kyte-Doolittle index is computed using Protscale online tool (http://web.expasy.org/cgi-bin/protscale/protscale.pl).

Chapter 5: Using IRES vectors to control LC:HC ratio for studying effect of the ratio on mAb expression in stably transfected CHO cells

The effect of LC:HC ratio on mAb expression has been demonstrated in in-silico and transient experiments but not in stably transfected conditions . In this chapter, we used four variations of IRES vectors to control LC and HC at different ratios in stable transfections. Due to the reported issues of using F2A in chapter 4, redesigned IRES vectors were used to generate cell lines with equal amounts of LC and HC. MAb expression level and quality at the different ratios are determined and discussed.

*The following was first published in "**Ho, S. C. L.**, Koh, E. Y. C., van Beers, M., Mueller, M., Wan, C., Teo, G., Song, Z., Tong, Y. W., Bardor, M. and Yang, Y. (2013). "Control of IgG LC:HC ratio in stably transfected CHO cells and study of the impact on expression, aggregation, glycosylation and conformational stability." Journal of Biotechnology **165**(3–4): 157-166".*

5.1 Abstract

Immunoglobulin G (IgG), the most common class of commercial monoclonal antibodies (mAbs), exists as multimers of two identical light chains (LC) and two identical heavy chains (HC) assembled together by disulfide bridges. Due to the kinetics of mAb assembly, it is suggested that expression of LC and HC in equal amounts is not optimal for IgG production. We designed a set of vectors using internal ribosome entry site (IRES) elements to control LC and HC expression. Using those IRES-mediated vectors, it was demonstrated that the intracellular LC:HC ratio of stable IgG expressing Chinese hamster ovary (CHO) cell pools can be controlled effectively at four different ratios of 3.4, 1.2, 1.1, 0.3. The stable pools were used to study the impact of LC:HC ratio on mAb expression and quality. Gene amplification was most effective for pools with excess LC and generated the highest mAb titers among the transfected pools. When LC:HC ratio was greater than one, more than 97% of the secreted products were IgG monomers. The products also have similar N-glycosylation profiles and conformational stabilities at those ratios. For pools which presented a lower LC:HC ratio (0.3), monomers only constituted half of the product with the other half being aggregates and mAb fragments. High mannose-type N-glycans increased while fucosylated and galactosylated glycans decreased significantly at the lowest LC:HC ratio. Product stability was also adversely affected.

5.2 Introduction

Monoclonal antibodies (mAbs) are the best-selling class of biologics on the market (Aggarwal 2011). The most common type of mAb, immunoglobulin G (IgG), is composed of two identical light chains (LC) and two identical heavy chains (HC) linked by disulfide bonds. Assembly in the endoplasmic reticulum (ER) involves interactions between partly folded HC dimers, LC monomers, BiP chaperones and catalysts like protein disulfide isomerase (PDI) (Lee et al. 1999; Vanhove et al. 2001; Gonzalez et al. 2002; Feige et al. 2010). Although there is an equal numbers of LC and HC in each IgG mAb, having LC and HC peptides at a balanced ratio may not be optimal for its expression (Gonzalez et al. 2002; Davies et al. 2011). Mathematical modeling of the IgG mAb synthesis pathway indicated that assembly time decreases as the relative amount of LC to HC increases (Gonzalez et al. 2002). It has been shown that for CHO cells, excess LC is favorable for transient mAb expression (Li et al. 2007; Yang et al. 2009; Ho et al. 2012) and high producing stably transfected cell lines typically express LC in excess (Schlatter et al. 2005; Lee et al. 2009; O'Callaghan et al. 2010). Most natural lymphoid cells and IgG expressing myeloma cells also express light chain in excess (Shapiro et al. 1966; Baumal and Scharff 1973). Incompletely formed heavy chains can be prone to aggregation (Vanhove et al. 2001; Ellgaard and Helenius 2003) and there is evidence that higher relative HC level is a possible cause for aggregation (Vanhove et al. 2001; Lee et al. 2009). N-glycosylation of HC takes place co-translationally within the ER and complements the assembly of secreted mAb (Sakaguchi 1997). The degree of late glycan modifications occurring in the golgi apparatus is influenced by the protein

conformation as well (Krambeck and Betenbaugh 2005; Butler 2006). The ratio of LC:HC expression may thus affect mAb glycosylation as the ratio affects both mAb folding and assembly.

MAb expression in CHO cells can be achieved by having LC and HC genes under the control of individual promoters and either co-transfected on separate vectors or on the same vector (Trill et al. 1995; Costa et al. 2010). Ratio of LC: HC expression can be controlled by changing the relative amounts of each plasmid of two co-transfected vectors carrying LC and HC, respectively (Lee et al. 1999; Schlatter et al. 2005). Controlling LC:HC ratio by this approach is affected by variations in transfection efficiencies. It is also not appropriate for studies in stably transfected cells as vector integration is highly random and the integration site has significant effect on the expression level (Fussenegger et al. 1999; Mielke et al. 2000). Control LC:HC ratio can also be achieved using one large vector carrying all the required expression cassettes and varying the relative expression using promoters (Yahata et al. 2005) or poly-adenylation signals (Yang et al. 2009) with different strengths. Although all genes are integrated at the same site, one issue that arises with having multiple promoters in close proximity is transcriptional interference (Eszterhas et al. 2002). Incomplete vectors can also get integrated due to vector fragmentation and affect the gene ratios (Barnes et al. 2007; Chusainow et al. 2009; Ng et al. 2010).

Single vectors with genes linked together in one transcript would allow all genes to be integrated at the same site for stricter control of relative LC to HC expression. This can be achieved by using internal ribosome entry site (IRES) elements to express all genes of interest in one transcript under a single

promoter. When placed between two genes, IRES allows ribosomes to bind in the middle of the transcript for cap-independent translation of the second gene (Mountford and Smith 1995; Martinez-Salas 1999). IRES driven translation of the second gene is less efficient than a typical cap-dependent translation, resulting in lower peptide levels for the second gene. IRES elements can be used to control the relative level of two genes. The technique has been applied to transient studies of mAb expression in CHO cells where an intracellular excess of HC was observed to decrease IgG yield (Li et al. 2007). We have previously used an IRES-mediated tricistronic vector to maintain LC:HC at a constant ratio of excess LC in stable clones (Ho et al. 2012). Those clones exhibited high expression levels, low aggregation and consistent N-glycosylation profiles possibly due to the controlled LC:HC ratio.

Reports where LC:HC ratio is controlled for studying the impact on mAb expression and quality have mainly been performed in transient transfections (Schlatter et al. 2005; Li et al. 2007; Yang et al. 2009). However, the industry relies mainly on stably transfected cell lines for therapeutic mAb production. There are currently no reports of controlling LC:HC ratio at different levels in stably transfected mAb producing cell lines for study of both mAb expression and quality. In this work, we designed four IRES-mediated tricistronic vectors to control LC:HC at different ratios. Depending on the position of LC, HC and the selection marker gene on the vector, stably transfected pools exhibited either excess of LC, excess of HC or similar levels for both. Product titers and quality characteristics such as aggregation, N-glycosylation and conformational stability were compared. Three biosimilar mAbs, Herceptin (anti-HER2 IgG1), Humira (anti-TNFα IgG1) and Avastin

(anti-VEGF IgG1), were generated at various LC:HC ratios. MAb produced at the highest LC:HC ratio and of the best quality. As ratio decreased, it was observed that expression dropped, aggregates increased and other quality attributes changed.

5.3 Materials and methods

5.3.1 Cell culture and media

DHFR deficient CHO DG44 cells (Life Technologies, Carlsbad, CA) were grown in protein free media (PFM) as described in section 4.3.1. Cells were passaged every 3 to 4 days by diluting the cultures to 2×10^5 cells mL^{-1} in fresh media. Cell viability and density were determined by Trypan blue exclusion method using a Vi-Cell XR cell viability analyzer (Beckman Coulter, CA).

5.3.2 Construction of vectors for control of LC:HC ratio and cell engineering

Vectors were designed as shown in figure 5.1. LIHID and HILID were constructed by replacing the neomycin phosphotransferase gene of two previously described IRES-mediated tricistronic vectors in section 3.3.2 with a dihydrofolate reductase (DHFR) gene. DILIH was constructed by modifying LIHID. Firstly, IRES-DHFR-pA was replaced with only a pA sequence. Next, IRES-LC was cloned from HILID and used to replace LC. Finally, DHFR was inserted between the CMV promoter and the first IRES. DIHIL was constructed in a similar method through modification of HILID.

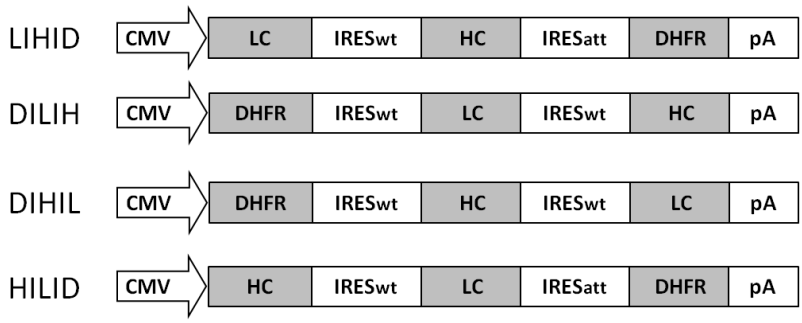

Figure 5.1 Schematic representation of IRES-mediated tricistronic vectors for mAb expression. CMV, human cytomegalovirus IE gene promoter; pA, simian virus 40 early polyadenylation signal; IRESwt, wild type encephalomyocarditis virus (EMCV) internal ribosomal entry site; IRESatt, mutated EMCV IRES with attenuated translation efficiency; LC, light chain cDNA; HC, heavy chain cDNA; DHFR, dihydrofolate reductase.

IRES-driven expression is known to be lower than cap-dependent expression (Martinez-Salas 1999; Hennecke et al. 2001). This characteristic of IRES was used to vary the LC:HC ratio. We had shown earlier that by placing the LC downstream of the promoter and the HC downstream of the wild-type IRES (IRESwt) all stably transfected clones expressed LC:HC at a ratio of around 4:1 (section 3.4.3). For vectors DIHIL and DILIH, DHFR is in the first cistron downstream of the promoter and both LC and HC expression were driven by identical IRESwt. LC and HC expression was expected to be similar for these designs. Vector HILID, with promoter driven HC expression and IRES driven LC expression should have a LC:HC ratio less than one due to HC being expressed in excess of LC.

Vectors for cell engineering experiments to reduce aggregates were modified from LIHID vector. DHFR sequence was changed to a Zeocin selection marker cloned from a pCDNA 3.1/Zeo vector (Life Technologies).

Subsequently, LC-IRES-HC was replaced with either LC or CHO BiP cDNA (Genbank: GCA_000223135.1).

5.3.3 Transfection and cell line generation

All transfections were performed using Nucleofection kits from Lonza (Cologne, Germany) following the manufacturer's instructions. Transient transfections were performed using 2×10^6 cells, 2 µg of each plasmid and 0.2 µg of pMAX-GFP (Lonza). Transfected cells were placed in 6-well suspension culture plates containing 2 mL of HT supplemented with PFM. After 48 hours, supernatant was collected for quantification of mAb expression by an enzyme linked immunosorbent assay (ELISA) as previously described in section 3.3.5 and cells were collected to measure GFP fluorescent intensity using a FACS Calibur (Becton Dickinson, MA).

Stable transfections were performed using 1×10^7 cells and 5 µg of each linearized plasmid in duplicates. Cells were transferred to 6-well plates containing 2 mL of HT supplemented with PFM for 24 hours. Next, cells were inoculated to shake flasks and the media was replaced with 25 mL of PFM for selection. Cells were seeded at densities of 4×10^5 cells mL^{-1} during the selection process. Selection and recovery was considered complete for each selection step when viability was above 95%. Stepwise methotrexate (MTX) amplification was then carried out with concentrations of 50 nM, 250 nM, 1000 nM, 5000 nM and 25000 nM. MTX concentrations of 50 nM, 250 nM, 1000 nM were used for LIHID and HILID. Higher concentrations up to 25000 nM MTX were used for DIHIL and DILIH as their promoter driven DHFR expression were higher than the IRES driven expression for LIHID and HILID. Batch cultures were seeded at 2×10^5 cells mL^{-1} and maintained until

viability dropped to 50% for supernatant collection. The supernatant was used for product quantification and characterization. Cell pellets were collected during either day 3 or 4 for analysis of intracellular LC and HC polypeptide abundance. Titers were measured using an IMMAGE 800 immunochemistry nephelometer (Beckman Coulter, Buckinghamshire, England) and cell counts were carried out using the Vi-Cell XR (Beckman Coulter).

5.3.4 Intracellular LC and HC polypeptide ELISA

Cell pellets were washed with phosphate buffered saline (PBS; 1st BASE, Singapore) and lysed in RIPA buffer (Thermo Scientific, Waltham, MA) supplemented with ProteoBlock protease inhibitor cocktail (Fermentas, Thermo Scientific). Concentrations of LC and HC polypeptides were quantified using ELISA as previously described in section 3.3.5 and 3.3.6.

5.3.5 Western blotting of cell lysates and supernatant

Cell lysates prepared for ELISA and supernatant collected at the end-point of batch cultures were used for western blot analysis. NuPAGE sample loading buffer and reducing buffer (Life Technologies) were added as required for each sample. Non-reduced and reduced samples were heated at 70 °C for 2 min and 10 min, respectively. Protocols were as listed in section 4.3.5.

5.3.6 Purifying mAb using protein A column

Purification was performed using a GE *Ä*KTA Explorer 100 (GE Healthcare, Uppsala, Sweden) and UV detection at 280 nm. Buffers used differ from that described in 3.3.8 to improve the purification process. Cleared culture supernatant was loaded on a Tricorn 5/150 Protein A column packed with MabSelect SuRe (GE Healthcare) pre-equilibrated using PBS. Sample

was injected at a flow rate of 3 mL/min. A terminator wash buffer of 2 M sodium chloride (Merck, Darmstadt, Germany), 250 mM imidazole (Merck), 10 mM EDTA (Sigma-Aldrich), 4 M urea (Sigma-Aldrich) adjusted to pH 7.0 was passed through the column followed by an elution buffer of 100 mM acetate (Sigma-Aldrich) and 100 mM arginine (Sigma-Aldrich) at pH 3.5. Eluted samples were neutralized using 1 M Tris (Sigma-Aldrich) and column was regenerated using 0.1 M glycine (Merck) adjusted to pH 2.5.

5.3.7 Aggregation and glycosylation analysis of purified mAb

Aggregation of protein A purified mAb was analyzed immediately after the purification using size exclusion chromatography (SEC) in order to avoid formation of aggregates during storage similar to the protocol listed in section 3.3.10. The N-glycan distribution was analyzed using matrix assisted laser desorption ionization-time of flight mass spectrometry (MALDI-TOF MS) using methods listed in section 3.3.9.

5.3.8 Conformational stability analysis of purified mAb

Differential scanning calorimetric (DSC) measurements were performed using a VP-Capillary DSC system (Microcal Inc, Northampton, MA, USA) which was equipped with tantalum cells with an active volume of 130 µL. The samples were analyzed at a concentration of 1 mg mL^{-1} in 50 mM HEPES buffer at pH 7.0 using a scan range from 35 to 100°C and a scan rate of 1°C per minute. HEPES buffer at pH 7.0 was used as a blank reference. Data were analyzed using Origin 7.0 software (OriginLab Corporation, Northampton, MA, USA). Thermograms were corrected by subtraction of buffer blank scans and normalization to the protein concentration. The

transition curves were fitted using a non-2-state model to obtain the temperature midpoint of transition (T_m).

5.4 Results

5.4.1 Anti-HER2 mAb expression using the four IRES-mediated vectors designed

We designed four IRES-mediated vectors to control LC:HC ratio in stably transfected IgG expressing pools. Transient expression levels of a model anti-HER2 biosimilar mAb using the four vectors were first evaluated (Fig. 5.2A). LIHID vector was used as a reference and GFP was co-transfected as a control for transfection efficiency variations. Pools transfected with the LIHID vector which was designed to express LC in excess had the highest expression, followed by vectors designed for balanced LC:HC ratio. DIHIL and DILIH had expression levels about half that of LIHID. HILID transfected pools had the lowest transient expression at only 30% that of LIHID. These observations fit well with earlier reports that excess LC is beneficial to mAb expression in CHO cells (Schlatter et al. 2005; Yang et al. 2009).

The vectors were transfected into CHO DG44 cells and underwent stepwise MTX amplification to generate stably transfected pools. Titer was measured after each amplification step using a nephelometer (Fig. 5.2B). Amplification of stable pools generated by LIHID was most effective. There was 3-fold titer increase when MTX was stepped up from 50 nM to 250 nM, followed by a 1.5-fold titer increase to reach a final titer of 380 mg L^{-1} at 1000 nM MTX. Titers of stably transfected pools generated using DIHIL and

DILIH increased gradually during MTX amplification, reaching 110 mg L^{-1} and 79.5 mg L^{-1}, respectively, at 25000 nM MTX. Titer for HILID was 68.3 mg L^{-1} at 50 nM MTX and reached a peak of 83 mg L^{-1} at 250 nM MTX with no improvements at 1000 nM MTX.

LIHID pools at 50 nM MTX, DIHIL and DILIH pools at 5000 nM MTX and HILID pools at 50 nM MTX had similar titers and were chosen for subsequent studies of LC:HC ratios and the effects on mAb quality. Western blot analysis of supernatant from pools generated by each vector was performed using anti-LC and anti-Fc detection antibodies (Fig. 5.2C). For LIHID, IgG monomer (HC_2LC_2) was the main product detected together with some excess of LC dimers (LC_2). Those were possibly due to expression of excess LC. Only IgG monomers were detected for pools DIHIL and DILIH. Product from HILID consisted of IgG monomer and HC dimers (HC_2) reflecting an excess of HC production.

(A)

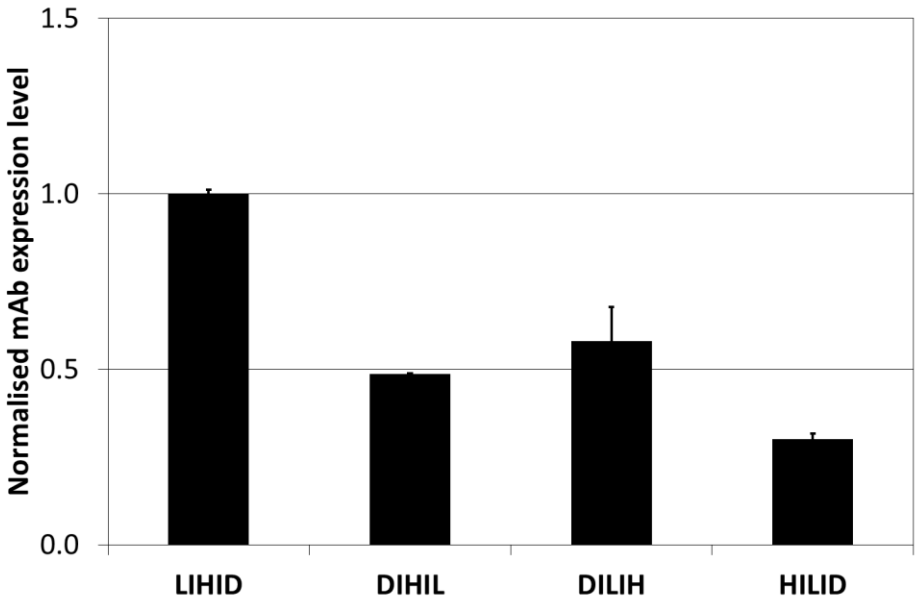

(B)

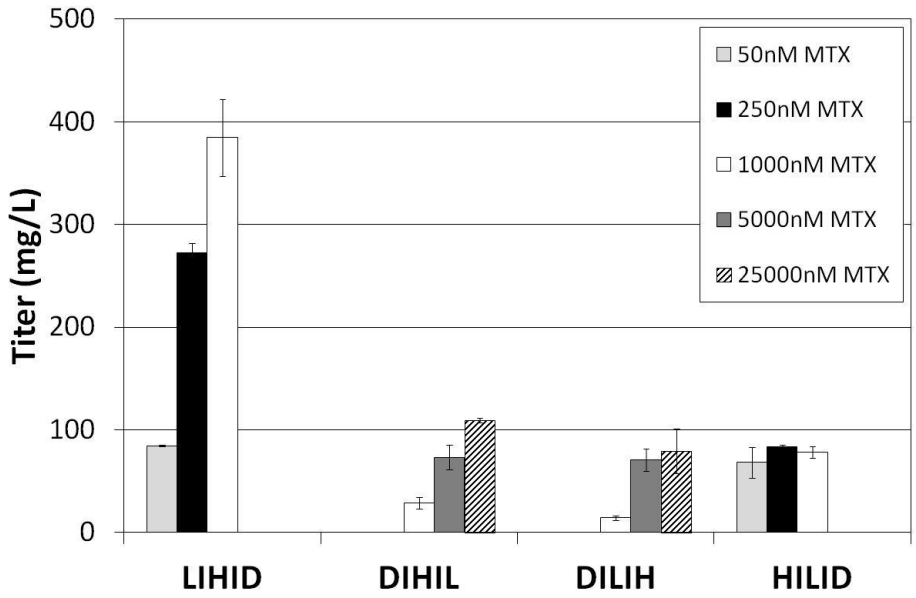

(C)

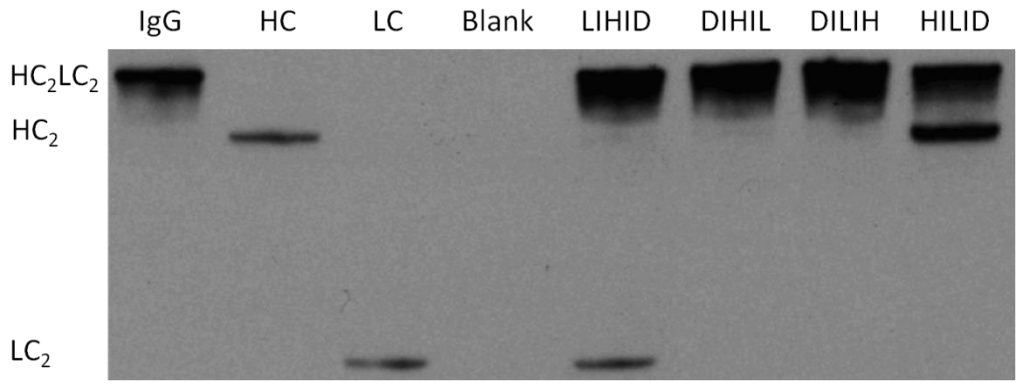

Figure 5.2 Comparison of IRES-mediated tricistronic vectors for expression of anti-HER2 in transient and stable transfections. (A) Comparison of transient expression of CHO DG44 cells transfected with each of the four vectors, LIHID, DIHIL, DILIH and HILID. mAb expression was quantified by ELISA 48 h post transfection and normalized to an internal GFP control. GFP normalized expression was further normalized to LIHID results. (B) Titers of stably transfected pools generated using each tricistronic vector. The transfected cells next underwent selection and amplification at various MTX concentrations. (C) Western blot analysis of non-reduced supernatants in stably transfected pools from LIHID at 50 nM MTX, DIHIL and DILIH at 5000 nM MTX and HILID at 50 nM MTX. Each point in (A) and (B) represents the average and standard deviation of duplicate measurements from two independently transfected pools.

5.4.2 Stable intracellular LC:HC ratio

Intracellular LC and HC peptide abundances in LIHID stable pools at 50 nM MTX, DIHIL and DILIH stable pools at 5000 nM MTX, and HILID stable pools at 50 nM MTX were measured using ELISA to obtain the LC:HC ratio for each vector (Fig. 5.3A). LIHID exhibited a LC:HC ratio of 3.43. This high ratio indicated that there was an excess of intracellular LC and is a possible reason for LC_2 detection in the supernatant. DIHIL had a LC:HC ratio of 1.24 while DILIH had a ratio of 1.12. A ratio of 0.32 was measured for HILID pools, indicating that these pools had excess intracellular HC. This excess HC could be a reason for the detection HC_2 products.

(A)

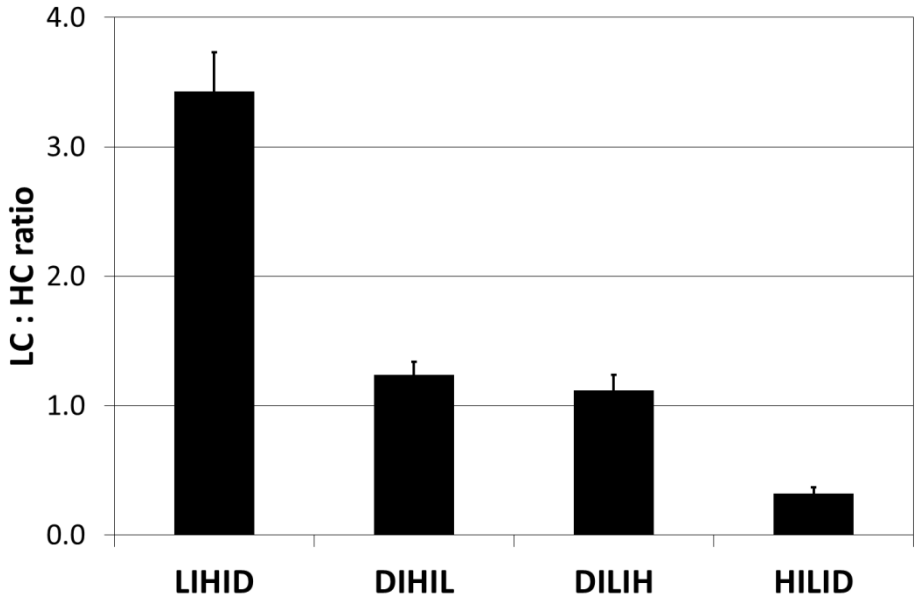

(B)

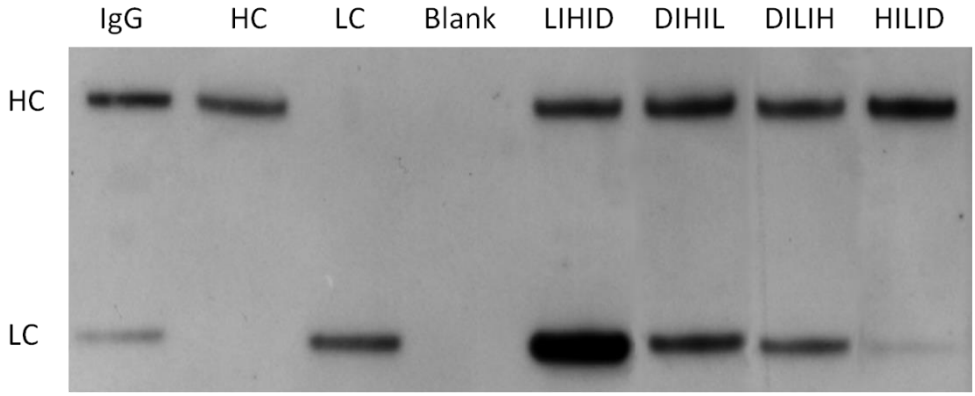

(C)

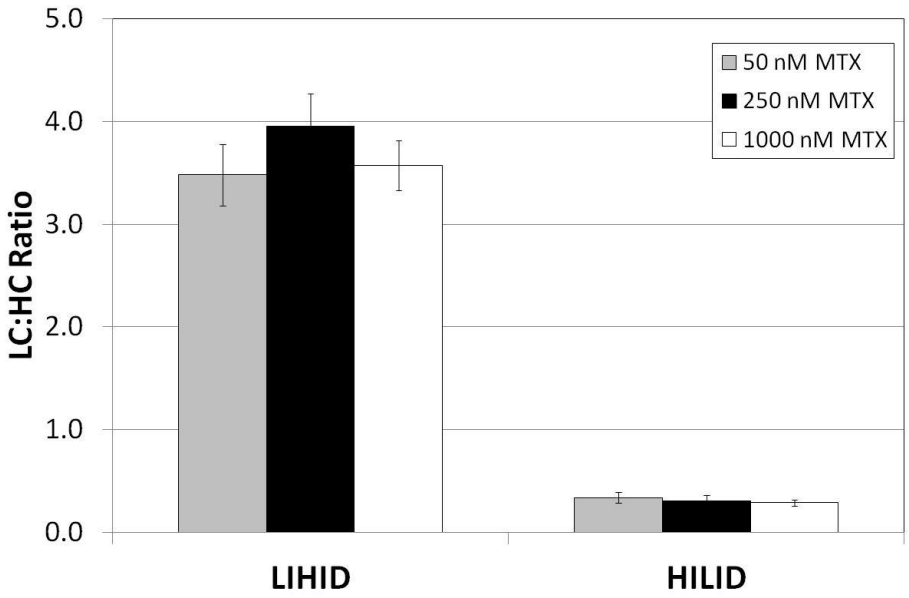

Figure 5.3 Comparison of intracellular LC:HC ratio for CHO DG44 stably expressing anti-HER2 IgG. (A) ELISA analysis of the ratios of intracellular abundance of LC over HC polypeptides in stably transfected. LC:HC ratio was calculated as the concentration of intracellular LC polypeptides determined by ELISA divided by the HC polypeptides. (B) Western blot analysis of intracellular abundance of LC and HC polypeptides in stably transfected pools under reducing conditions. (C) LC:HC ratio for LIHID and HILID at different MTX concentrations. Each point in (A) and (C) represents the average and standard deviation of duplicate measurements of lysates from two independently transfected stable pools.

Western blot was performed using the same intracellular lysates to verify the LC:HC ratio differences determined by ELISA between the samples (Fig. 5.3B). Samples were reduced before analysis and detection was performed using antibodies for both LC and HC monomers. The band intensity corresponding to HC was similar for all four samples as sample loading was based on the amount of IgG Fc measured during ELISA. LIHID presented the darkest LC band, corresponding to the highest LC:HC ratio. At a similar amount of HC, DIHIL and DILIH had fainter LC bands than LIHID, indication of lower LC levels. HILID with the lowest LC:HC ratio also had the faintest band corresponding to the LC species. Intensities of all the bands observed were as expected when compared to the ELISA results.

To further ascertain that we were able to control LC:HC ratio using IRES-based vectors, LC:HC ratios for LIHID and HILID at 250 MTX and 1000 MTX were also measured (Fig. 5.3C). LC:HC ratios for LIHID were 3.96 and 3.58 at 250 nM MTX and 1000 nM MTX, respectively. HILID had ratios of 0.31 and 0.29 at the higher MTX concentrations. LC:HC ratios remained similar for all pools at all the MTX concentrations analyzed, showing that the vector designs were indeed able to control LC:HC ratio.

5.4.3 Aggregation at different LC:HC ratios

Protein A purified supernatant was analyzed by size exclusion chromatography and species were identified using UV detectors (Fig. 5.4). The respective amounts of IgG monomer, higher molecular weight aggregates and lower molecular weight mAb fragments were quantified by calculating the peak areas detected by the UV detector. When there was a greater excess of LC in LIHID pools, 99.6% of the product was IgG monomers while

aggregates and incomplete mAb fragments contributed only to 0.2% each (Fig. 5.4A). Product from DIHIL with LC:HC ratio of 1.24 was similar to LIHID with 99.3% monomers, 0.5% aggregates and 0.2% fragments (Fig. 5.4B). Aggregation increased to 2.2% when LC:HC ratio dropped to 1.12 in DILIH (Fig. 5.4C). Monomers and fragments contributed 97.5% and 0.2%, respectively. For HILID with excess HC, the aggregates and incomplete mAb fragments increased to 13.5% and 26.5%, respectively. Only around 60% of the total product was composed of IgG monomers (Fig. 5.4D). Average distributions of each product type at each ratio measured from two independently transfected pools are shown in figure 5.4E.

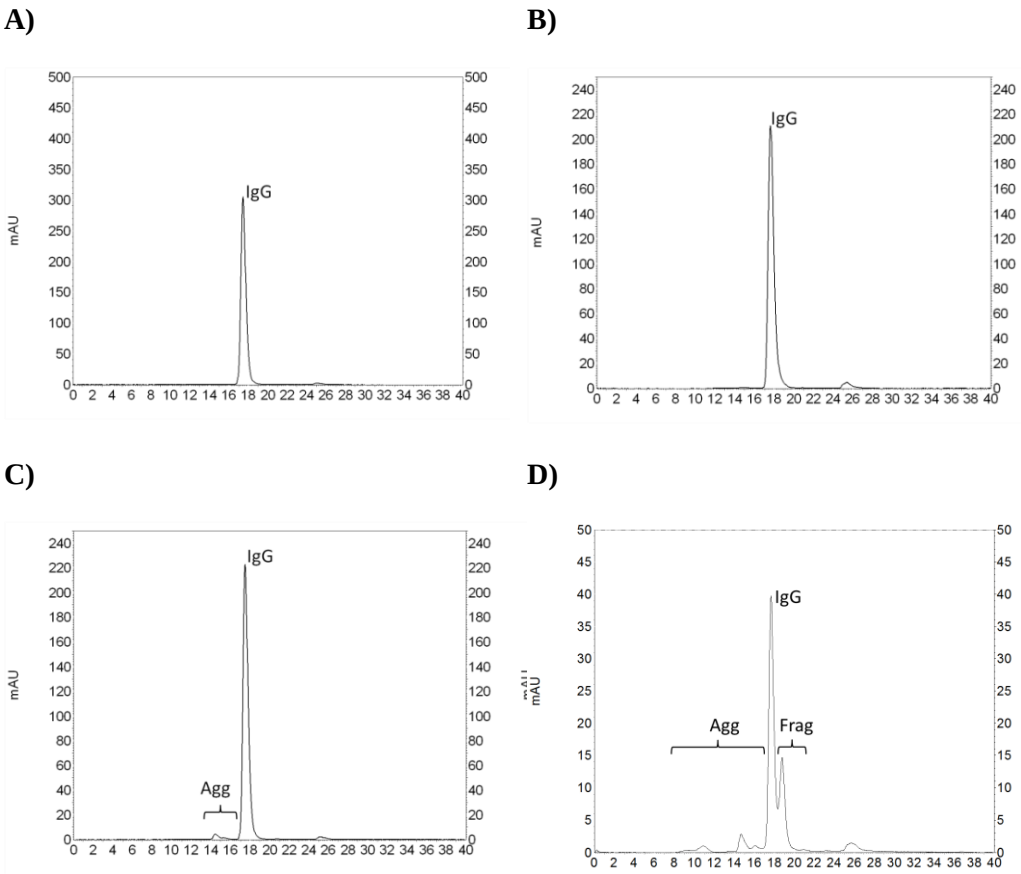

(E)

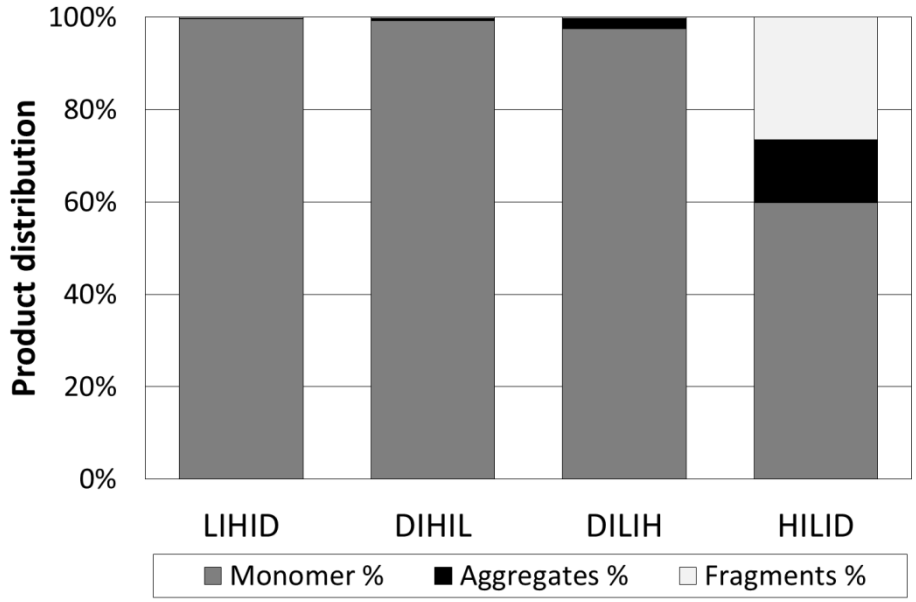

Figure 5.4 Representative SEC chromatograms and distribution of the monomer, aggregates and fragments for the mAb produced with the different versions of the IRES-mediated tricistronic vectors. SEC chromatograms were registered using a UV detector and anti-HER2 mAb purified from stably transfected pools generated using (A) LIHID, (B) DIHIL, (C) DILIH, (D) HILID vectors. Agg: Aggregates, IgG: Full mAb monomer, Frag: mAb fragments. (E) Quantitative comparison of the different species detected for each mAb vector. Protein A purified product from two independently transfected pools for each vector were quantified but only the chromatogram of the first pool is shown in (A) to (D) as the replicates are highly similar. Values shown in (E) are the average of two measurements of two independently generated stable pools.

5.4.4 Glycosylation at different LC:HC ratios

MALDI-TOF mass spectrometry was used to identify the glycans on protein A purified anti-HER2 IgG. Relative quantification was calculated based on the MALDI-TOF analysis of permethylated N-glycans. To summarize the results, N-glycans were categorized into high mannose type, sialylated, fucosylated, G0 (complex type glycans not bearing any terminal galactose), G1 (bearing one terminal galactose) and G2 (bearing two terminal galactose) N-glycan species (Fig. 5.5). A similar set of around 20 glycans was

observed for mAb generated at ratios of 3.43, 1.24 and 1.12, consisting as expected of mainly high mannose type N-glycans and bi-antennary complex type N-glycans (Fig. 5.5A, B and C). Vector HILID, which generated pools with LC:HC ratio of 0.32, exhibited 34 different glycans (Fig. 5.5D for mass peaks below 2500, 5.5E for peaks above 2500) with the appearance of more tri-antennary and tetra-antennary complex type N-glycans not seen previously. Relative quantification of the different major N-glycans showed variations between the different LC:HC ratios (Fig. 5.5F). For example, the percentage of high mannose increased with decreasing LC:HC ratios. LIHID with a LC:HC ratio of 3.43 had the lowest high mannose fraction, 14.5%. A slight increase to 19% was observed in DIHIL and DILIH pools with LC:HC ratios controlled at 1.24 and 1.12, respectively, while a dramatic increase of high mannose fraction to 32.95% was observed in HILID pools with a LC:HC ratio of 0.32. Accordingly, products from LIHID, DIHIL, and DILIH exhibited similar percentage of fucosylated species around 78%, while a dramatic drop to 60 % was observed on products from HILID. A similar trend was observed for G1.

(A)

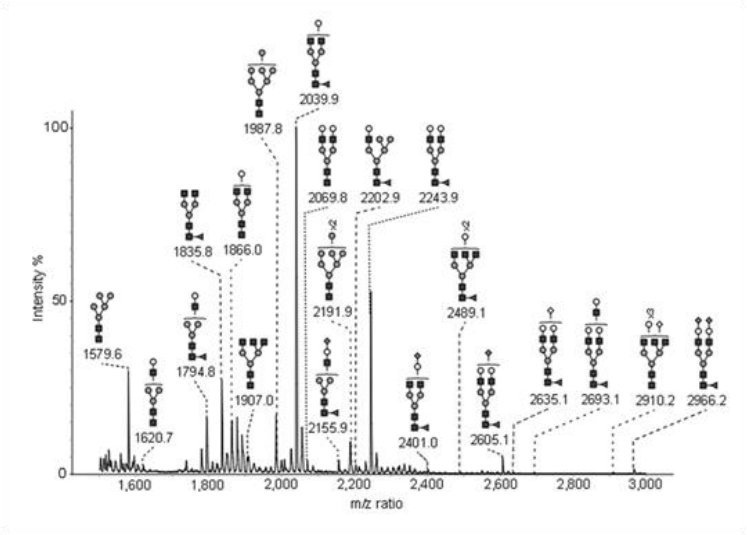
Intensity %
m/z ratio
1579.6
1620.7
1794.8
1835.8
1866.0
1907.0
1987.8
2039.9
2069.8
2155.9
2191.9
2202.9
2243.9
2401.0
2489.1
2605.1
2635.1
2693.1
2910.2
2966.2

(B)

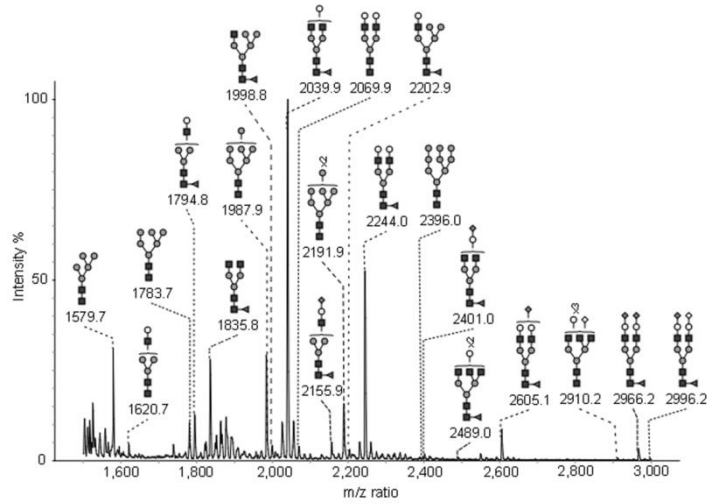
Intensity %
m/z ratio
1579.7
1620.7
1783.7
1794.8
1835.8
1967.9
1998.8
2039.9
2069.9
2155.9
2191.9
2202.9
2244.0
2396.0
2401.0
2489.0
2605.1
2910.2
2966.2
2996.2

(C)

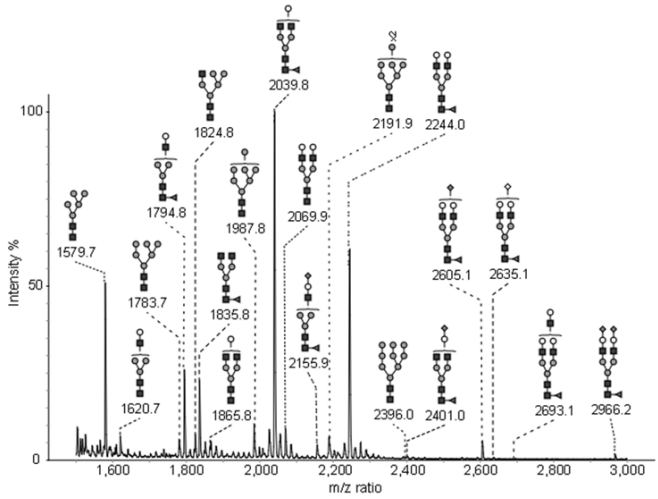
Intensity %
m/z ratio
1579.7
1620.7
1783.7
1794.8
1824.8
1835.8
1865.8
1987.8
2039.8
2069.9
2155.9
2191.9
2244.0
2396.0
2401.0
2605.1
2635.1
2693.1
2966.2

(D)

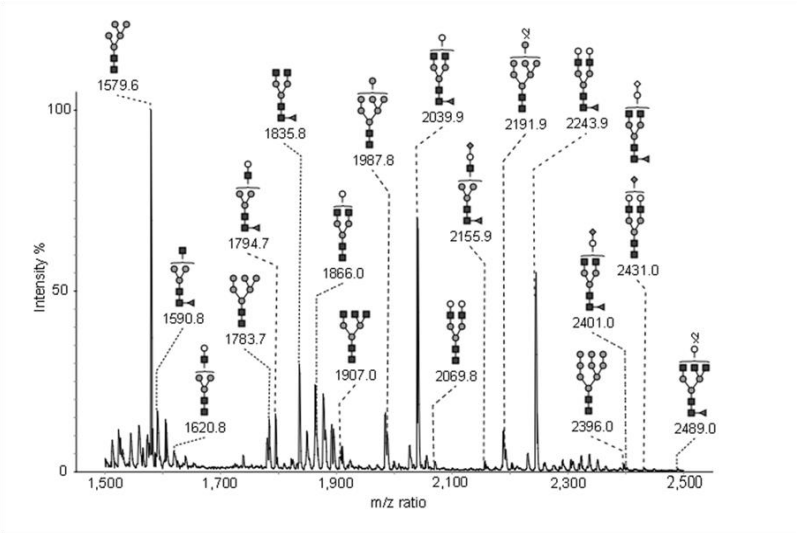
1579.6
1590.8
1620.8
1783.7
1794.7
1835.8
1866.0
1907.0
1987.8
2039.9
2069.8
2155.9
2191.9
2243.9
2396.0
2401.0
2431.0
2489.0
Intensity %
100
50
0
1,500
1,700
1,900
2,100
2,300
2,500
m/z ratio

(E)

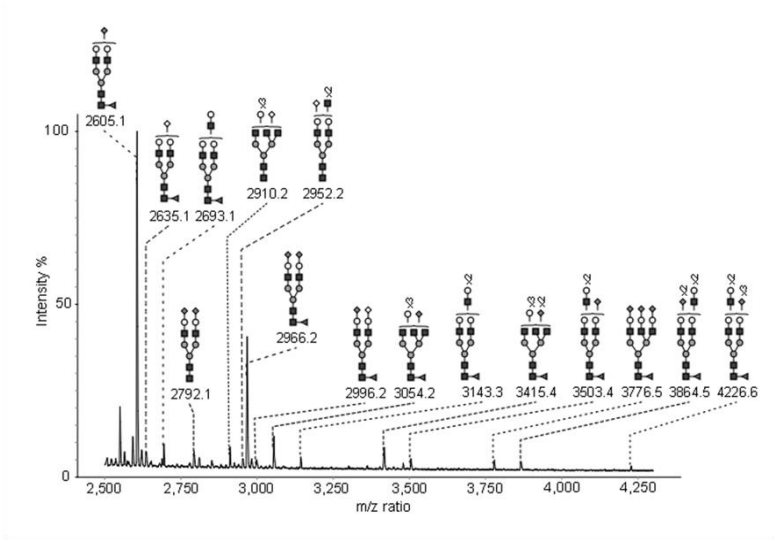
2605.1
2635.1
2693.1
2792.1
2910.2
2952.2
2966.2
2996.2
3054.2
3143.3
3415.4
3503.4
3776.5
3864.5
4226.6
Intensity %
100
50
0
2,500
2,750
3,000
3,250
3,500
3,750
4,000
4,250
m/z ratio

(F)

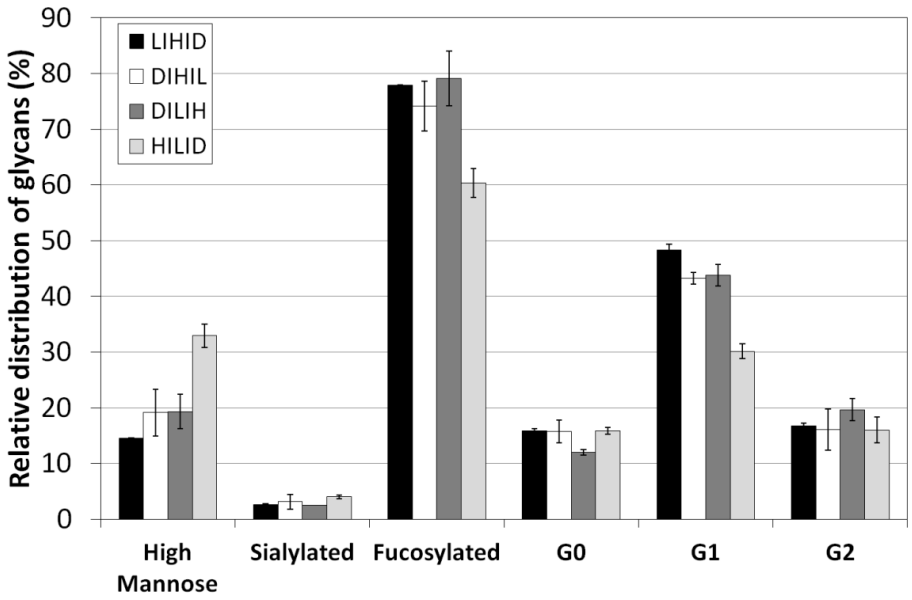

Figure 5.5 Representative MALDI-TOF mass spectra and N-glycan distribution obtained for anti-HER2 mAb generated at different LC:HC ratio. MALDI-TOF analysis of the permethylated N-glycans released from the purified mAb produced by pools generated using (A) LIHID, (B) DIHIL, (C) DILIH, (D,E) HILID, respectively. Solid square, N-acetylglucosamine; solid circle, mannose; open circle, galactose; solid triangle, fucose; solid diamond, sialic acid and open diamond, N-glycolylneuraminic acid. (F) Glycan distribution for the product generated at the different ratios is shown. LC:HC ratios of 3.43, 1.24, 1.12 and 0.32 were observed for LIHID, DIHIL, DILIH and HILID, respectively. N-glycans were categorized into high-mannose type, sialylated type that carry at least one terminal sialic acid, fucosylated complex type N-glycans, G0 glycans which carry no galactose residues, G1 which carry one terminal galactose residue and G2 which carry two terminal galactose residues. Each bar represents the average of the results collected from two independently generated pools. Protein A purified product from two independently transfected pools were quantified but only the spectra of the first pool is shown in (A) to (E) as the replicates are highly similar.

5.4.5 Conformational stability at different LC:HC ratios

Conformational stabilities of the protein A purified products collected for the different LC:HC ratios were measured by DSC at neutral pH. IgGs can have either two or three thermal transitions indicated by the unfolding temperatures (T_m). Those are contributed by the unfolding of the Fc (CH2 and

CH3 regions) and Fab segments (Garber and Demarest 2007; Ionescu et al. 2008). A higher T_m represents greater stability. The DSC profiles observed for the anti-HER2 LIHID, DIHIL and DILIH pools were similar to those reported previously (Ionescu et al. 2008). Three transitions around 70°C, 80°C and 82°C were observed (Fig. 5.6. and Table 5.1). Product from LIHID, the pools with excess LC, had the highest melting points for all transitions. HILID had lower T_m1, which corresponds to unfolding of the CH2 domain (Ionescu et al. 2008; Mueller et al. 2013).

5.4.6 Effect of excess LC and HC on product quality of other mAbs

We next generated stably transfected CHO cell lines expressing anti-TNFα and anti-VEGF IgG antibodies to investigate whether the impact of LC:HC ratio on mAb expression level and quality is mAb dependent. LIHID and HILID (Fig. 5.1) vectors were used to generate pools which expressed LC or HC in excess for these two other mAbs. Expression level, intracellular LC:HC ratio and product quality were determined and consolidated in Table 5.2. Regardless of the IgG studied, LIHID generated pools exhibited high LC:HC ratios while HILID pools had low ratios, albeit with some differences in the values. LIHID generated pools exhibited LC:HC ratios of 2.77 and 3.53, while using a HILID design generated ratios of 0.35 and 0.38 for anti-TNFα and anti-VEGF, respectively. LC:HC ratio for anti-TNFα produced using LIHID was lower possibly due decreased translation efficiency or increased clearance for LC. Consistent with the observed impact of LC:HC ratios on anti-HER2 expression, expression of LC in excess enhanced expression of anti-TNFα and anti-VEGF. Amplified pools of LIHID had titers four-fold higher than HILID for both antibodies.

The impact of LC:HC ratio on aggregation of anti-TNFα and anti-VEGF was similar to that observed for anti-HER2. Under excess LC conditions using LIHID, anti-TNFα had 99.01% IgG monomers, 0.49% aggregates and 0.50% fragments and anti-VEGF mAb had 98.71% monomers, 1.10% aggregates and 0.19% fragments. While HILID pools with HC expressed in excess displayed increased levels of aggregation of 22.36% for anti-TNFα and 14.96% for anti-VEGF. Incomplete mAb fragments were also observed for these two antibodies at low LC:HC ratios although the amount was less than that observed for anti-HER2. Anti-TNFα had 9.05% fragments while anti-VEGF had 1.02% of fragments.

Similar changes in glycosylation at different LC:HC ratios were also observed for these two antibodies as seen earlier for anti-HER2. There was still an increase in variety of glycans and the appearance of more matured tetra-antennary glycans for mAb generated with excess HC (data not shown). High mannose type N-glycans were elevated even more significantly for anti-TNFα and anti-VEGF as compared to anti-HER2. Only 6.42% and 13.05% of glycans were high mannose for anti-TNFα and anti-VEGF, respectively, at high LC:HC ratios. This increased dramatically to 54.23% and 44.11% for pools at low LC:HC ratios. The amount of fucosylated glycans in excess LC pools when compared to excess HC pools decreased from 84.49% to 41% and from 78.77% to 50.42% for anti-TNFα and anti-VEGF.

Pools with excess LC also displayed superior stability as compared to excess HC pools. Two transitions and T_ms were detected at around 70°C and 80°C for both antibodies generated using LIHID. DSC analysis for both

antibodies at low LC:HC ratio could not be performed successfully due to rapid aggregation during sample preparation, indicating low stability.

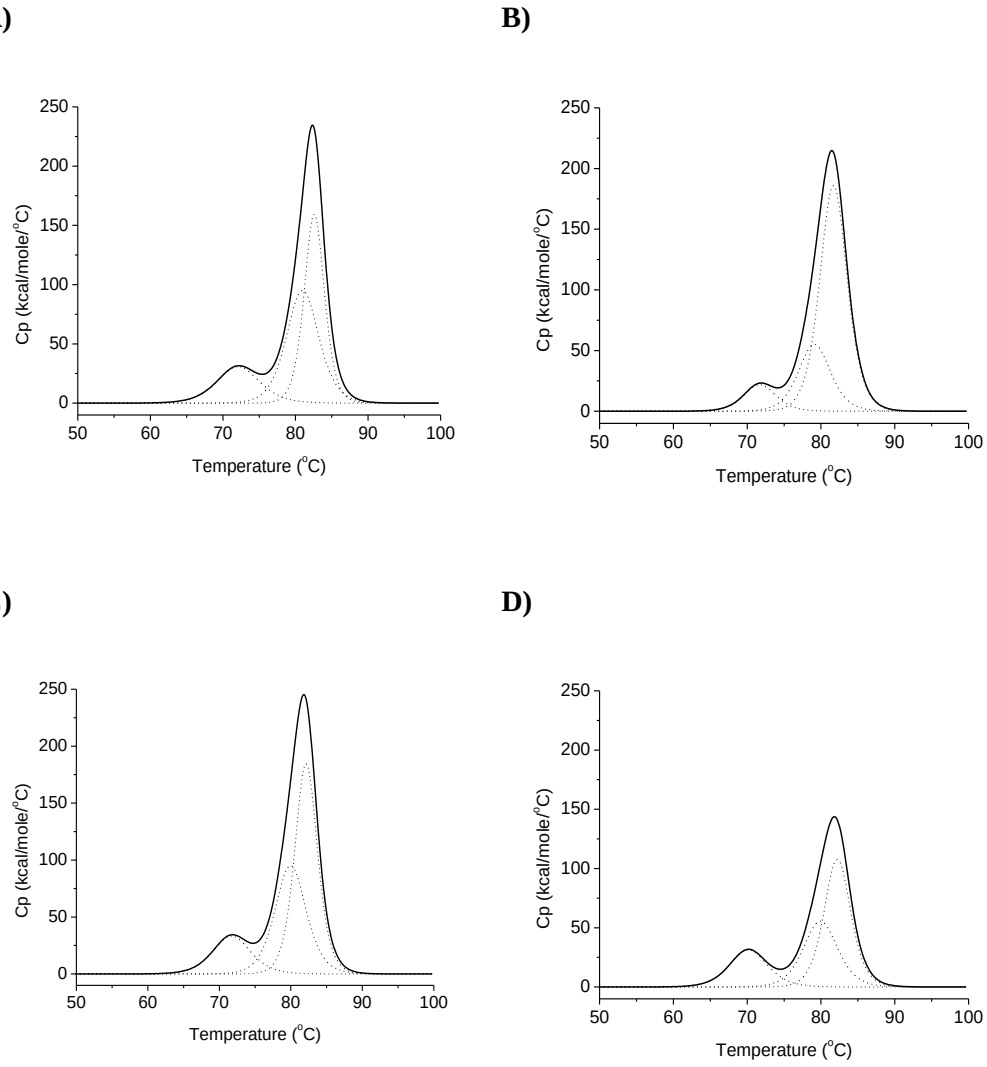

Figure 5.6 Representative thermograms for differential scanning calorimetry (DSC) observed for anti-HER2 purified mAb produced in stably transfected pools generated using the A) LIHID, B) DIHIL, C) DILIH, D) HILID vectors. Dotted curves symbolize deconvolution analysis for the different thermal transitions. Protein A purified product from two independently transfected pools were quantified but only the thermogram of the first pool is shown in (A) to (D) as the replicates are highly similar. T_ms are listed in table 1.

Table 5.1 Conformation stability of the anti-HER2 mAb in stably transfected pools generated using different IRES-mediated tricistronic vectors

		anti-HER2 IgG1			
		LIHID	**DIHIL**	**DILIH**	**HILID**
Stability (°C)	**T_m1**	72.1 ± 0.1	71.8 ± 0.1	71.6 ± 0.3	69.9 ± 0.2
	T_m2	80.9 ± 0.2	79.3 ± 0.3	80.1± 0.2	79.7± 0.5
	T_m3	82.6 ± 0.0	81.8 ± 0.2	82.2 ± 0.1	82.2 ± 0.1

Table 5.2 Expression level, aggregation, N-glycosylation and conformation stability of anti-TNFα and anti-VEGF mAb in stably transfected pools generated at different LC:HC ratios.

		anti-TNFα IgG1		**anti-VEGF IgG1**	
		LIHID	**HILID**	**LIHID**	**HILID**
LC:HC		2.77 ± 0.05*	0.35 ± 0.02	3.53 ± 0.34	0.38 ± 0.01
Titer (mg L^{-1})		54.6 ± 10.18	14.05 ± 2.47	102 ± 11.31	21.4 ± 0.85
Aggregation (%)	**IgG**	99.01 ± 0.15	68.59 ± 2.74	98.71 ± 0.11	84.02 ± 1.21
	Aggregates	0.49 ± 0.05	22.36 ± 1.97	1.10 ± 0.12	14.96 ± 1.80
	Fragments	0.50 ± 0.20	9.05 ± 0.78	0.19 ± 0.02	1.02 ± 0.59
Glycosylation (%)	**High Mannose**	6.42 ± 0.46	54.23 ± 0.06	13.05 ± 3.15	44.11 ± 3.98
	Sialylated	3.03 ± 0.61	3.38 ± 0.49	2.46 ± 0.83	3.57 ± 1.49
	Fucosylated	84.49 ± 0.07	41.00 ± 0.20	78.77 ± 3.99	50.42 ± 4.56
	G0	27.66 ± 0.52	15.30 ± 0.16	21.17 ± 0.41	11.96 ± 0.16
	G1	43.87 ± 0.46	17.41 ± 0.05	45.58 ± 0.12	24.36 ± 3.01
	G2	16.74 ± 1.41	9.02 ± 0.41	15.54 ± 0.92	14.73 ± 2.89
Stability (°C)	**T_m1**	73.0 ± 0.1	ND	72.7 ± 0.0	ND
	T_m2	83.5 ± 0.3	ND	83.2 ± 0.2	ND

* Value is significantly different from anti-Her2 LIHID based on two-tailed student t-test.

ND: could not be determined because of high aggregation during sample preparation for DSC.

5.5 Discussion

Previous studies which controlled LC:HC ratio at different levels to study its impact on mAb expression in CHO cells were conducted in transient conditions (Schlatter et al. 2005; Li et al. 2007). Control of LC:HC ratio in stably transfected CHO cells with high IgG expression has yet to be reported. We designed four IRES-mediated vectors and verified that LC:HC ratios could be controlled at ratios of 3.43, 1,24, 1,12 and 0.32 in CHO DG44 cell lines stably expressing anti-HER2 IgG. Strict control of the LC:HC ratio was achieved by our vector design as indicated by the consistent ratio for each vector even under gene-amplified conditions (Fig. 5.3C). Our results demonstrated that the LC:HC ratio affects both mAb expression level and quality and this impact is not antibody dependent.

LC:HC ratios reported here are based on peptide amounts measured by ELISA while the ratio is reported at gene or mRNA level in other studies (Lee et al. 2009; Yang et al. 2009). We chose peptide quantification for two reasons: (1) as our LC and HC genes would be on one transcript linked by IRES, there would be no differences in their relative mRNA levels, (2) protein folding and glycosylation would be affected at peptide level and thus peptide ratios would be more relevant to this study. Amplification was more effective and achieved higher mAb titers at LC:HC ratio of 3.43 as the excess LC allows for more efficient mAb folding and assembly and HC clearance (Gonzalez et al. 2002; Schlatter et al. 2005; O'Callaghan et al. 2010). Schlatter et al. (2005) had observed and reported similar LC:HC peptide ratios of 2, 2.5 and 3.1 in three stable high mAb producing cell lines. The absence of mAb fragments in the product generated by the pools with more balanced LC:HC

ratios is a possible sign that LC and HC peptides are used more efficiently for mAb assembly with no wasted resources. However, the peak titers achieved at balanced LC:HC ratios were much less than when expressing LC in excess even though MTX concentration was increased to a much higher level. The lower titer achieved at balanced LC:HC ratios may be also due to the stronger DHFR expression. We also observed higher mAb expression from the LIHID vector than the DIHIL and DILIH vectors in transient transfection to support that expression of excess LC is indeed more favorable for mAb expression. It is interesting that there are contrary reports which observed excess HC being beneficial to IgG expression levels in CHO cells (Jiang et al. 2006; Fallot et al. 2009). Based on our results, titers at 50 nM MTX were indeed comparable for anti-HER2 IgG for both excess LC pools (LIHID) and excess HC pools (HILID) when detection was performed using HC-specific antibodies (Fig. 5.2B). It was only upon further analysis of the product that we noticed a significant proportion of the product was not the desired IgG monomers (Fig. 5.2C and 5.4). This false detection of high titer in pools or clones could be an issue when generating mAb expressing cell lines with poor control of LC:HC ratio.

Maintaining low mAb aggregation is of critical importance during production as it reduces efficacy and may cause immunogenicity (Hermeling et al. 2004; Cromwell et al. 2006). Earlier observations of a correlation between LC:HC ratio and aggregation were at a clonal level and it is unclear if the reported effects could have been due to a clone specific effect (Lee et al. 2009; Gomez et al. 2012). When LC:HC ratio decreased from 3.43 to 1.24, aggregation levels remained at a level below 0.5%, but aggregation increased

to above 2% when ratio further decreased slightly to 1.12, suggesting there is a threshold between LC:HC ratios of 1.12 and 1.24 for aggregation to occur. An earlier report which selected clones expressing a different unknown mAb with LC:HC mRNA ratios above 1.5 to minimize product aggregation issues were still unable to identify all clones with low aggregation (Lee et al. 2009), suggesting that the threshold of LC:HC ratio causing aggregation may be different from mAb to mAb. Based on our observation of low levels of aggregates for all mAbs generated with greater excess LC, having LC in greater excess is likely a better method to minimize aggregation. Aggregation increased significantly when HC was in excess at LC:HC ratios of around 0.3 for all mAbs tested. Excess HC which are unable to be properly folded with limited LC is one possible source of aggregation (Vanhove et al. 2001). The excess HC had different effects on different mAb products. Significant mAb fragments were observed only in pools of anti-HER2 and anti-TNFα. Although all mAbs produced under excess HC conditions had aggregates, aggregation for anti-TNFα and anti-VEGF worsened more significantly to form visible aggregates quickly upon sample preparation after purification.

It is still unclear how LC:HC ratios can cause changes in glycosylation in stably transfected cell lines. mAb glycosylation affects product efficacy and immunogenicity (Jefferis 2005). The distribution of N-glycans on anti-HER2 was similar between pools generated using DIHIL and DILIH with LC:HC ratios close to one. When LC:HC ratio was increased to 3.43 using LIHID, there was a drop in high mannose species and an increase in the complex-type N-glycans, especially the galactosylated ones. Decreasing LC:HC ratio to 0.32 resulted in elevated high mannose glycans, less fucosylated and appearance of

tri- and tetra-antennary structures which can result from an abnormal folding of the mAb. Protein folding and glycosylation are indeed parallel processes which could compete and affect each other (Gonzalez et al. 2001). There is possibly a better folding and assembly with excess of LC, resulting in an enhanced fraction of the desired complex glycans. High mannose glycans play a part in the protein quality control process occurring within the ER (Fagioli and Sitia 2001). The elevated level of high mannose species detected is a possible sign of the cell's folding and quality control machinery being overloaded. As protein A purified mAb at low LC:HC ratios contained incomplete fragments, highly matured N-glycans such as tri- and tetra-antennary N-glycans observed could be due to mAb fragments with altered conformations having the glycosylation site more exposed, allowing for a greater level of glyco-modifications within the Golgi apparatus.

The increased aggregation, altered N-glycosylation, and decreased conformation stability we observed when there was excess HC are possibly correlated as protein folding, glycosylation, and conformation stability are closely related events (Krambeck and Betenbaugh 2005; Butler 2006). Several reports have indicated that the type and presence of glycosylation plays an important role in the likelihood of protein aggregating (Hristodorov et al. 2012; Schaefer and Plückthun 2012). It has also been reported that glycosylation does affect the stability of mAb products (Liu et al. 2006; Hristodorov et al. 2012). Glycans destabilize the unfolded state, making the folded state more desirable (Shental-Bechor and Levy 2008). Melting temperature for the CH_2 domain which was observed to be most affected is also the region where N-glycosylation takes place. When the CH_2 domain is

less stable and unfolds more easily, stability of the other domains are affected as well. Glycosylation is not the only factor contributing to the differences in conformational stability as even though glycosylation for the product from pools of the balanced ratio were similar to the excess LC pools, stability was still lower. This difference could be due to LC:HC ratios affecting the early stages of protein folding and glycosylation. An interesting follow-up to this work could be to study how long LC and HC are retained within the ER at each ratio. It is possible that having excess LC to minimize the retention time of the incomplete HC dimers within the ER is preferred, giving the best folding conditions and thus the greatest stability. Near and far UV circular dichroism analysis of the two different products could be carried out to observe for differences in their secondary and tertiary structures.

The observations we made at the different LC:HC ratios for a variety of mAbs in stably transfected mAb show that LC:HC ratio plays an important role in mAb expression and quality. Having LC in excess is not only beneficial for mAb expression, it also keeps aggregate and fragment levels low. This is beneficial in ensuring maximal product yield. Protein A purification would be more efficient and less polishing steps would be needed. The glycosylation profile is more consistent and high mannose species which can reduce circulation time is lower. Methods to improve the product from cells with low LC:HC ratio were also tested. In recent years, there has been a push for implementation of Quality by Design (QbD) principles for development of biologics. The aim of QbD is to ensure consistency of product quality through understanding and optimization of the production process instead of through rigorous testing (Rathore and Winkle 2009; van Beers and Bardor 2012). This

can be achieved partly through control of LC:HC ratio by using specific vector designs. More work is required to validate that excess LC is beneficial to product quality as several other factors like culture condition, media formulation and cell types are also important. The ratio which we have controlled our LC and HC levels at are possibly not optimal due to wastage of excess LC. The high excess LC could still be beneficial when dealing with difficult to express mAbs where transfected LC:HC ratios of up to 9:1 were tested and shown to improve expression (Pybus et al. 2014). Future work could include further studies using more refined vector designs to identify ratios where peptide usage is maximized, mAb expression level is highest, and mAb quality is not compromised.

Chapter 6: IgG aggregation in cells expressing excess HC and strategies to reduce the aggregates

When there is excess HC in mAb producing CHO cells, the mAb produced was observed to be aggregation prone. In this chapter, we identified some reasons for the aggregates forming and evaluated some methods to reduce the aggregates like over-expression of chaperones and increasing LC expression.

*The following results are undergoing minor revision at the time of writing of the thesis to be published in "**Ho, S. C. L.**, Wang T., Song, Z., and Yang, Y. (2015). "IgG aggregation mechanism for CHO cells expressing excess heavy chains ." Molecular Biotechnology".*

6.1 Abstract

Aggregates in protein therapeutics like IgG monoclonal antibodies (mAb) are detrimental to product safety and efficacy. It has been reported that aggregates form in Chinese hamster ovary (CHO) cell lines expressing greater amount of heavy chain (HC) than light chain (LC). In this study, we observed that aggregates could form within the cells with excess HC and was partially secreted into the supernatant. The aggregates in the supernatant consisted of mainly HC and were partially dissociated under either reducing or denaturing conditions. Mutation of a predicted free cysteine on HC to prevent disulfide bonding did not reduce aggregation. Re-transfecting CHO cells with excess HC with more BiP, an important IgG molecular chaperone, reduced unwanted aggregates and fragments possibly by helping retain more incomplete products within the cell for either proper assembly or degradation. A second transfection of LC into CHO cells with excess HC to increase the LC expression to a level greater than the HC expression successfully removed all aggregates and fragments. mAb product aggregation in CHO cells with excess HC occur due to a combination of limited chaperones and LC:HC ratio. These results provide added insights to aggregate formation in and would be useful for development of mAb cell lines with reduced aggregates.

6.2 Introduction

All proteins including monoclonal antibody (mAb) therapeutics have the tendency to aggregate. Aggregates can be classified by their covalent/non-covalent bonds, reversible/non-reversible nature, size and conformation (Cromwell et al. 2006; Mahler et al. 2009). The presence of aggregates in protein therapeutics like IgG mAb can result in immunogenic reactions, complications during product administration and impair product quality and efficacy (Cromwell et al. 2006). Aggregation can occur during the various steps of the mAb manufacturing process, starting from cell line generation to the scale up culture process followed by purification, formulation all the way to storage (Cromwell et al. 2006; Mahler et al. 2009; Joubert et al. 2011). The presence of aggregates after filtration and centrifugation of the culture complicates the purification steps as the commonly used protein A affinity mAb purification method does not discriminate between monomers and aggregates as long as the Fc region is intact (Phillips et al. 2001). Several extra polishing steps like size exclusion and ion-exchange chromatography are required after affinity purification to remove aggregates (Phillips et al. 2001; Yoo and Ghosh 2012).

It is beneficial to minimize aggregation from the early steps of production during clone selection and culturing. In order to maximize yields, high amounts of recombinant mAb peptides are expressed by each cell. This could lead to intracellular aggregation due to the high amount of unfolded proteins or inefficiencies of the molecular chaperones at controlling proper protein folding (Zhang et al. 2004). This has been demonstrated in Chinese hamster ovary (CHO) cells where the expression of a simple ATIII

glycoprotein above a threshold triggered aggregation and lowered yield (Schröder et al. 2002). mAb expression is further complicated by its multimeric nature where the heavy chain (HC) and light chain (LC) peptides are translated separately before being assembled with the aid of various ER proteins (Gonzalez et al. 2002; Feige et al. 2010). One study observed that aggregate levels were reversibly correlated to the LC:HC mRNA ratios in stable mAb producing clones and high level of aggregates formed in clones with the LC:HC mRNA ratio over 1.5 (Lee et al. 2009). It was also observed that increased aggregates were associated with decreased LC:HC mRNA ratios in response to a temperature shift from 37 °C to lower temperatures (Gomez et al. 2012). We had generated two mAb producing stably transfected CHO cell pools, LIHID and HILID, with controlled intracellular LC:HC ratios of 3.4 and 0.3 respectively. The mAb produced by HILID stable pools with excess HC comprised of over 10% aggregates while LIHID stable pools with excess LC had less than 1% aggregate (Ho et al. 2013). Further analysis of the nature and mechanism of mAb aggregation in CHO cells with excess HC was not reported in our previous study.

In this work, we studied where aggregates formed in HILID cells with excess HC, characterized and investigated the nature of aggregates. Cell engineering of molecular chaperones have mostly been performed to improve cell productivity (Borth et al. 2005; Hayes et al. 2010; Mohan and Lee 2010), with little reports of chaperone engineering to reduce product aggregation (Gomez et al. 2012). Chaperone engineering is not always a straight-forward experiment due to the complexity of the mammalian protein folding machinery (Borth et al. 2005; Nishimiya 2014). We studied how CHO cells

with excess HC would respond to the accumulation of intracellular HC polypeptides and the effect of overexpressing a BiP chaperone on the mAb aggregate formation. An extra transfection of only LC had been suggested as a solution to reduce aggregates arising due to excess HC but was not evaluated as the authors had considered that the mechanisms of aggregation was unknown and simply altering the LC:HC ratio could be insufficient (Lee et al. 2009). We designed a strategy to increase LC expression in HILID stable pools using stringent selection markers and demonstrated that a second transfection of LC was effective at reducing aggregates. The results obtained would provide insights to the causes of mAb aggregation and to generate cell lines with reduced aggregates.

6.3 Materials and methods

6.3.1 Vector construction

Vectors used were modified from a previously described LIHID vector which LC, HC, and dihydrofolate reductase (DHFR) genes were linked by internal ribosome entry site elements (IRES) (Ho et al. 2013). The HID vector was constructed by replacing LC-IRES-HC with HC (Fig. 6.1A). The IRES upstream of the DHFR selection marker was replaced with a mutant IRES variant we had generated, IRESv11 (Koh et al. 2013). Variants of the HID vector with mutations to the cysteine on the HC which normally forms a disulfide bond with a LC to either alanine (nucleotide substitutions of T725G and G725C) or serine (substitution of G725C) were obtained by using QuikChange multi site-directed mutagenesis kits (Agilent, Santa Clara, CA). The variants were labelled as H_{ala}ID and H_{ser}ID. To generate LIZ and BIZ

vectors (Fig. 6.1B and C), the DHFR selection marker on the LIHID vector was first replaced by a Zeocin antibiotics selection marker cloned from pCDNA3.1/Zeo (Life Technologies, Carlsbad, CA). Following which, LC-IRES-HC was replaced with either just LC or CHO BiP cDNA (genbank: GCA_000223135.1). Finally, the IRES sequence upstream of Zeocin for LIZ vector was replaced with a mutant IRESv18 with an estimated 1.4% strength of the wild-type IRES, and the IRES sequence upstream of Zeocin for BIZ was replaced with either IRESv18 or IRESv11 with a relative 25% strength of the wild-type IRES. HID, H_{ala}ID and H_{ser}ID were transfected to DG44 cells while LIZ and BIZ were used to re-transfect earlier generated HILID stable pools with excess HC.

(A)

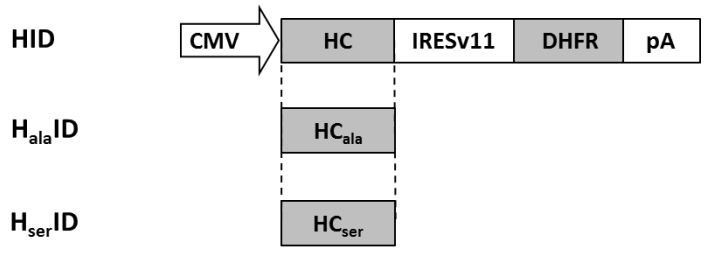

(B)

(C)

Figure 6.1 Plasmid vectors used in the study. (A) Vectors for expression of HC and HC mutants, (B) vector re-transfected into HILID pool to increase BiP expression, (C) vector re-transfected into HILID pool to increase LC expression.

6.3.2 Cell culture and transfections

DHFR deficient CHO DG44 cells (Life Technologies) were grown in protein free media (PFM) supplemented with 0.1 mM sodium hypoxanthine and 0.016 mM thymine (HT; Life Technologies). PFM was prepared from a 1:1 mixture of HyQ PF (Hyclone, Logan, UT) and CD CHO (Life Technologies), supplemented with 1 g/L sodium bicarbonate (Sigma-Aldrich, St-Louis, MO), 6mM Glutamine (Sigma-Aldrich) and 0.05% Pluronic F-68 (Life Technologies). Cell lines LIHID and HILID were generated in an earlier report (Ho et al. 2013) and cultured in PFM supplemented with 50 mM methotrexate (MTX, Sigma-Aldrich). Cells were passaged every 3 to 4 days by diluting the cultures to 2×10^5 cells/mL in fresh media. Cell viability and density were determined by trypan blue exclusion method using a Vi-Cell XR cell viability analyzer (Beckman Coulter, CA).

Transfections were performed using SG solution and program FF-137 on a 4D-Nucleofector system (Lonza, Cologne, Germany). 1×10^7 cells and 5 µg of plasmid were used for each experiment. Transfected DG44 cells with HID vector series were transferred to selection media of PFM media without HT followed by gene amplification using 50 mM MTX. HILID pools that were re-transfected with LIZ or BIZ vectors underwent selection using 200 µg/mL Zeocin™ (Invivogen, San Diego, CA). Selection was deemed completed when cell viability reached above 95%. Recovered cultures were seeded at 2×10^5 cells/mL and supernatant was collected after 10-11 days when viability dropped to 50% for further experiments. All transfections were performed in duplicates.

6.3.3 ELISA and Western blotting

Cell lysis was performed using CellLytic^{TM} M with added protease inhibitor cocktail (both from Sigma-Aldrich). Intracellular protein from 1×10^7 cells was extracted using 200 µL of the mix. Cell lysates were used to determine intracellular polypeptides of LC:HC ratio by enzyme linked immunosorbent assay (ELISA) and identify intracellular mAb components by western blotting. ELISA and western blotting were performed as previously described (Ho et al. 2013). Precision Plus dual color protein pre-stained standards (Bio-Rad, Hercules, CA) were added to each blot to identify species sizes. Undiluted cell lysates and 10 ng of mAb in the supernatant were used for western blotting.

6.3.4 Purifying of mAb products

mAb was purified using a Tricorn 5/150 protein A column packed with MabSelect SuRe (GE Healthcare, Uppsala, Sweden) loaded on a GE *Ä*KTA Explorer 100 (GE Healthcare). Sample was injected at a flow rate of 3 mL/min. A terminator wash buffer of 2 M sodium chloride (Merck, Darmstadt, Germany), 250 mM imidazole (Merck), 10 mM EDTA (Sigma-Aldrich), 4 M urea (Sigma-Aldrich) adjusted to pH 7.0 was passed through the column followed by an elution buffer of 100 mM acetate (Sigma-Aldrich) and 100 mM arginine (Sigma-Aldrich) at pH 3.5. Eluted samples were neutralized using 1 M Tris (Sigma-Aldrich) and the column was regenerated using 0.1 M glycine (Merck) adjusted to pH 2.5.

6.3.5 Aggregation analysis of protein A purified mAb

The aggregation of protein A purified mAb was determined using size exclusion chromatography (SEC). The instrument setup consisted of a HPLC

system (Shimadzu, Kyoto, Japan), with a binary pump, an auto injector, a thermostated column oven and a UV-visible detector. The chromatography columns used were TSK Guard column SWXL, 6×40 mm and TSK gel G3000 SWXL, 7.8×300 mm (Tosoh Corporation, Tokyo, Japan). Column Oven temperature was set at 25ºC and the regular mobile phase included 0.2M sodium phosphate (Merck) and 0.1M potassium sulfate buffer at pH 6.0 (Merck). Flow rate was 0.5 mL/min. All samples were analyzed immediately after protein A purification.

Subsequent SEC analysis of aggregates was performed using methods with modified mobile phases similar to that previously reported by Gomez et al (2012). One experiment was performed using mobile phase with added 6 M guanidine (Sigma Aldrich). Another was performed with 30mins incubation at 37 °C of the product with 10 mM DTT (Promega) prior to injection and running with mobile phase containing 10 mM DTT. The final experiment was performed with doubling K_2SO_4 salt concentration from 0.1 M to 0.2 M. Duplicate measurements were performed for two separately collected samples for each experiment.

6.3.6 Quantitative real-time PCR (qRT-PCR)

Total RNA was isolated from LIHID and HILID pools using a RNeasy® Mini Kit (Qiagen, Valencia, CA). mRNA levels for binding immunoglobulin protein (BiP) were then analyzed using a two-step qRT-PCR protocol. β-actin was used as the internal control. Briefly, 100 ng of RNA was reverse transcribed to cDNA using the ImProm II™ reverse transcription system (Promega) in a 40 µL reaction. These cDNA samples were analyzed on an iQ-5 Real-time PCR System (Bio-Rad) using a recipe of 10.0 µL of

SsoFast™ Evagreen® Supermix (Bio-Rad), 500 nM (final concentration) of forward and reverse primers (Research Biolabs, Singapore), 2.0 µL of above synthesized cDNA, and topped up with HPLC water (Merck, San Diego, CA, USA) for a 20 µL reaction. Primers used are shown in table 1. mRNA was extracted from two independently transfected cultures and analyzed with duplicate measurements for each sample. The collected threshold cycle (Ct) values were analyzed using a $2^{-\Delta\Delta Ct}$ method (Livak and Schmittgen 2001).

Table 6.1 Primers used for qRT-PCR

Primer	Sequence
BiP-Forw	5'- CGGTGGAACCTTCGATGTG -3'
BiP-Rev	5'- TCCATAACCCGCTGATCAAAG -3'
Actin-Forw	5'- AGCTGAGAGGGAAATTGTGCG -3'
Actin-Rev	5'- GCAACGGAACCGCTCATT -3'

6.4 Results

6.4.1 Analysis of aggregate formation

We performed western blotting analysis of the cell lysate and supernatant to determine where aggregates formed in HILID stable pools with excess HC (LC:HC ratio of 0.3) and to identify the possible components within the aggregates. Cell lysate and supernatant for LIHID cell pools with excess LC and low mAb aggregates (LC:HC ratio of 3.4) were also analyzed for comparison. The samples were analyzed separately using anti-HC and anti-LC detection antibodies (Fig. 6.2). Over-exposure during development of the blot ensured even small amounts of aggregates present would be visualized. LIHID lysate and supernatant samples had similar results for both detection antibodies and no aggregates were observed. HILID lysates exhibited a myriad of species with HC which appeared as a smear starting from 50 kDa, the size of a single HC to the start of the gel. Appearance of these unwanted products was likely exacerbated by the excess HC as the smearing was not visible using the anti-LC primary antibody. While this might not represent the actual species present within the cell due to differences between the cellular environment and the blot, this shows that HC species highly prone to aggregation are abundant within HILID pools. This smearing was not as evident in the HILID supernatant with slight smearing above the 150 kDa IgG monomer band and a high molecular weight band above. The high molecular weight species (above 150 kDa) comprised mostly of HC as the band was significantly darker using the anti-HC antibody compared to the faint band using anti-LC even with the over-exposure.

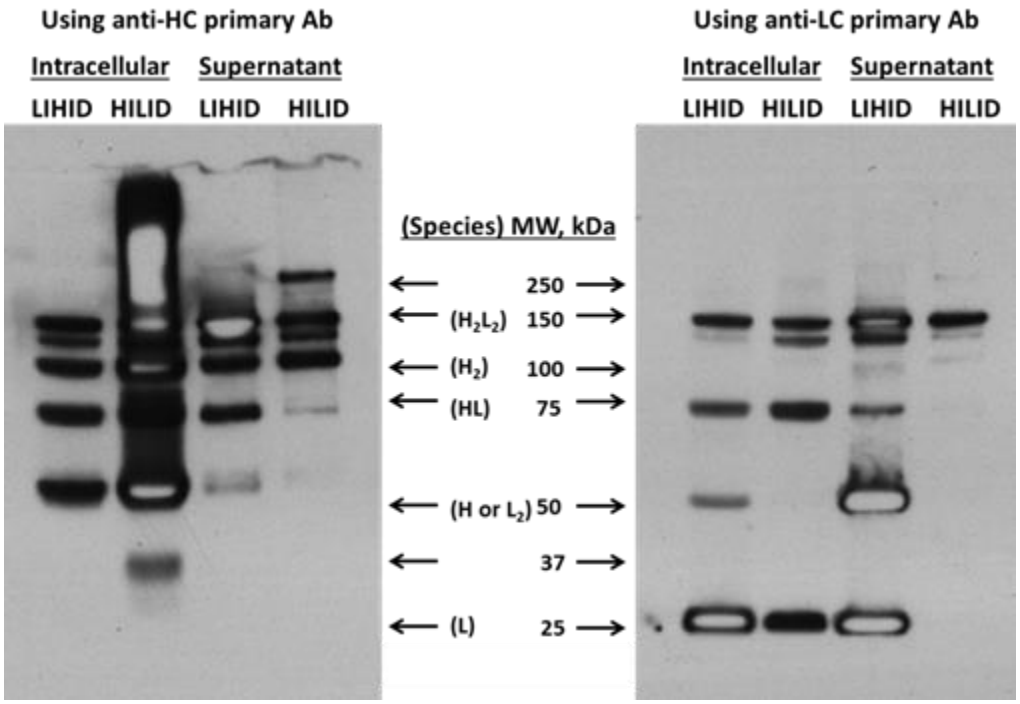

Figure 6.2 Western blotting of intracellular proteins and supernatant from LIHID and HILID using separate anti-HC and anti-LC detection antibodies. Samples were non-reduced and the increased exposure was performed to enable visualization of products present in small amounts.

SEC analysis was performed on the protein A purified anti-HER2 IgG from HILID pools to identify the mechanisms causing the aggregates to form. Three conditions were tested: reducing condition with 10 mM DTT, denaturing condition with 6 M guanidine and increased salt concentration to 0.4 M K_2SO_4. The conditions were determined based on a previous report (Gomez et al. 2012). The reducing condition would test for disulfide bonding, the denaturing conditions for hydrophobic interactions and the change to salt concentration for charge interactions. Purified sample from LIHID and HILID were first analyzed using the regular mobile phase buffer as a control (Fig. 6.3A and E). LIHID only had a single monomer peak. HILID had 13% aggregates, 60% monomers and 27% of IgG fragments. Testing the various processes on IgG monomers from a LIHID pool ensured the treatments did not

affect IgG monomers. Only a single monomer peak was observed during SEC analysis for all three conditions (Fig. 6.3B, C and D). Treatment of HILID samples resulted in a drop in the amount of aggregates from 13% to 4% and 6% in the reducing and denaturing conditions respectively (Fig. 6.3F and G). Peaks on the chromatogram profile for HILID in the mobile phase with 6M guanidine was less distinct compared to the regular mobile phase and the aggregate and fragment peaks became a shoulder off the main IgG peak (Fig. 6.3G). The aggregate peak in this case was identified by comparing the LIHID and HILID chromatograms obtained using the same buffer. There was no change in the amount of aggregates in the increased salt buffer (Fig. 6.3H). Analysis was done for samples from two sets of LIHID and HILID cell pools and similar results were observed. The average amount of aggregates measured after each treatment of duplicate cell pools is shown in Fig. 6.3I. Based on these observations, the aggregates in HILID CHO cell pools with excess HC likely formed due to a combination of disulfide bonding and hydrophobic interactions between free extra HC polypeptides.

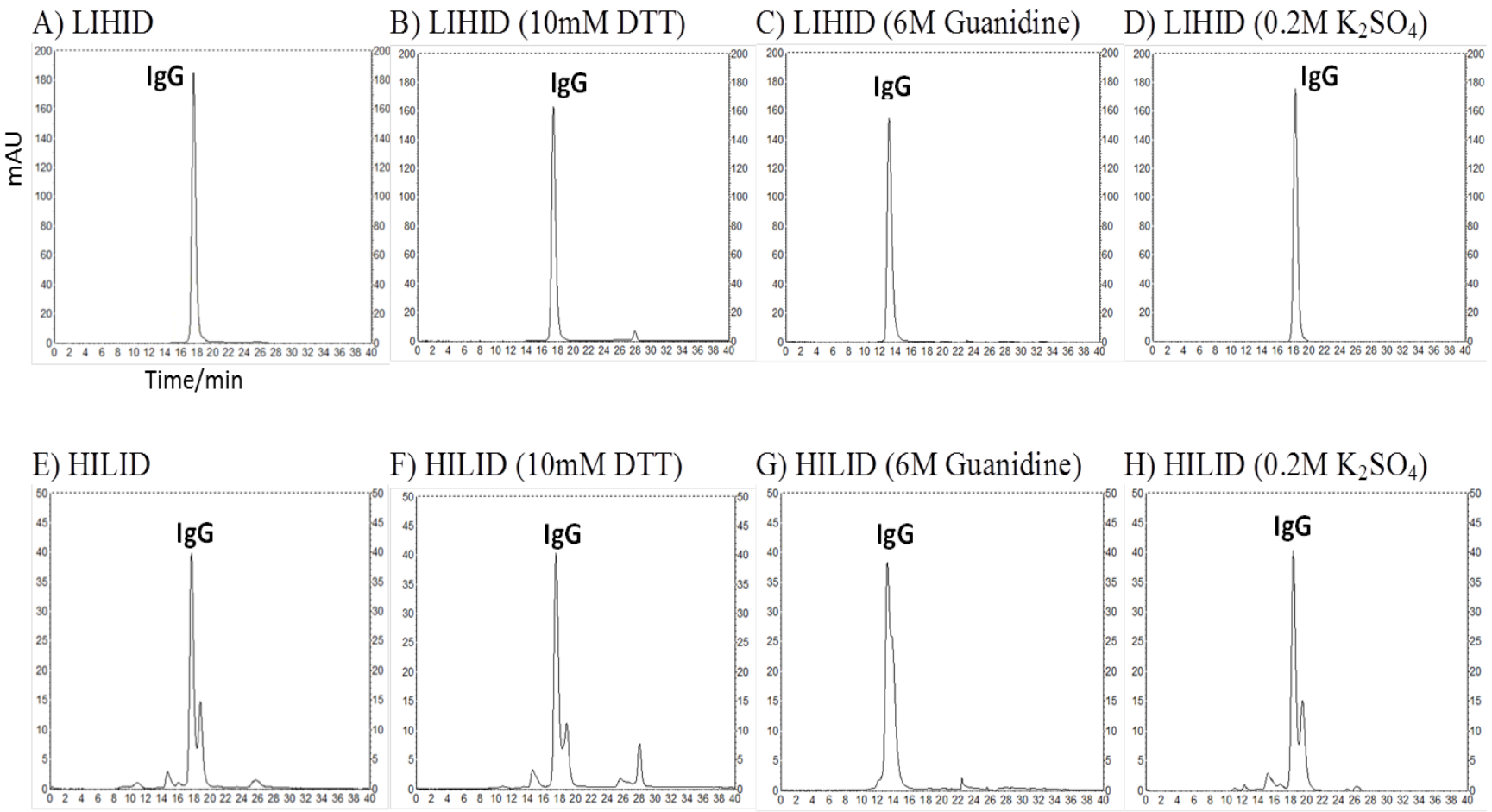
A) LIHID
B) LIHID (10mM DTT)
C) LIHID (6M Guanidine)
D) LIHID (0.2M K_2SO_4)
E) HILID
F) HILID (10mM DTT)
G) HILID (6M Guanidine)
H) HILID (0.2M K_2SO_4)
IgG
mAU
Time/min

(I)

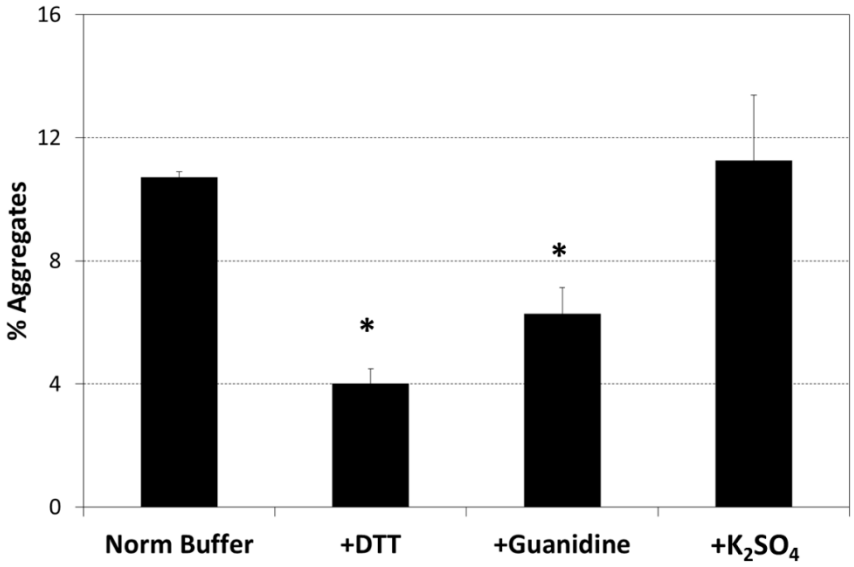

Figure 6.3 Chromatograms of protein A purified mAb produced by LIHID (A,B,C,D) and HILID (E,F,G,H). Samples analyzed with addition of either 10 mM DTT, 6 M guanidine or 0.2M K2SO4 to the liquid phase during SEC analysis. The main peaks labelled IgG are peaks for full IgG monomers. Peaks or peak shoulders appearing before the IgG were considered higher molecular weight aggregates. Peaks and shoulders after the main peak are low molecular weight IgG fragments. (I) Amount of aggregates detected in the normal SEC mobile phase and with the various additions. Each experiment was performed in replicates. * denotes the change was statistically significant using a two-tailed student t-test ($p<0.05$).

mAb synthesis involves formation of HC_2 dimers before folded LC are added (Feige et al. 2010; O'Callaghan et al. 2010). HC polypeptides are highly hydrophobic and inclined to aggregate. BIP binds to exposed HC hydrophobic region to prevent aggregation. BIP is released when a folded LC becomes available. HC dimer pairs with LC through disulfide bonding at fifth cysteine on HC (C223) and the last cysteine on LC (C236) (Liu and May 2012). Under the condition of excess HC and limited BIP, hydrophobic regions of variable region and first constant domains would be exposed. We hypothesized incomplete mAb fragments, HC_2 and HC_2LC would aggregate through

disulfide bonding at free cysteine 223 and hydrophobic interactions. We designed three experiments to test this hypothesis: (1) Mutation of cysteine on HC (C223A, C223S), (2) overexpression of BIP, and (3) a second transfection of only LC.

6.4.2 Effect of mutating cysteine 223 on HC on aggregate formation

As aggregates mainly consisted of HC polypeptides, we had hypothesized that one reason for the aggregates forming in the HILID pools was due to excess HC with unpaired free cysteines forming unwanted disulfide bonding. To test this hypothesis, a series of plasmids expressing only HC were generated (Fig. 6.1A). HID has the same HC sequence as used on the HILID plasmid, and another two with the cysteine which was to pair with a cysteine on a LC mutated to either alanine or serine, H_{ala}ID and H_{ser}ID. HC expressed from H_{ala}ID and H_{ser}ID vectors should not form high molecular weight aggregates due to disulfide bonding. Aggregates were visible in HC with mutation of the free cysteine to either alanine or serine, suggesting that mechanisms other than disulfide bonds were contributing to the aggregates (Fig. 6.4). This result complemented the earlier observations that the aggregates were comprised by a majority of HC and formed with a combination of different bonds like disulfide bonding and hydrophobic interactions.

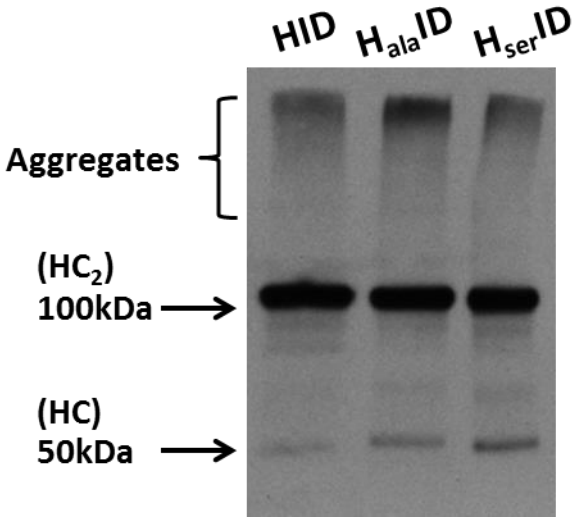

Figure 6.4 HC aggregates after cysteine mutation. Expression of only IgG HC (HID) and HC mutants with the cysteine for disulfide paring with LC mutated to alanine ($H_{ala}ID$) and serine ($H_{ser}ID$). Samples were probed with anti-FC detection antibody.

6.4.3 Increased expression of BIP to reduce aggregates

BiP expression levels were examined for non-transfected CHO DG44 cells, LIHID and HILID pools by qRT-PCR (Fig. 6.5A). BIP was upregulated at 4.3 and 7 fold higher for LIHID and HILID respectively compared to non-transfected CHO DG44 cells (NT). This could be due to the cell having to cope with the increased IgG expression for LIHID and large amounts of excess HC for HILID. BiP overexpression is linked to the unfolded protein response (UPR) that cells activate to handle the protein overload. Although BiP binds directly to incorrectly folded HC to aid in retaining them in the ER, we observed incomplete products being secreted. It is possible that the cell's own BiP upregulation could be still insufficient, leading to a breakdown in the cell's quality control mechanism and elevated product aggregation.

In order to test if an increase BIP expression could reduce aggregates, a HILID pool was re-transfected in duplicates with the BIZ vector carrying the

CHO BiP cDNA and a Zeocin selection marker (Fig. 6.1B). The transfected HILID pools underwent a second selection using Zeocin antibiotics to generate new stable pools referred to as HILID+BiP. Transfected cells failed to survive selection using the weaker IRESv18 on Zeocin selection marker. HILID+BiP pools generated using IRESv11, with greater translation efficiency than IRESv18, to drive Zeocin selection marker expression survived selection. Cells were collected for qRT-PCR analysis of chaperone expression levels and the supernatant collected to check product aggregate levels. Analysis of mRNA expression levels for the re-transfected HILID+BiP cells showed that BiP expression increased 2.7 fold compared to the original HILID pool (Fig. 5A). The amount of aggregates decreased to 8.2% for HILID+BiP compared to the initial 12% of the HILID pool and an increase in monomers from 62.9% to 68.7% (Fig. 6.5B and C). IgG titer detected increased from 70 mg/L to 80 mg/L. There are currently no reports of how BiP chaperone over-expression could affect IgG product quality. It is possible that the increased BiP levels helped retain more incomplete and aggregation prone IgG within the cell for reassembly or degradation.

(A)

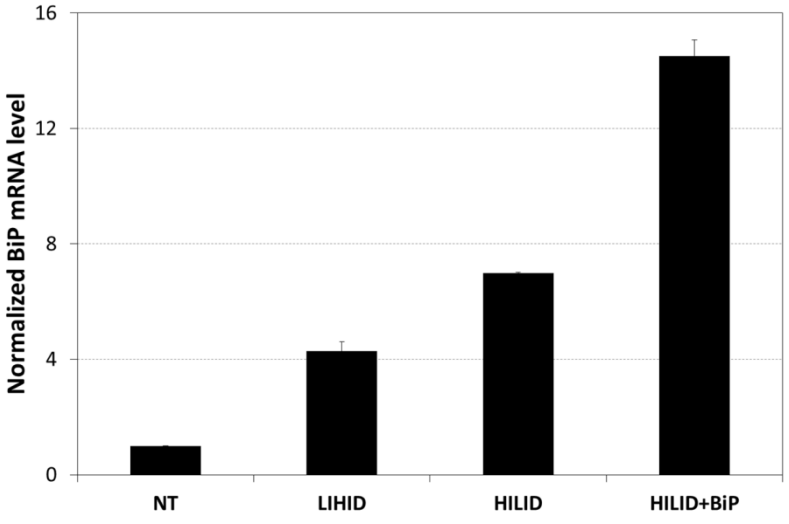
Normalized BiP mRNA level
16
12
8
4
0
NT
LIHID
HILID
HILID+BiP

(B)

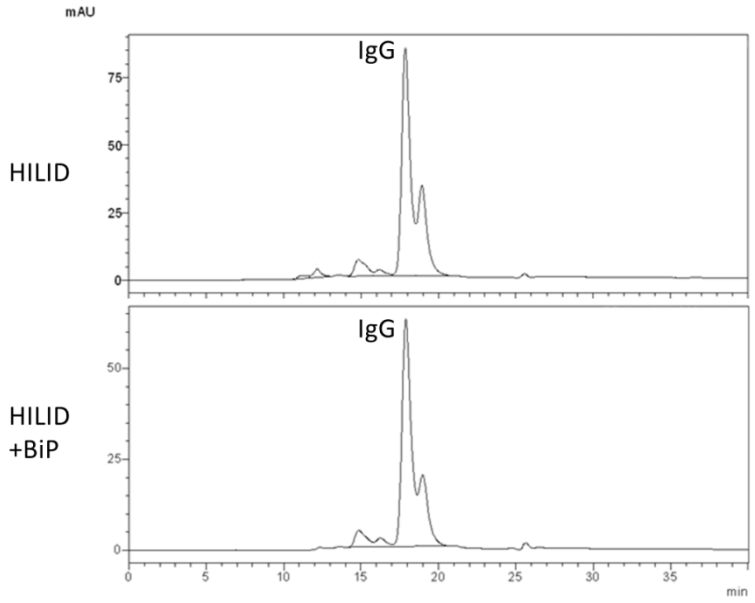
mAU
IgG
HILID
IgG
HILID
+BiP
75
50
25
0
50
25
0
0
5
10
15
20
25
30
35
min

(C)

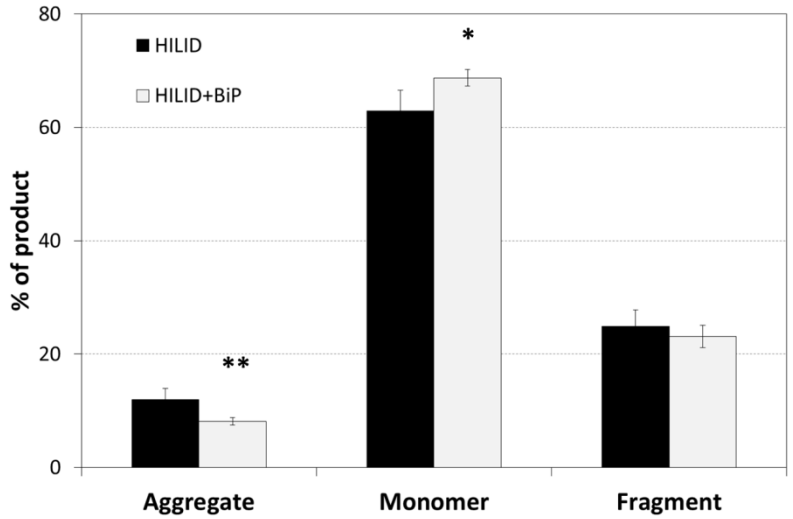

Figure 6.5 Analysis of BiP expression. (A) mRNA expression level of BiP for non-transfected DG44 cells (NT), LIHID, HILID and HILID+BiP were checked using qRT-PCR with β-actin used as the internal control. Samples were normalized to NT. (B) SEC chromatograms for HILID before (top) and after increasing BiP expression (HILID+BiP, bottom). Monomer peak is labelled as IgG. Peaks appearing before the main peak were considered high molecular weight aggregates and peaks after considered fragments. (C) Product distribution comparison of HILID and HILID+BIP. Each bar and standard deviations are obtained from two measurements each of biological replicates. * and ** denotes the differences were statistically significant using a two-tailed student t-test at $p<0.1$ and $p<0.05$ respectively.

6.4.4 A second transfection of LC to reduce aggregates

Over-expression of BiP chaperone did not completely remove the aggregates. We next explored an alternative method to reduce product aggregation in the HILID pools by re-transfecting the cells with more LC cDNA to increase the intracellular LC peptide amount and thus LC:HC ratio. A HILID pool was re-transfected with the LIZ vector carrying the LC cDNA and a Zeocin selection marker (Fig. 1C) and underwent antibiotics selection similar to how HILID+BiP pools were generated. IRESv18 was applied onto Zeocin to enhance selection stringency and maximize LC expression. The

newly generated stable cell pools were labeled as HILID+LC. Intracellular LC:HC ratio was verified to have increased from the initial 0.3 for HILID to 1.3 in HILID+LC pools (Fig. 6.6A). Titer for HILID+LC increased to 160 mg/L as compared to 70 mg/L for HILID. Only a single IgG monomer peak was observed for purified HILID+LC product during SEC analysis (Fig. 6.6B). Cells producing mAb with poor product quality due to low LC:HC ratio would thus likely benefit from a second transfection of only LC.

(A)

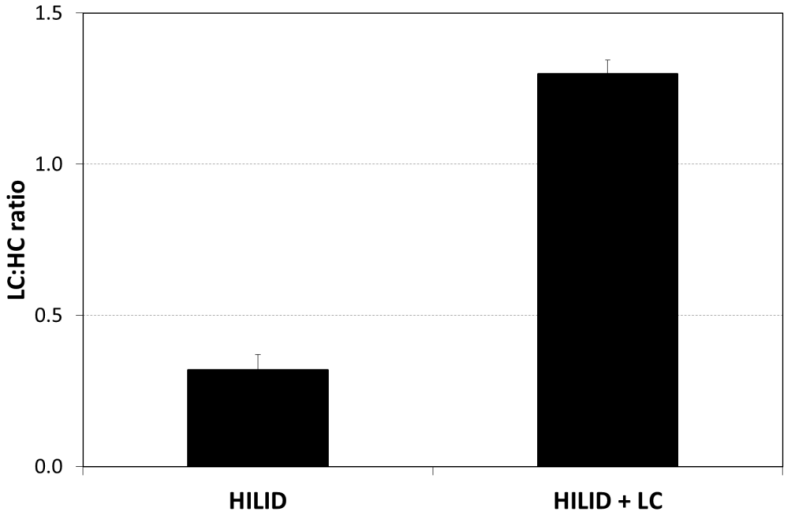

(B)

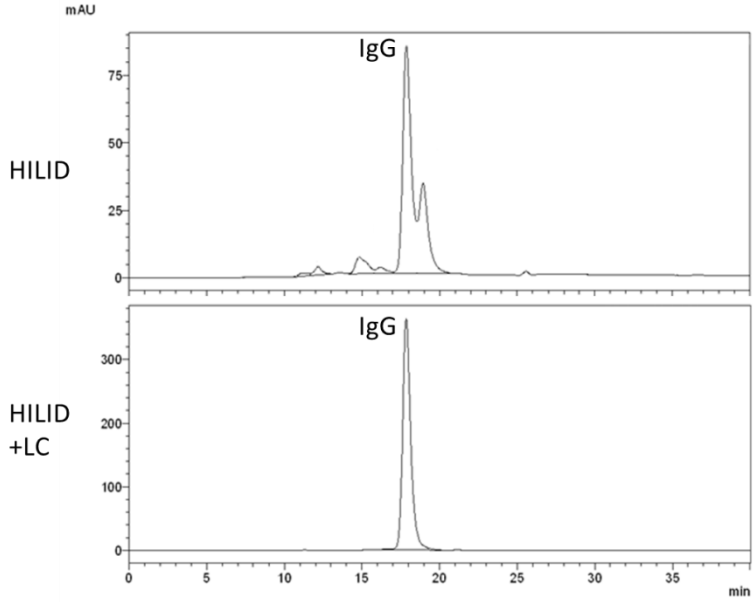

Figure 6.6 Increasing expression of LC to reduce aggregates and fragments in HILID pools. (A) Intracellular LC:HC ratio of HILID and after second transfection of LC only vector (HILID+LC). Data and standard deviation are from two measurements each of biological duplicates. (B) SEC chromatograms for HILID before (top) and after increasing LC expression (HILID+LC, bottom). Monomer peak is labelled IgG. Species appearing before the peak are aggregates and after the peak are fragments.

6.5 Discussion

In this study, we used a previously generated set of mAb producing CHO cell lines with LC:HC ratio controlled at either 3.4 (LIHID) or 0.3 (HILID) to understand the mechanism of aggregation formed under the condition of excess HC. Analytical studies of product from the HILID pool revealed that the aggregates consists a majority of HC polypeptides and were partially dissociated under reducing and denaturing conditions. We hypothesized that incomplete mAb fragments containing excess HC, such as HC_2 and HC_2LC were inclined to aggregate due to free cysteines and exposed hydrophobic regions on HC. HC was secreted when expressed in the absence

of LC and aggregates still formed between HC polypeptides when the free cysteine was mutated to alanine and serine. The level of aggregate was not significantly reduced compared to the wild-type HC as determined by western blotting. In a study using COS-7 cells expressing murine IgG, HC was only secreted in the absence of LC when cysteines on the first HC constant region (C_H1) were removed (Elkabetz et al. 2005). Unmodified HC and HC_2 were still being secreted in our CHO cells likely due to its high expression level under a DHFR/MTX amplification system exceeding the cell's capacity. Most of the aggregation prone motifs on IgG1 (class of the IgG used in this study) are concentrated around the hinge region of the HC (Chennamsetty et al. 2009). This is also the region where the free cysteine due to LC absence resides. This could explain why we did not see increased aggregation in the wild-type HC as the two main aggregating mechanisms, disulfide bonding at free cysteines and hydrophobic interactions, likely occur at the same region. A previous report conducted a similar study on aggregates but only observed aggregate levels decreasing upon adding guanidine and not in DTT (Gomez et al. 2012). In that study, LC:HC peptide ratios not determined but they reported a greater increase in HC mRNA levels as compared to LC mRNA levels for two of the three cell lines studied. It is possible that at the protein level, the LC:HC ratio was still close to one and the incomplete products composed of more mAbs lacking only one LC. In our study, more HC dimers were formed.

BiP upregulation to handle increased protein expression is part of the cell's unfolded protein response (UPR) (Lee et al. 1999; Schröder and Kaufman 2005). Over-expressing BiP in mAb expressing CHO cell lines had been reported to reduce specific secretion rate and increase HC accumulation

(Borth et al. 2005). There are still no reports on the effect of over-expressing BiP on mAb aggregation. The result here provides evidence that BiP over-expression could help reduce secretion of mAb aggregates and fragments caused by excess HC. BiP binds to the C_H1 domain of the unfolded HC to aid retention within the ER and release is triggered by LC (Hendershot et al. 1987; Vanhove et al. 2001). The increased BiP could help with retention of the excess HC within the ER, reducing the secretion of fragments like the HC_2 which are more prone to aggregation. Weakening the selection marker is effective to increase the stable expression of a gene as only clones with more copies of the integrated vector and/or vectors integrated into transcriptionally active site in chromosomes can survive the selection (Ho et al. 2012). We attempted to control BiP expression by using IRES variants with different strengths to control the resistance gene (Koh et al. 2013). Over-expression of BiP using the BIZ vector with Zeocin under the control of IRESv11 did not prevent aggregates forming possibly due to a combination of the limitations of the cell and insufficient BiP to handle all the excess HC. When we tried to maximize BiP expression by using a weaker IRESv18 on Zeocin on BIZ, the transfected cells failed to survive selection. IRESv18 had been successfully used with Zeocin in this report for LC re-transfection. We speculate that the higher BiP levels, due to greater selection stringency from the weaker IRES, resulted in over-accumulation of unfolded IgG and eventually cell death due to inability to cope with the load. The protein folding machinery is a complex process involving multiple enzymes and engineering of the pathway would likely require more than one target to successfully remove more of the aggregates. Further work is needed to understand how over-expression of

chaperones lowers aggregation and if a combination of BiP with other chaperones would have a greater effect.

Cell lines generated using commonly used vectors, co-transfection and multi-promoter single vector have varied ratios of LC:HC. Lee et al., had previously found that product from clones with low LC:HC mRNA levels were prone to aggregate and suggested super-transfection of LC into clones exhibiting high levels of mAb aggregation but did not perform the experiment (2009). In our study, we show that re-transfecting of cells with low LC:HC ratio with more LC to increase the ratio was an effective method to reduce aggregation. The excess LC expression was obtained by using a very weak IRESv18 to drive low levels of Zeocin expression to increase the stringency of selection for high producers in stably transfected pools. LC:HC ratios affect expression level and is a critical parameter for mAb aggregation and other quality parameters, such as glycosylation (van Berkel et al. 2009; Yang et al. 2009; Ho et al. 2013; Koh et al. 2013). It is favorable to generate cell lines using vectors with the ability to control LC:HC at optimal ratios for both expression level and quality. For cell lines forming aggregate due to excess HC, re-transfection of LC is the easiest and most effective way to reduce aggregates HC.

Aggregates in protein therapeutics like IgG monoclonal antibodies (mAb) are detrimental to product safety and efficacy. We studied the underlying mechanism causing product aggregation in mAb producing CHO cell lines with excess HC. Product was highly aggregation prone within the cell but the majority of these aggregates were not secreted. The poorly folded mAb which managed to escape the cell's quality control mechanisms and

enter the supernatant could be dissociated by reducing and denaturing conditions. Interestingly, mutation of a potential free cysteine on HC did not reduce the amount of aggregates observed between HC dimers. Aggregates could be reduced by over-expression of BiP chaperone and totally removed by a second transfection of LC. mAb aggregation in CHO cells with excess HC occurs due to a combination of limitations of the chaperone levels and LC:HC ratio. Further experiments using clones with varying levels of intracellular HC and BiP before BiP over-expression could yield even more interesting results. Overall, the results here would be useful for designing methods to break up aggregates post-purification or to rescue previously generated mAb cell lines with poor product quality.

Chapter 7: Conclusion and future work

In this chapter, we conclude the work done in this thesis and suggest some possible future work which can be performed.

7.1 Conclusion

The main aim of this thesis was to design a single vector system which expressed the LC, HC and selection marker genes required for mAb expression in CHO cells on a single transcript. This would reduce non-expressing clones due to vector fragmentation and aid in controlling LC:HC ratio. The vector can subsequently be used to evaluate the effect of different LC:HC ratios had on stable mAb expression. The final vector we designed and optimized was the first IRES tricistronic vector for expressing high levels of mAb in CHO cells and a patent has been awarded based on this work (US patent no. 8,809,01). We first established in chapter 3 that the benefits of using IRES to link the genes on a single vector compared to the other traditional vector designs include: 1) improved proportion of isolated clones expressing full mAb with the tighter coupling of the genes on one transcript, 2) increased stringency during drug selection by linking the selection marker to an attenuated IRES leads to higher titers, 3) control of relative LC and HC amounts.

We next evaluated another way of linking the multiple genes together by comparing the use of F2A elements with IRES in chapter 4. MAb produced using F2A had poor product quality due to incorrect protein cleavage and could not be used for any further mAb production or studies. The ability to use IRES to express multiple genes correctly without much optimization would be a major benefit and allow easier vector design. In the fifth chapter, the ability to control LC:HC ratio at consistent levels in stably transfected cells using IRES was used to determine the best arrangement of genes on the vector and to study how the ratio affects mAb production. We observed that expression

levels and product quality were the best at the controlled LC:HC ratio of 3.4 when placing LC in the first cistron. There was significant product aggregation due to hydrophobic interactions and disulfide bonding between incompletely formed IgG when ratio was at 0.3. This aggregation could be reduced by increasing BiP chaperone expression or re-transfecting the cells with more LC.

Using IRES to link LC and HC and placing LC as the first cistron directly downstream of the promoter, similar to the vector design of LIHID in figure 5.1, is an effective way to ensure LC is expressed in excess of HC. This design has shown to be beneficial for obtaining high mAb producing cells with low aggregation. The design was also flexible and worked with both antibiotic (NPT, chapter 3) and amplifiable selection markers (DHFR, chapter 4 and 5). The IRES tricistronic design provides a novel vector for generation of mAb producing CHO cells with greater efficiency and better quality. The IRES tricistronic vector could be part of a QbD system, helping to control LC:HC ratio for better mAb expression and consistent product quality. The excess LC could also aid in producing difficult to express mAbs. Finally, the solutions tested to reduce mAb aggregates that arise due to excess HC should also be effective for cell lines generated with other vector systems.

7.2 Future work

In this thesis, we focused only on IgG1 mAb production in CHO cells as they are the best-selling biologics and most commonly used mammalian cell line respectively. The IRES vector design could be extended to other forms of immunoglobulins which are also assembled from multiple different proteins to determine how the relative amounts of each protein would affect

product expression. The study should also be replicated using other novel cell types like the Per.C6 human cell lines.

The vector still holds much potential for improvements to increase the final mAb titer. Firstly, the hCMV promoter used can be replaced with other strong promoters like the murine CMV promoter and promoter from the CHO elongation factor. The promoter can also be replaced by synthetic promoters generated by screening large libraries of randomly evolved mutations or constructed based on bioinformatics data of known promoters to maximize transcription factor binding and optimize for tissue specificity (Ho and Yang 2014). Another possible area of improvement would be to use the codon optimization tools discussed in section 2.5.1 to create expression cassettes optimized for CHO cells. While chromatin modifying elements introduced in section 2.5.4 can also be included, there exists possible issues of intellectual property rights for many of these elements. The vector could also be combined with targeted integration techniques discussed in 2.4.5 to increase the rate of integration into an active site for higher productivity. Another benefit of targeted integration is the minimizing of gene copies within the host cell to reduce the occurrence of tandem induced gene silencing. The site and gene copies integrated into the host cell are parameters required for authority approval of the cell line for biologics production, this information would be more easily obtained using a gene targeted cell line. The site of targeted can be chosen based on the CHO genome database obtained to avoid unwanted gene mutations.

Despite not working well during our evaluation, F2A elements are still interesting for multi-gene expression studies as it allows for a 1:1 balanced

ratio of the genes. F2A has been successfully reported for use previously and could still work for our vector design with some optimization like testing different signal peptides and increasing the expression of furin endoprotease. Another area of this thesis which could be further explored is an expanded range of LC:HC ratios spread over smaller intervals. Either IRES from other sources could be tested or synthetic IRES sequences can be generated to alter the expression of the gene downstream of IRES and create a wider range of LC:HC ratios. The effect of BiP on product aggregation has yet to be reported and further work could be done to identify how the increased BiP aided in lowering the fragments and aggregates.

As mentioned in the literature review, the growing biosimilar market is creating a rising demand for mAb producing cell lines. In this study, the materials used were influenced largely by in-house availability and experience. An optimized cell generation kit comprising hydrolysate- and protein-free chemically defined culture media with optimized feed systems and vectors that work with other selection systems like the glutamine synthetase (GS) marker could be developed. Scale-up studies of mAb producing cell lines in bioreactors could also be conducted to more closely replicate actual production conditions.

Bibliography

Aggarwal, S. (2010). "What's fueling the biotech engine - 2009 to 2010." Nature Biotechnology **28**(11): 1165-1171.

Aggarwal, S. (2011). "What's fueling the biotech engine - 2010 to 2011." Nature Biotechnology **29**(12): 1083-1089.

Aggarwal, S. (2012). "What's fueling the biotech engine - 2011 to 2012." Nature Biotechnology **30**(12): 1191-1197.

Agrawal, V. and M. Bal (2012). "Strategies for rapid production of therapeutic proteins in mammalian cells." BioProcess International **10**(4): 32-48.

Ahmed, I., B. Kaspar, et al. (2012). "Biosimilars: Impact of Biologic Product Life Cycle and European Experience on the Regulatory Trajectory in the United States." Clinical Therapeutics **34**(2): 400-419.

Aldrich, T. L., A. Viaje, et al. (2003). "EASE vectors for rapid stable expression of recombinant antibodies." Biotechnology Progress **19**(5): 1433-1438.

Angov, E. (2011). "Codon usage: Nature's roadmap to expression and folding of proteins." Biotechnology Journal **6**(6): 650-659.

Arden, N. and M. J. Betenbaugh (2006). "Regulating apoptosis in mammalian cell cultures." Cytotechnology **50**(1-3): 77-92.

Bailey, L. A., D. Hatton, et al. (2012). "Determination of Chinese hamster ovary cell line stability and recombinant antibody expression during long-term culture." Biotechnology and Bioengineering **109**(8): 2093-2103.

Baker, K. N., M. H. Rendall, et al. (2001). "Metabolic control of recombinant protein N-glycan processing in NS0 and CHO cells." Biotechnology and Bioengineering **73**(3): 188-202.

Balcarcel, R. R. and G. Stephanopoulos (2001). "Rapamycin reduces hybridoma cell death and enhances monoclonal antibody production." Biotechnology and Bioengineering **76**(1): 1-10.

Barnes, L. M., C. M. Bentley, et al. (2007). "Molecular analysis of successful cell line selection in transfected GS-NS0 myeloma cells." Biotechnology and Bioengineering **96**(2): 337-348.

Barok, M., J. Isola, et al. (2007). "Trastuzumab causes antibody-dependent cellular cytotoxicity-mediated growth inhibition of submacroscopic JIMT-1 breast cancer xenografts despite intrinsic drug resistance." Molecular Cancer Therapeutics **6**(7): 2065-2072.

Barron, N., N. Kumar, et al. (2011). "Engineering CHO cell growth and recombinant protein productivity by overexpression of miR-7." Journal of Biotechnology **151**(2): 204-211.

Baumal, R. and M. D. Scharff (1973). "Synthesis, Assembly and Secretion of Mouse Immunoglobulin." Immunological Reviews **14**(1): 163-183.

Baumal, R. and M. D. Scharff (1973). "Synthesis, Assembly and Secretion of γ-Globulin by Mouse Myeloma Cells: V. Balanced and Unbalanced Synthesis of Heavy and Light Chains by IgG-Producing Tumors and Cell Lines." The Journal of Immunology **111**(2): 448-456.

Baycin-Hizal, D., D. L. Tabb, et al. (2012). "Proteomic Analysis of Chinese Hamster Ovary Cells." Journal of Proteome Research **11**(11): 5265-5276.

Bebbington, C. R., G. Renner, et al. (1992). "High-level expression of a recombinant antibody from myeloma cells using a glutamine synthetase gene as an amplifiable selectable marker." Nature Biotechnology **10**(2): 169-175.

Beck, A. and J. M. Reichert (2012). "Marketing approval of mogamulizumab: A triumph for glyco-engineering." MAbs **4**(4): 419-425.

Becker, J., M. Hackl, et al. (2011). "Unraveling the Chinese hamster ovary cell line transcriptome by next-generation sequencing." Journal of Biotechnology **156**(3): 227-235.

Benton, T., T. Chen, et al. (2002). "The use of UCOE vectors in combination with a preadapted serum free, suspension cell line allows for rapid production of large quantities of protein." Cytotechnology **38**(1-3): 43-46.

Bibikova, M., M. Golic, et al. (2002). "Targeted Chromosomal Cleavage and Mutagenesis in Drosophila Using Zinc-Finger Nucleases." Genetics **161**(3): 1169-1175.

Birch, J. R. and A. J. Racher (2006). "Antibody production." Advanced Drug Delivery Reviews **58**(5-6): 671-685.

Bochkov, Y. A. and A. C. Palmenberg (2006). "Translational efficiency of EMCV IRES in bicistronic vectors is dependent upon IRES sequence and gene location." Biotechniques **41**(3): 283-284, 286, 288 passim.

Böhm, E., R. Voglauer, et al. (2004). "Screening for improved cell performance: Selection of subclones with altered production kinetics or improved stability by cell sorting." Biotechnology and Bioengineering **88**(6): 699-706.

Borman, A. M., J. L. Bailly, et al. (1995). "Picornavirus internal ribosome entry segments: Comparison of translation efficiency and the requirements for optimal internal initiation of translation in vitro." Nucleic Acids Research **23**(18): 3656-3663.

Borman, A. M., P. Le Mercier, et al. (1997). "Comparison of Picornaviral IRES-Driven Internal Initiation of Translation in Cultured Cells of Different Origins." Nucleic Acids Research **25**(5): 925-932.

Borman, A. M., P. LeMercier, et al. (1997). "Comparison of picornaviral IRES-driven internal initiation of translation in cultured cells of different origins." Nucleic Acids Research **25**(5): 925-932.

Borth, N., D. Mattanovich, et al. (2005). "Effect of Increased Expression of Protein Disulfide Isomerase and Heavy Chain Binding Protein on Antibody Secretion in a Recombinant CHO Cell Line." Biotechnology Progress **21**(1): 106-111.

Braakman, I. and N. J. Bulleid (2011). "Protein folding and modification in the mammalian endoplasmic reticulum." Annual Review of Biochemistry **80**: 71-99.

Brennan, F. M., A. Jackson, et al. (1989). "Inhibitory effect of TNFα antibodies on synovial cell interleukin-1 production in rheumatoid arthritis." Lancet **2**(8657): 244-247.

Brezinsky, S. C., G. G. Chiang, et al. (2003). "A simple method for enriching populations of transfected CHO cells for cells of higher specific productivity." Journal of Immunological Methods **277**(1-2): 141-155.

Bronson, J., M. Dhar, et al. (2012). Chapter Thirty-One - To Market, To Market—2011. Annual Reports in Medicinal Chemistry. C. D. Manoj, Academic Press. **Volume 47:** 499-569.

Brooks, S. (2004). "Appropriate glycosylation of recombinant proteins for human use." Molecular Biotechnology **28**(3): 241-255.

Brown, M. E., G. Renner, et al. (1992). "Process development for the production of recombinant antibodies using the glutamine synthetase (GS) system." Cytotechnology **9**(1-3): 231-236.

Butler, M. (2005). "Animal cell cultures: recent achievements and perspectives in the production of biopharmaceuticals." Applied Microbiology and Biotechnology **68**(3): 283-291.

Butler, M. (2006). "Optimisation of the cellular metabolism of glycosylation for recombinant proteins produced by mammalian cell systems." Cytotechnology **50**(1-3): 57-76.

Butler, M. and A. Meneses-Acosta (2012). "Recent advances in technology supporting biopharmaceutical production from mammalian cells." Applied Microbiology and Biotechnology **96**(4): 885-894.

Cacciatore, J. J., L. A. Chasin, et al. (2010). "Gene amplification and vector engineering to achieve rapid and high-level therapeutic protein production using the Dhfr-based CHO cell selection system." Biotechnology Advances **28**(6): 673-681.

Cairns, V. R., C. T. Demaria, et al. (2011). "Utilization of non-AUG initiation codons in a flow cytometric method for efficient selection of recombinant cell lines." Biotechnology and Bioengineering **108**(11): 2611-2622.

Camper, N., T. Byrne, et al. (2011). "Stable expression and purification of a functional processed Fab' fragment from a single nascent polypeptide in CHO cells expressing the mCAT-1 retroviral receptor." Journal of Immunological Methods **372**(1-2): 30-41.

Carlage, T., R. Kshirsagar, et al. (2012). "Analysis of dynamic changes in the proteome of a Bcl-XL overexpressing Chinese hamster ovary cell culture during exponential and stationary phases." Biotechnology Progress **28**(3): 814-823.

Carroll, D. (2014). "Genome Engineering with Targetable Nucleases." Annual Review of Biochemistry **83**(1): 409-439.

Chan, A. C. and P. J. Carter (2010). "Therapeutic antibodies for autoimmunity and inflammation." Nature Reviews Immunology **10**(5): 301-316.

Chan, H. Y., V. Sivakamasundari, et al. (2011). "Comparison of IRES and F2A-based locus-specific multicistronic expression in stable mouse lines." PLoS One **6**(12).

Chen, L., Z. Xie, et al. (2004). "Highly efficient selection of the stable clones expressing antibody-IL-2 fusion protein by a dicistronic expression vector containing a mutant neo gene." Journal of Immunological Methods **295**(1-2): 49-56.

Chennamsetty, N., B. Helk, et al. (2009). "Aggregation-prone motifs in human immunoglobulin G." Journal of Molecular Biology **391**(2): 404-413.

Chiang, G. G. and W. P. Sisk (2005). "Bcl-xL mediates increased production of humanized monoclonal antibodies in Chinese hamster ovary cells." Biotechnology and Bioengineering **91**(7): 779-792.

Chung, B. K.-S., F. N. K. Yusufi, et al. (2013). "Enhanced expression of codon optimized interferon gamma in CHO cells." Journal of Biotechnology **167**(3): 326-333.

Chusainow, J., Y. S. Yang, et al. (2009). "A study of monoclonal antibody-producing CHO cell lines: what makes a stable high producer?" Biotechnology and Bioengineering **102**(4): 1182-1196.

Ciucanu, I. and F. Kerek (1984). "A simple and rapid method for the permethylation of carbohydrates." Carbohydrate Research **131**(2): 209-217.

Cockett, M. I., C. R. Bebbington, et al. (1990). "High Level Expression of Tissue Inhibitor of Metalloproteinases in Chinese Hamster Ovary Cells Using Glutamine Synthetase Gene Amplification." Nature Biotechnology **8**(7): 662-667.

Cost, G. J., Y. Freyvert, et al. (2010). "BAK and BAX deletion using zinc-finger nucleases yields apoptosis-resistant CHO cells." Biotechnology and Bioengineering **105**(2): 330-340.

Costa, A. R., M. E. Rodrigues, et al. (2010). "Guidelines to cell engineering for monoclonal antibody production." European Journal of Pharmaceutics and Biopharmaceutics **74**(2): 127-138.

Costa, A. R., M. E. Rodrigues, et al. (2012). "Evaluation of the OSCAR™ system for the production of monoclonal antibodies by CHO-K1 cells." International Journal of Pharmaceutics **430**(1-2): 42-46.

Crameri, A., E. A. Whitehorn, et al. (1996). "Improved Green Fluorescent Protein by Molecular Evolution Using DNA Shuffling." Nature Biotechnology **14**(3): 315-319.

Cromwell, M. E., E. Hilario, et al. (2006). "Protein aggregation and bioprocessing." AAPS J **8**(3): E572-579.

Cromwell, M. E., E. Hilario, et al. (2006). "Protein aggregation and bioprocessing." AAPS Journal **8**(3): E572-579.

Davies, M. V. and R. J. Kaufman (1992). "The Sequence Context Of The Initiation Codon In The Encephalomyocarditis Virus Leader Modulates Efficiency Of Internal Translation Initiation." Journal Of Virology **66**(4): 1924-1932.

Davies, S. L., P. M. O'Callaghan, et al. (2011). "Impact of gene vector design on the control of recombinant monoclonal antibody production by chinese hamster ovary cells." Biotechnology Progress **27**(6): 1689-1699.

De Felipe, P., G. A. Luke, et al. (2010). "Inhibition of 2A-mediated 'cleavage' of certain artificial polyproteins bearing N-terminal signal sequences." Biotechnology Journal **5**(2): 213-223.

de Felipe, P., G. A. Luke, et al. (2006). "E unum pluribus: multiple proteins from a self-processing polyprotein." Trends in Biotechnology **24**(2): 68-75.

Dell, A., A. J. Reason, et al. (1994). "Mass spectrometry of carbohydrate-containing biopolymers." Methods in Enzymology **230**: 108-132.

DeMaria, C. T., V. Cairns, et al. (2007). "Accelerated clone selection for recombinant CHO CELLS using a FACS-based high-throughput screen." Biotechnology Progress **23**(2): 465-472.

Dharshanan, S., H. Chong, et al. (2011). "Rapid automated selection of mammalian cell line secreting high level of humanized monoclonal

antibody using Clone Pix FL system and the correlation between exterior median intensity and antibody productivity." Electronic Journal of Biotechnology **14**: 8-8.

Dietmair, S., L. K. Nielsen, et al. (2011). "Engineering a mammalian super producer." Journal of Chemical Technology & Biotechnology **86**(7): 905-914.

Dietmair, S., L. K. Nielsen, et al. (2012). "Mammalian cells as biopharmaceutical production hosts in the age of omics." Biotechnology Journal **7**(1): 75-89.

Dinnis, D. M. and D. C. James (2005). "Engineering mammalian cell factories for improved recombinant monoclonal antibody production: lessons from nature?" Biotechnology and Bioengineering **91**(2): 180-189.

Donnelly, M. L., G. Luke, et al. (2001). "Analysis of the aphthovirus 2A/2B polyprotein 'cleavage' mechanism indicates not a proteolytic reaction, but a novel translational effect: a putative ribosomal 'skip'." Journal of General Virology **82**(Pt 5): 1013-1025.

Dorai, H., S. Corisdeo, et al. (2012). "Early prediction of instability of chinese hamster ovary cell lines expressing recombinant antibodies and antibody-fusion proteins." Biotechnology and Bioengineering **109**(4): 1016-1030.

Dorai, H., B. Csirke, et al. (2006). "Correlation of heavy and light chain mRNA copy numbers to antibody productivity in mouse myeloma production cell lines." Hybridoma **25**(1): 1-9.

Doronina, V. A., P. de Felipe, et al. (2008). "Dissection of a co-translational nascent chain separation event." Biochemical Society Transactions **36**: 712-716.

Doronina, V. A., C. Wu, et al. (2008). "Site-specific release of nascent chains from ribosomes at a sense codon." Molecular and Cellular Biology **28**(13): 4227-4239.

Durocher, Y. and M. Butler (2009). "Expression systems for therapeutic glycoprotein production." Current Opinion in Biotechnology **20**(6): 700-707.

Eisenstein, M. (2006). "Automatic for the people." Nature Methods **3**(10): 855-866.

Elkabetz, Y., Y. Argon, et al. (2005). "Cysteines in CH1 Underlie Retention of Unassembled Ig Heavy Chains." Journal of Biological Chemistry **280**(15): 14402-14412.

Ellgaard, L. and A. Helenius (2003). "Quality control in the endoplasmic reticulum." Nature Reviews Molecular Cell Biology **4**(3): 181-191.

Eon-Duval, A., H. Broly, et al. (2012). "Quality attributes of recombinant therapeutic proteins: An assessment of impact on safety and efficacy as part of a quality by design development approach." Biotechnology Progress **28**(3): 608-622.

Eszterhas, S. K., E. E. Bouhassira, et al. (2002). "Transcriptional interference by independently regulated genes occurs in any relative arrangement of the genes and is influenced by chromosomal integration position." Molecular and Cellular Biology **22**(2): 469-479.

European Medicines Agency. (2008). "Guideline on development, production, characterisation and specifications for monoclonal antibodies and related products." 2014, from http://www.ema.europa.eu/ema/.

Fagioli, C., A. Mezghrani, et al. (2001). "Reduction of Interchain Disulfide Bonds Precedes the Dislocation of Ig-μ Chains from the Endoplasmic Reticulum to the Cytosol for Proteasomal Degradation." Journal Of Biological Chemistry **276**(44): 40962-40967.

Fagioli, C. and R. Sitia (2001). "Glycoprotein quality control in the endoplasmic reticulum. Mannose trimming by endoplasmic reticulum mannosidase I times the proteasomal degradation of unassembled immunoglobulin subunits." Journal Of Biological Chemistry **276**(16): 12885-12892.

Fallot, S., R. Ben Naya, et al. (2009). "Alternative-splicing-based bicistronic vectors for ratio-controlled protein expression and application to recombinant antibody production." Nucleic Acids Research **37**(20): e134.

Fan, L., I. Kadura, et al. (2012). "Improving the efficiency of CHO cell line generation using glutamine synthetase gene knockout cells." Biotechnology and Bioengineering **109**(4): 1007-1015.

Fang, J., J. J. Qian, et al. (2005). "Stable antibody expression at therapeutic levels using the 2A peptide." Nature Biotechnology **23**(5): 584-590.

Fang, J., S. Yi, et al. (2007). "An antibody delivery system for regulated expression of therapeutic levels of monoclonal antibodies In Vivo." Molecular Therapy **15**(6): 1153-1159.

Fath, S., A. P. Bauer, et al. (2011). "Multiparameter RNA and Codon Optimization: A Standardized Tool to Assess and Enhance Autologous Mammalian Gene Expression." PLoS One **6**(3): e17596.

Feige, M. J., L. M. Hendershot, et al. (2010). "How antibodies fold." Trends in Biochemical Sciences **35**(4): 189-198.

Ferrara, N. (2004). "Vascular Endothelial Growth Factor: Basic Science and Clinical Progress." Endocrine Reviews **25**(4): 581-611.

Ferrara, N., K. J. Hillan, et al. (2004). "Case history: Discovery and development of bevacizumab, an anti-VEGF antibody for treating cancer." Nature Reviews Drug Discovery **3**(5): 391-400.

Fischer, S., N. Charara, et al. (2012). "Transient recombinant protein expression in a human amniocyte cell line: The CAP-T® cell system." Biotechnology and Bioengineering **109**(9): 2250-2261.

Fishwild, D. M., S. L. O'Donnell, et al. (1996). "High-avidity human IgG[kappa] monoclonal antibodies from a novel strain of minilocus transgenic mice." Nature Biotechnology **14**(7): 845-851.

Freimark, D., V. Jerome, et al. (2010). "A GFP-based method facilitates clonal selection of transfected CHO cells." Biotechnology Journal **5**(1): 24-31.

Fussenegger, M., J. E. Bailey, et al. (1999). "Genetic optimization of recombinant glycoprotein production by mammalian cells." Trends In Biotechnology **17**(1): 35-42.

Fussenegger, M., X. Mazur, et al. (1998). "pTRIDENT, a novel vector family for tricistronic gene expression in mammalian cells." Biotechnology and Bioengineering **57**(1): 1-10.

Fussenegger, M., S. Moser, et al. (1998). "Regulated multicistronic expression technology for mammalian metabolic engineering." Cytotechnology **28**(1-3): 111-125.

Galbete, J. L., M. Buceta, et al. (2009). "MAR elements regulate the probability of epigenetic switching between active and inactive gene expression." Molecular BioSystems **5**(2): 143-150.

Gammell, P., N. Barron, et al. (2007). "Initial identification of low temperature and culture stage induction of miRNA expression in suspension CHO-K1 cells." Journal of Biotechnology **130**(3): 213-218.

Garber, E. and S. J. Demarest (2007). "A broad range of Fab stabilities within a host of therapeutic IgGs." Biochemical and Biophysical Research Communications **355**(3): 751-757.

Geisse, S. (2009). "Reflections on more than 10 years of TGE approaches." Protein Expression and Purification **64**(2): 99-107.

Geisse, S. and B. Voedisch (2012). Transient expression technologies: Past, present, and future. **899:** 203-219.

Gersbach, C. A., T. Gaj, et al. (2014). "Synthetic Zinc Finger Proteins: The Advent of Targeted Gene Regulation and Genome Modification Technologies." Accounts of Chemical Research **47**(8): 2309-2318.

Girod, P. A., D. Q. Nguyen, et al. (2007). "Genome-wide prediction of matrix attachment regions that increase gene expression in mammalian cells." Nature Methods **4**(9): 747-753.

Girod, P. A., M. Zahn-Zabal, et al. (2005). "Use of the chicken lysozyme 5′ matrix attachment region to generate high producer CHO cell lines." Biotechnology and Bioengineering **91**(1): 1-11.

Goetze, A. M., Y. D. Liu, et al. (2011). "High-mannose glycans on the Fc region of therapeutic IgG antibodies increase serum clearance in humans." Glycobiology **21**(7): 949-959.

Gomez, N., J. Subramanian, et al. (2012). "Culture temperature modulates aggregation of recombinant antibody in CHO cells." Biotechnology and Bioengineering **109**(1): 125-136.

Gonzalez, R., B. A. Andrews, et al. (2001). "Metabolic control analysis of monoclonal antibody synthesis." Biotechnology Progress **17**(2): 217-226.

Gonzalez, R., B. A. Andrews, et al. (2002). "Kinetic model of BiP- and PDI-mediated protein folding and assembly." Journal of Theoretical Biology **214**(4): 529-537.

Greber, D. and M. Fussenegger (2007). "Multi-gene engineering: simultaneous expression and knockdown of six genes off a single platform." Biotechnology and Bioengineering **96**(5): 821-834.

Gura, T. (2002). "Therapeutic antibodies: Magic bullets hit the target." Nature **417**(6889): 584-586.

Gurtu, V., G. Yan, et al. (1996). "IRES bicistronic expression vectors for efficient creation of stable mammalian cell lines." Biochemical and Biophysical Research Communications **229**(1): 295-298.

Hackl, M., T. Jakobi, et al. (2011). "Next-generation sequencing of the Chinese hamster ovary microRNA transcriptome: Identification, annotation and profiling of microRNAs as targets for cellular engineering." Journal of Biotechnology **153**(1-2): 62-75.

Hammond, S., J. C. Swanberg, et al. (2011). "Genomic sequencing and analysis of a Chinese hamster ovary cell line using Illumina sequencing technology." BMC Genomics **12**.

Hammond, S., J. C. Swanberg, et al. (2012). "Profiling conserved microRNA expression in recombinant CHO cell lines using illumina sequencing." Biotechnology and Bioengineering **109**(6): 1371-1375.

Harraghy, N., A. Regamey, et al. (2011). "Identification of a potent MAR element from the mouse genome and assessment of its activity in stable and transient transfections." Journal of Biotechnology **154**(1): 11-20.

Hayes, N. V. L., C. M. Smales, et al. (2010). "Protein disulfide isomerase does not control recombinant IgG4 productivity in mammalian cell lines." Biotechnology and Bioengineering **105**(4): 770-779.

Hellen, C. U. T. and P. Sarnow (2001). "Internal ribosome entry sites in eukaryotic mRNA molecules." Genes & Development **15**(13): 1593-1612.

Hendershot, L., D. Bole, et al. (1987). "Assembly and secretion of heavy chains that do not associate posttranslationally with immunoglobulin heavy chain-binding protein." The Journal of Cell Biology **104**(3): 761-767.

Hennecke, M., M. Kwissa, et al. (2001). "Composition and arrangement of genes define the strength of IRES-driven translation in bicistronic mRNAs." Nucleic Acids Research **29**(16): 3327-3334.

Hermeling, S., D. J. Crommelin, et al. (2004). "Structure-immunogenicity relationships of therapeutic proteins." Pharmaceutical Research **21**(6): 897-903.

Higgins, E. (2010). "Carbohydrate analysis throughout the development of a protein therapeutic." Glycoconjugate Journal **27**(2): 211-225.

Ho, S. C. L., M. Bardor, et al. (2012). "IRES-mediated Tricistronic vectors for enhancing generation of high monoclonal antibody expressing CHO cell lines." Journal Of Biotechnology **157**(1): 130-139.

Ho, S. C. L., E. Y. C. Koh, et al. (2013). "Control of IgG LC:HC ratio in stably transfected CHO cells and study of the impact on expression, aggregation, glycosylation and conformational stability." Journal of Biotechnology **165**(3–4): 157-166.

Ho, S. C. L. and Y. Yang (2014). "Identifying and engineering promoters for high level and sustainable therapeutic recombinant protein production in cultured mammalian cells." Biotechnology Letters **36**(8): 1569-1579.

Hobbs, S., S. Jitrapakdee, et al. (1998). "Development of a bicistronic vector driven by the human polypeptide chain elongation factor 1alpha promoter for creation of stable mammalian cell lines that express very high levels of recombinant proteins." Biochemical and Biophysical Research Communications **252**(2): 368-372.

Hoeksema, F., R. Van Blokland, et al. (2011). "The use of a stringent selection system allows the identification of DNA elements that augment gene expression." Molecular Biotechnology **48**(1): 19-29.

Hossler, P., S. F. Khattak, et al. (2009). "Optimal and consistent protein glycosylation in mammalian cell culture." Glycobiology **19**(9): 936-949.

Hou, J. J. C., J. Codamo, et al. (2011). "New frontiers in cell line development: challenges for biosimilars." Journal of Chemical Technology & Biotechnology **86**(7): 895-904.

Houdebine, L. M. and J. Attal (1999). "Internal ribosome entry sites (IRESs): reality and use." Transgenic Research **8**(3): 157-177.

Hristodorov, D., R. Fischer, et al. (2012). "Generation and Comparative Characterization of Glycosylated and Aglycosylated Human IgG1 Antibodies." Molecular Biotechnology.

Hung, F., L. Deng, et al. (2010). "mRNA stability and antibody production in CHO cells: improvement through gene optimization." Biotechnology Journal **5**(4): 393-401.

ICH. (1999). "ICH Q6B, Specifications: Test procedures and acceptance criteria for biotechnological/biological products." 2014, from http://www.ich.org/products/guidelines/quality/article/quality-guidelines.html.

Imai-Nishiya, H., K. Mori, et al. (2007). "Double knockdown of alpha1,6-fucosyltransferase (FUT8) and GDP-mannose 4,6-dehydratase (GMD) in antibody-producing cells: a new strategy for generating fully non-fucosylated therapeutic antibodies with enhanced ADCC." BMC Biotechnology **7**: 84.

Ionescu, R. M., J. Vlasak, et al. (2008). "Contribution of variable domains to the stability of humanized IgG1 monoclonal antibodies." Journal of Pharmaceutical Sciences **97**(4): 1414-1426.

Jadhav, V., M. Hackl, et al. (2012). "A screening method to assess biological effects of microRNA overexpression in Chinese hamster ovary cells." Biotechnology and Bioengineering **109**(6): 1376-1385.

Jayapal, K. P., K. F. Wlaschin, et al. (2007). "Recombinant protein therapeutics from CHO Cells - 20 years and counting." Chemical Engineering Progress **103**(10): 40-47.

Jefferis, R. (2005). "Glycosylation of recombinant antibody therapeutics." Biotechnology Progress **21**(1): 11-16.

Jefferis, R. (2009). "Glycosylation as a strategy to improve antibody-based therapeutics." Nature Reviews Drug Discovery **8**(3): 226-234.

Jenkins, N. (2007). "Modifications of therapeutic proteins: challenges and prospects." Cytotechnology **53**(1-3): 121-125.

Jiang, Z., Y. Huang, et al. (2006). "Regulation of recombinant monoclonal antibody production in chinese hamster ovary cells: a comparative study of gene copy number, mRNA level, and protein expression." Biotechnology Progress **22**(1): 313-318.

Johnson, K. C., N. M. Jacob, et al. (2011). "Conserved MicroRNAs in Chinese hamster ovary cell lines." Biotechnology and Bioengineering **108**(2): 475-480.

Jones, P. T., P. H. Dear, et al. (1986). "Replacing the complementarity-determining regions in a human antibody with those from a mouse." Nature **321**(6069): 522-525.

Jostock, T., Z. Dragic, et al. (2010). "Combination of the 2A/furin technology with an animal component free cell line development platform process." Applied Microbiology and Biotechnology **87**(4): 1517-1524.

Jostock, T., M. Vanhove, et al. (2004). "Rapid generation of functional human IgG antibodies derived from Fab-on-phage display libraries." Journal of Immunological Methods **289**(1-2): 65-80.

Joubert, M. K., Q. Luo, et al. (2011). "Classification and characterization of therapeutic antibody aggregates." Journal of Biological Chemistry **286**(28): 25118-25133.

Jun, S. C., M. S. Kim, et al. (2005). "Selection strategies for the establishment of recombinant Chinese hamster ovary cell line with dihydrofolate reductase-mediated gene amplification." Applied Microbiology and Biotechnology **69**(2): 162-169.

Jun, S. C., M. S. Kim, et al. (2006). "Limitations to the development of humanized antibody producing Chinese hamster ovary cells using glutamine synthetase-mediated gene amplification." Biotechnology Progress **22**(3): 770-780.

Junttila, T. T., K. Parsons, et al. (2010). "Superior in vivo efficacy of afucosylated trastuzumab in the treatment of HER2-amplified breast cancer." Cancer Research **70**(11): 4481-4489.

Kalwy, S., J. Rance, et al. (2006). "Toward more efficient protein expression." Molecular Biotechnology **34**(2): 151-156.

Kaminski, A., G. J. Belsham, et al. (1994). "Translation Of Encephalomyocarditis Virus-Rna - Parameters Influencing The Selection Of The Internal Initiation Site." Embo Journal **13**(7): 1673-1681.

Kaminski, A., M. T. Howell, et al. (1990). "Initiation of encephalomyocarditis virus RNA translation: The authentic initiation site is not selected by a scanning mechanism." Embo Journal **9**(11): 3753-3759.

Kaneko, Y., F. Nimmerjahn, et al. (2006). "Anti-Inflammatory Activity of Immunoglobulin G Resulting from Fc Sialylation." Science **313**(5787): 670-673.

Kang, P., Y. Mechref, et al. (2007). "Comparative glycomic mapping through quantitative permethylation and stable-isotope labeling." Analytical Chemistry **79**(16): 6064-6073.

Kaufman, R. J., M. V. Davies, et al. (1991). "Improved Vectors For Stable Expression Of Foreign Genes In Mammalian-Cells By Use Of The Untranslated Leader Sequence From Emc Virus." Nucleic Acids Research **19**(16): 4485-4490.

Kaufman, R. J., L. C. Wasley, et al. (1985). "Coamplification and coexpression of human tissue-type plasminogen activator and murine dihydrofolate reductase sequences in Chinese hamster ovary cells." Molecular and Cellular Biology **5**(7): 1750-1759.

Kelley, B. (2009). "Industrialization of mAb production technology: The bioprocessing industry at a crossroads." MAbs **1**(5): 443-452.

Khawli, L. A., S. Goswami, et al. (2010). "Charge variants in IgG1." mAbs **2**(6): 613-624.

Kim, C. H., Y. Oh, et al. (1997). "Codon optimization for high-level expression of human erythropoietin (EPO) in mammalian cells." Gene **199**(1–2): 293-301.

Kim, H. and J.-S. Kim (2014). "A guide to genome engineering with programmable nucleases." Nature Reviews Genetics **15**(5): 321-334.

Kim, J. Y., Y. G. Kim, et al. (2012). "CHO cells in biotechnology for production of recombinant proteins: Current state and further potential." Applied Microbiology and Biotechnology **93**(3): 917-930.

Kim, N. S., T. H. Byun, et al. (2001). "Key determinants in the occurrence of clonal variation in humanized antibody expression of cho cells during dihydrofolate reductase mediated gene amplification." Biotechnol Prog **17**(1): 69-75.

Kim, S. J., N. S. Kim, et al. (1998). "Characterization of chimeric antibody producing CHO cells in the course of dihydrofolate reductase-mediated gene amplification and their stability in the absence of selective pressure." Biotechnology and Bioengineering **58**(1): 73-84.

Kim, Y. G., B. Park, et al. (2012). "New cell line development for antibody-producing Chinese hamster ovary cells using split green fluorescent protein." BMC Biotechnology **12**.

Kling, J. (2012). "Fresh from the biotech pipeline 2011." Nature Biotechnology **30**(2): 128-131.

Kober, L., C. Zehe, et al. (2012). "Development of a novel ER stress based selection system for the isolation of highly productive clones." Biotechnology and Bioengineering **109**(10): 2599-2611.

Kober, L., C. Zehe, et al. (2013). "Optimized signal peptides for the development of high expressing CHO cell lines." Biotechnology and Bioengineering: n/a-n/a.

Koh, E. Y. C., S. C. L. Ho, et al. (2013). "An Internal Ribosome Entry Site (IRES) Mutant Library for Tuning Expression Level of Multiple Genes in Mammalian Cells." PLoS ONE **8**(12): e82100.

Kohler, G. and C. Milstein (1975). "Continuous cultures of fused cells secreting antibody of predefined specificity." Nature **256**(5517): 495-497.

Konstantinidis, S., S. Kong, et al. (2013). "Identifying analytics for high throughput bioprocess development studies." Biotechnology and Bioengineering: n/a-n/a.

Kotsopoulou, E., H. Bosteels, et al. (2010). "Optimised mammalian expression through the coupling of codon adaptation with gene amplification: Maximum yields with minimum effort." Journal of Biotechnology **146**(4): 186-193.

Kozak, M. (1989). "Context effects and inefficient initiation at non-AUG codons in eucaryotic cell-free translation systems." Molecular and Cellular Biology **9**(11): 5073-5080.

Krambeck, F. J. and M. J. Betenbaugh (2005). "A mathematical model of N-linked glycosylation." Biotechnology and Bioengineering **92**(6): 711-728.

Krämer, O., S. Klausing, et al. (2010). "Methods in mammalian cell line engineering: from random mutagenesis to sequence-specific approaches." Applied Microbiology and Biotechnology **88**(2): 425-436.

Ku, S. C., D. T. Ng, et al. (2008). "Effects of overexpression of X-box binding protein 1 on recombinant protein production in Chinese hamster ovary and NS0 myeloma cells." Biotechnology and Bioengineering **99**(1): 155-164.

Kuczewski, M., E. Schirmer, et al. (2011). "A single-use purification process for the production of a monoclonal antibody produced in a PER.C6 human cell line." Biotechnology Journal **6**(1): 56-65.

Kumar, N. and N. Borth (2012). "Flow-cytometry and cell sorting: An efficient approach to investigate productivity and cell physiology in mammalian cell factories." Methods **56**(3): 366-374.
Kunes, Y. Z., W. R. Gion, et al. (2009). "Expression of antibodies using single-open reading frame vector design and polyprotein processing from mammalian cells." Biotechnology Progress **25**(3): 735-744.
Kwaks, T. H., P. Barnett, et al. (2003). "Identification of anti-repressor elements that confer high and stable protein production in mammalian cells." Nature Biotechnology **21**(5): 553-558.
Kyte, J. and R. F. Doolittle (1982). "A simple method for displaying the hydropathic character of a protein." Journal of Molecular Biology **157**(1): 105-132.
Lee, C. J., G. Seth, et al. (2009). "A clone screening method using mRNA levels to determine specific productivity and product quality for monoclonal antibodies." Biotechnology and Bioengineering **102**(4): 1107-1118.
Lee, Y. K., J. W. Brewer, et al. (1999). "BiP and immunoglobulin light chain cooperate to control the folding of heavy chain and ensure the fidelity of immunoglobulin assembly." Molecular Biology of the Cell **10**(7): 2209-2219.
Lenny, N. and M. Green (1991). "Regulation of endoplasmic reticulum stress proteins in COS cells transfected with immunoglobulin μ heavy chain cDNA." Journal Of Biological Chemistry **266**(30): 20532-20537.
Li, J., C. Menzel, et al. (2007). "A comparative study of different vector designs for the mammalian expression of recombinant IgG antibodies." Journal of Immunological Methods **318**(1-2): 113-124.
Li, J., C. Zhang, et al. (2007). "Analysis of IgG heavy chain to light chain ratio with mutant Encephalomyocarditis virus internal ribosome entry site." Protein Engineering, Design and Selection **20**(10): 491-496.
Li, M., Y. M. Wu, et al. (2012). "2A Peptide-based, Lentivirus-mediated Anti-death Receptor 5 Chimeric Antibody Expression Prevents Tumor Growth in Nude Mice." Molecular Therapy **20**(1): 46-53.
Lim, S. F., K. H. Chuan, et al. (2006). "RNAi suppression of Bax and Bak enhances viability in fed-batch cultures of CHO cells." Metabolic Engineering **8**(6): 509-522.
Lim, Y., N. S. C. Wong, et al. (2010). "Engineering mammalian cells in bioprocessing – current achievements and future perspectives." Biotechnology and Applied Biochemistry **55**(4): 175-189.
Liu, H., G. G. Bulseco, et al. (2006). "Effect of posttranslational modifications on the thermal stability of a recombinant monoclonal antibody." Immunology Letters **106**(2): 144-153.
Liu, H. and K. May (2012). "Disulfide bond structures of IgG molecules: Structural variations, chemical modifications and possible impacts to stability and biological function." mAbs **4**(1): 17-23.
Liu, P.-Q., E. M. Chan, et al. (2010). "Generation of a triple-gene knockout mammalian cell line using engineered zinc-finger nucleases." Biotechnology and Bioengineering **106**(1): 97-105.
Livak, K. J. and T. D. Schmittgen (2001). "Analysis of relative gene expression data using real-time quantitative PCR and the 2(T)(-Delta Delta C) method." Methods **25**(4): 402-408.

Lonberg, N., L. D. Taylor, et al. (1994). "Antigen-specific human antibodies from mice comprising four distinct genetic modifications." Nature **368**(6474): 856-859.

Mahler, H. C., W. Friess, et al. (2009). "Protein aggregation: Pathways, induction factors and analysis." Journal of Pharmaceutical Sciences **98**(9): 2909-2934.

Majors, B. S., M. J. Betenbaugh, et al. (2009). "Mcl-1 overexpression leads to higher viabilities and increased production of humanized monoclonal antibody in Chinese hamster ovary cells." Biotechnology Progress **25**(4): 1161-1168.

Malphettes, L., Y. Freyvert, et al. (2010). "Highly efficient deletion of FUT8 in CHO cell lines using zinc-finger nucleases yields cells that produce completely nonfucosylated antibodies." Biotechnology and Bioengineering **106**(5): 774-783.

Martin, P., O. Albagli, et al. (2006). "Development of a new bicistronic retroviral vector with strong IRES activity." BMC Biotechnology **6**: 4.

Martinez-Salas, E. (1999). "Internal ribosome entry site biology and its use in expression vectors." Current Opinion in Biotechnology **10**(5): 458-464.

Matasci, M., D. L. Hacker, et al. (2009). "Recombinant therapeutic protein production in cultivated mammalian cells: current status and future prospects." Drug Discovery Today: Technologies **5**(2-3).

Mielke, C., M. Tümmler, et al. (2000). "Stabilized, long-term expression of heterodimeric proteins from tricistronic mRNA." Gene **254**(1-2): 1-8.

Mohan, C. and G. M. Lee (2010). "Effect of inducible co-overexpression of protein disulfide isomerase and endoplasmic reticulum oxidoreductase on the specific antibody productivity of recombinant Chinese hamster ovary cells." Biotechnology and Bioengineering **107**(2): 337-346.

Mohan, C., S. H. Park, et al. (2007). "Effect of doxycycline-regulated protein disulfide isomerase expression on the specific productivity of recombinant CHO cells: Thrombopoietin and antibody." Biotechnology and Bioengineering **98**(3): 611-615.

Mountford, P. S. and A. G. Smith (1995). "Internal Ribosome Entry Sites And Dicistronic Rnas In Mammalian Transgenesis." Trends In Genetics **11**(5): 179-184.

Mueller, M., M. Q. Loh, et al. (2013). "Liquid Formulations for Long-Term Storage of Monoclonal IgGs." Applied biochemistry and biotechnology **169**(4): 1431-1448.

Müller, D., H. Katinger, et al. (2008). "MicroRNAs as targets for engineering of CHO cell factories." Trends in Biotechnology **26**(7): 359-365.

Nair, A. R., X. Jinger, et al. (2011). "Effect of different UCOE-promoter combinations in creation of engineered cell lines for the production of Factor VIII." BMC Research Notes **4**.

Nakayama, K. (1997). "Furin: A mammalian subtilisin/Kex2p-like endoprotease involved in processing of a wide variety of precursor proteins." Biochemical Journal **327**(3): 625-635.

Nehlsen, K., S. Herrmann, et al. (2010). "Toxin–antitoxin based transgene expression in mammalian cells." Nucleic Acids Research **38**(5): e32.

Nelson, A. L., E. Dhimolea, et al. (2010). "Development trends for human monoclonal antibody therapeutics." Nature Reviews Drug Discovery **9**(10): 767-774.

Ng, S. K., W. Lin, et al. (2010). "Vector fragmentation: characterizing vector integrity in transfected clones by Southern blotting." Biotechnology Progress **26**(1): 11-20.

Ng, S. K., D. I. C. Wang, et al. (2007). "Application of destabilizing sequences on selection marker for improved recombinant protein productivity in CHO-DG44." Metabolic Engineering **9**(3): 304-316.

Nishimiya, D. (2014). "Proteins improving recombinant antibody production in mammalian cells." Applied Microbiology and Biotechnology **98**(3): 1031-1042.

Nolan, R. P. and K. Lee (2012). "Dynamic model for CHO cell engineering." Journal of Biotechnology **158**(1–2): 24-33.

North, S. J., H. H. Huang, et al. (2010). "Glycomics profiling of Chinese hamster ovary cell glycosylation mutants reveals N-glycans of a novel size and complexity." Journal Of Biological Chemistry **285**(8): 5759-5775.

Norton, P. A. and C. J. Pachuk (2003). Methods for DNA introduction into mammalian cells. New Comprehensive Biochemistry. S. C. Makrides, Elsevier. **Volume 38:** 265-277.

Nothwehr, S. F. and J. I. Gordon (1990). "Structural features in the NH2-terminal region of a model eukaryotic signal peptide influence the site of its cleavage by signal peptidase." Journal of Biological Chemistry **265**(28): 17202-17208.

Nowicki, M. (2007). "Basic Facts about Biosimilars." Kidney and Blood Pressure Research **30**(5): 267-272.

O'Callaghan, P. M., J. McLeod, et al. (2010). "Cell line-specific control of recombinant monoclonal antibody production by CHO cells." Biotechnology and Bioengineering **106**(6): 938-951.

Omasa, T., Y. Cao, et al. (2009). "Bacterial artificial chromosome library for genome-wide analysis of Chinese hamster ovary cells." Biotechnology and Bioengineering **104**(5): 986-994.

Omasa, T., M. Onitsuka, et al. (2010). "Cell engineering and cultivation of chinese hamster ovary (CHO) cells." Curr Pharm Biotechnol **11**(3): 233-240.

Osterlehner, A., S. Simmeth, et al. (2011). "Promoter methylation and transgene copy numbers predict unstable protein production in recombinant chinese hamster ovary cell lines." Biotechnology and Bioengineering **108**(11): 2670-2681.

Otte, A. P., T. H. Kwaks, et al. (2007). "Various expression-augmenting DNA elements benefit from STAR-Select, a novel high stringency selection system for protein expression." Biotechnology Progress **23**(4): 801-807.

Page, M., C. Ling, et al. (1995). "Fragmentation of Therapeutic Human Immunoglobulin Preparations." Vox Sanguinis **69**(3): 183-194.

Pelletier, J. and N. Sonenberg (1988). "Internal initiation of translation of eukaryotic mRNA directed by a sequence derived from poliovirus RNA." Nature **334**(6180): 320-325.

Petersen, T. N., S. Brunak, et al. (2011). "SignalP 4.0: discriminating signal peptides from transmembrane regions." Nature Methods **8**(10): 785-786.

Pfeilschifter, J., C. Chenu, et al. (1989). "Interleukin-1 and tumor necrosis factor stimulate the formation of human osteoclastlike cells in vitro." Journal of Bone and Mineral Research **4**(1): 113-118.

Pham, P., A. Kamen, et al. (2006). "Large-Scale transfection of mammalian cells for the fast production of recombinant protein." Molecular Biotechnology **34**(2): 225-237.

Phillips, J., A. Drumm, et al. (2001). "Manufacture and quality control of CAMPATH-1 antibodies for clinical trials." Cytotherapy **3**(3): 233-242.

Pichler, J., S. Galosy, et al. (2010). "Selection of CHO host cell subclones with increased specific antibody production rates by repeated cycles of transient transfection and cell sorting." Biotechnology and Bioengineering.

Pichler, J., F. Hesse, et al. (2009). "A study on the temperature dependency and time course of the cold capture antibody secretion assay." Journal of Biotechnology **141**(1–2): 80-83.

Pilbrough, W., T. P. Munro, et al. (2009). "Intraclonal protein expression heterogeneity in recombinant CHO cells." PLoS One **4**(12): e8432.

Pybus, L. P., D. C. James, et al. (2014). "Predicting the expression of recombinant monoclonal antibodies in Chinese hamster ovary cells based on sequence features of the CDR3 domain." Biotechnology Progress **30**(1): 188-197.

Qiao, J., V. Roy, et al. (2002). "High translation efficiency is mediated by the encephalomyocarditis virus internal ribosomal entry sites if the natural sequence surrounding the eleventh AUG is retained." Human Gene Therapy **13**(7): 881-887.

Raju, T. S. and R. Jordan (2012). "Galactosylation variations in marketed therapeutic antibodies." mAbs **4**(3): 385-391.

Rathore, A. S. and H. Winkle (2009). "Quality by design for biopharmaceuticals." Nature Biotechnology **27**(1): 26-34.

Rees, S., J. Coote, et al. (1996). "Bicistronic vector for the creation of stable mammalian cell lines that predisposes all antibiotic-resistant cells to express recombinant protein." Biotechniques **20**(1): 102-104, 106, 108-110.

Reichert, J. M. (2012). "Marketed therapeutic antibodies compendium." MAbs **4**(3): 413-415.

Reichert, J. M. (2012). "Which are the antibodies to watch in 2012?" MAbs **4**(1): 1-3.

Rouet, P., F. Smih, et al. (1994). "Introduction of double-strand breaks into the genome of mouse cells by expression of a rare-cutting endonuclease." Molecular and Cellular Biology **14**(12): 8096-8106.

Rudd, P. M., T. Elliott, et al. (2001). "Glycosylation and the immune system." Science **291**(5512): 2370-2376.

Ryan, M. D. and J. Drew (1994). "Foot-and-mouth disease virus 2A oligopeptide mediated cleavage of an artificial polyprotein." EMBO J **13**(4): 928-933.

Sakaguchi, M. (1997). "Eukaryotic protein secretion." Current Opinion in Biotechnology **8**(5): 595-601.

Sautter, K. and B. Enenkel (2005). "Selection of high-producing CHO cells using NPT selection marker with reduced enzyme activity." Biotechnology and Bioengineering **89**(5): 530-538.

Schaefer, J. V. and A. Plückthun (2012). "Engineering Aggregation Resistance in IgG by Two Independent Mechanisms: Lessons from Comparison of Pichia pastoris and Mammalian Cell Expression." Journal of Molecular Biology.

Schlatter, S., S. H. Stansfield, et al. (2005). "On the optimal ratio of heavy to light chain genes for efficient recombinant antibody production by CHO cells." Biotechnology Progress **21**(1): 122-133.

Schröder, M. and R. J. Kaufman (2005). "ER stress and the unfolded protein response." Mutation Research - Fundamental and Molecular Mechanisms of Mutagenesis **569**(1-2): 29-63.

Schröder, M., R. Schäfer, et al. (2002). "Induction of protein aggregation in an early secretory compartment by elevation of expression level." Biotechnology and Bioengineering **78**(2): 131-140.

Serpieri, F., A. Inocencio, et al. (2010). "Comparison of Humanized IgG and FvFc Anti-CD3 Monoclonal Antibodies Expressed in CHO Cells." Molecular Biotechnology **45**(3): 218-225.

Shapiro, A. L., M. D. Scharff, et al. (1966). "Synthesis of excess light chains of gamma globulin by rabbit lymph node cells." Nature **211**(5046): 243-245.

Shental-Bechor, D. and Y. Levy (2008). "Effect of glycosylation on protein folding: A close look at thermodynamic stabilization." Proceedings of the National Academy of Sciences **105**(24): 8256-8261.

Shields, R. L., J. Lai, et al. (2002). "Lack of Fucose on Human IgG1 N-Linked Oligosaccharide Improves Binding to Human FcγRIII and Antibody-dependent Cellular Toxicity." Journal Of Biological Chemistry **277**(30): 26733-26740.

Sigma-Aldrich. (2011). "CHOZN® DHFR-/- ZFN-Modified CHO Cell Line ", 2013, from http://www.sigmaaldrich.com/catalog/product/sigma/chodhfr.

Singh, R. P., M. Al.-Rubeai, et al. (1994). "Cell death in bioreactors: A role for apoptosis." Biotechnology and Bioengineering **44**(6): 720-726.

Sleiman, R. J., P. P. Gray, et al. (2008). "Accelerated cell line development using two-color fluorescence activated cell sorting to select highly expressing antibody-producing clones." Biotechnol Bioeng **99**(3): 578-587.

Stern, B., A. Optun, et al. (2011). "Enhanced protein synthesis and secretion using a rational signal-peptide library approach as a tailored tool." BMC Proceedings **5**(Suppl 8): O13.

Suzuki, E., R. Niwa, et al. (2007). "A Nonfucosylated Anti-HER2 Antibody Augments Antibody-Dependent Cellular Cytotoxicity in Breast Cancer Patients." Clinical Cancer Research **13**(6): 1875-1882.

Swiech, K., V. Picanço-Castro, et al. (2012). "Human cells: New platform for recombinant therapeutic protein production." Protein Expression and Purification **84**(1): 147-153.

Szymczak-Workman, A. L., K. M. Vignali, et al. (2012). "Design and Construction of 2A Peptide-Linked Multicistronic Vectors." Cold Spring Harbor Protocols **2012**(2): 199-204.

Tap Biosystems. (2014). "Tap Biosystems ambr15." 2014, from http://www.tapbiosystems.com/tap/cell_culture/ambr.htm.
Tey, B. T., R. P. Singh, et al. (2000). "Influence of Bcl-2 on cell death during the cultivation of a Chinese hamster ovary cell line expressing a chimeric antibody." Biotechnology and Bioengineering **68**(1): 31-43.
Tjio, J. H. and T. T. Puck (1958). "Genetics of Somatic Mammalian Cells." The Journal of Experimental Medicine **108**(2): 259-268.
Tracey, D., L. Klareskog, et al. (2008). "Tumor necrosis factor antagonist mechanisms of action: A comprehensive review." Pharmacology & Therapeutics **117**(2): 244-279.
Trill, J. J., A. R. Shatzman, et al. (1995). "Production of monoclonal antibodies in COS and CHO cells." Current Opinion in Biotechnology **6**(5): 553-560.
Underhill, M. F., C. M. Smales, et al. (2007). "Transient gene expression levels from multigene expression vectors." Biotechnology Progress **23**(2): 435-443.
Urlaub, G. and L. A. Chasin (1980). "Isolation of Chinese hamster cell mutants deficient in dihydrofolate reductase activity." Proceedings of the National Academy of Sciences **77**(7): 4216-4220.
Urlaub, G., E. Käs, et al. (1983). "Deletion of the diploid dihydrofolate reductase locus from cultured mammalian cells." Cell **33**(2): 405-412.
van Beers, M. M. C. and M. Bardor (2012). "Minimizing immunogenicity of biopharmaceuticals by controlling critical quality attributes of proteins." Biotechnology Journal **7**(12): 1473-1484.
Van Berkel, P. H. C., J. Gerritsen, et al. (2009). "N-linked glycosylation is an important parameter for optimal selection of cell lines producing biopharmaceutical human IgG." Biotechnology Progress **25**(1): 244-251.
van Blokland, H. J., T. H. Kwaks, et al. (2007). "A novel, high stringency selection system allows screening of few clones for high protein expression." Journal of Biotechnology **128**(2): 237-245.
Vanhove, M., Y. K. Usherwood, et al. (2001). "Unassembled Ig heavy chains do not cycle from BiP in vivo but require light chains to trigger their release." Immunity **15**(1): 105-114.
von Heijne, G. (1985). "Signal sequences: The limits of variation." Journal of Molecular Biology **184**(1): 99-105.
Wada, Y., P. Azadi, et al. (2007). "Comparison of the methods for profiling glycoprotein glycans - HUPO human disease glycomics/proteome initiative multi-institutional study." Glycobiology **17**(4): 411-422.
Wagner, S. D., G. T. Williams, et al. (1994). "Antibodies generated from human immunoglobulin miniloci in transgenic mice." Nucleic Acids Research **22**(8): 1389-1393.
Walsh, G. and R. Jefferis (2006). "Post-translational modifications in the context of therapeutic proteins." Nature Biotechnology **24**(10): 1241-1252.
Walter, P. and G. Blobel (1983). "Subcellular distribution of signal recognition particle and 7SL-RNA determined with polypeptide-specific antibodies and complementary DNA probe." The Journal of cell biology **97**(6): 1693-1699.

Wang, T. Y., J. H. Zhang, et al. (2010). "Positional effects of the matrix attachment region on transgene expression in stably transfected CHO cells." Cell Biology International **34**(2): 141-145.

Werner, R. G., K. Kopp, et al. (2007). "Glycosylation of therapeutic proteins in different production systems." Acta Paediatrica **96**(455): 17-22.

Westwood, A. D., D. A. Rowe, et al. (2010). "Improved recombinant protein yield using a codon deoptimized DHFR selectable marker in a CHEF1 expression plasmid." Biotechnology Progress **26**(6): 1558-1566.

Winter, G., A. D. Griffiths, et al. (1994). "Making Antibodies by Phage Display Technology." Annual Review of Immunology **12**(1): 433-455.

Wong, C. F. D., K. Tin Kam Wong, et al. (2005). "Impact of dynamic online fed-batch strategies on metabolism, productivity and N-glycosylation quality in CHO cell cultures." Biotechnology and Bioengineering **89**(2): 164-177.

Wong, D. C. F., K. T. K. Wong, et al. (2006). "Targeting early apoptotic genes in batch and fed-batch CHO cell cultures." Biotechnology and Bioengineering **95**(3): 350-361.

Wu, S.-C. (2009). "RNA interference technology to improve recombinant protein production in Chinese hamster ovary cells." Biotechnology Advances **27**(4): 417-422.

Wurm, F. M. (2004). "Production of recombinant protein therapeutics in cultivated mammalian cells." Nature Biotechnology **22**(11): 1393-1398.

Xu, X., H. Nagarajan, et al. (2011). "The genomic sequence of the Chinese hamster ovary (CHO)-K1 cell line." Nature Biotechnology **29**(8): 735-741.

Yahata, K., H. Kishine, et al. (2005). "Multi-gene Gateway clone design for expression of multiple heterologous genes in living cells: Conditional gene expression at near physiological levels." Journal Of Biotechnology **118**(2): 123-134.

Yakes, F. M., W. Chinratanalab, et al. (2002). "Herceptin-induced Inhibition of Phosphatidylinositol-3 Kinase and Akt Is Required for Antibody-mediated Effects on p27, Cyclin D1, and Antitumor Action." Cancer Research **62**(14): 4132-4141.

Yamane-Ohnuki, N., S. Kinoshita, et al. (2004). "Establishment of FUT8 knockout Chinese hamster ovary cells: An ideal host cell line for producing completely defucosylated antibodies with enhanced antibody-dependent cellular cytotoxicity." Biotechnology and Bioengineering **87**(5): 614-622.

Yang, Y. S., Mariati, et al. (2009). "Mutated polyadenylation signals for controlling expression levels of multiple genes in mammalian cells." Biotechnology and Bioengineering **102**(4): 1152-1160.

Yenofsky, R. L., M. Fine, et al. (1990). "A mutant neomycin phosphotransferase II gene reduces the resistance of transformants to antibiotic selection pressure." Proceedings of the National Academy of Sciences **87**(9): 3435-3439.

Yoo, S. M. and R. Ghosh (2012). "Simultaneous removal of leached protein-A and aggregates from monoclonal antibody using hydrophobic interaction membrane chromatography." Journal of Membrane Science **390-391**: 263-269.

Zhang, Y. B., J. Howitt, et al. (2004). "Protein aggregation during overexpression limited by peptide extensions with large net negative charge." Protein Expression and Purification **36**(2): 207-216.

Zhou, H., Z.-g. Liu, et al. (2010). "Generation of stable cell lines by site-specific integration of transgenes into engineered Chinese hamster ovary strains using an FLP-FRT system." Journal of Biotechnology **147**(2): 122-129.